

Burning Rate Characteristics of Turbulent Rich Premixed Flames

**A dissertation submitted in partial fulfillment of
The requirements for the degree of
MSc in Sustainable Energy and Environment**

By

**Ahmed Al Makky
(BSc in Mechanical Engineering)**

**Supervisor
Professor Phil Bowen**

Cardiff University

September 2007

ABSTRACT

The challenges associated with a sustainable future in terms of energy utilisation will require the utilisation of non-traditional fuels and operating conditions for power generators such as gas turbines and reciprocating engines. Cardiff School of Engineering is undertaking a detailed programme of work to study and analyse the fundamental turbulent burning characteristics of alternative fuels under a range of ambient conditions. This thesis provides the first studies of a new atmospheric experimental facility, which forms part of the overall programme of work.

The Cardiff atmospheric combustion rig was designed and developed at the Cardiff University to investigate burning velocities for different types of fuels. However, it is known that due to the installation of different types of turbulence plates (in some references turbulence plates are referred to as turbulence discs) raises the turbulence intensity which results in changes on the flame parameters on the Borghi chart. The focus of the research concerns the turbulent burning velocity and the effects of turbulence plates on the flame burning rates and the flame stretch. As such, the main aim of this study was to undertake a first benchmarking study for this rig using methane-air mixtures, compare the recorded data with others that have used atmospheric combustion facilities, and hence determine a protocol for the interpretation of results from the Cardiff atmospheric combustion rig. This study found that the diameter of the holes in the turbulence discs, the discharge coefficient and holes layout has a great impact on the burning velocity. On the other hand, the disc thickness, the number of holes also has an effect on the burning velocity. The rise of pressure and its profile distribution on the turbulence plate surface has a great impact on increasing burning velocities. The work also pointed out where the turbulence plates are situated on the Borghi /Peters chart.

Acknowledgments

This case study is an effect of my research during a 3-month period at Cardiff school of engineering in Wales where I did my daily work in doing my literature review modeling taking notes and getting an in depth understanding of the field of combustion which I had no back ground in before.

I'd like to thank my mother, father and brother for their help, prayers, support and scientific guidance all my life and till now.

I thank Dr. Peter Kay who was my actual every-day boss at Cardiff school of engineering for his professional supervision, discussions and generous scientific support. I would also like to thank PhD student Audrius Bagdanavicius, for his follow up and kind help in setting up and taking samples .I thank the man in charge of our Combustion Research Laboratory, Professor Phil Bowen for his expertise and feedback. For the financial support I am grateful to Cardiff School of Engineering, especially to professor Phil Bowen.

DECLARATION

This work has not previously been accepted in substance for any degree and is not being concurrently submitted in candidature for any degree.

Signed..... (Candidate)
Date.....

Statement 1

This thesis is the result of my own investigations, except where otherwise stated.

Other sources are acknowledged by footnotes giving explicit references. A bibliography is appended.

Signed..... (Candidate)
Date.....

Statement 2

I hereby give consent for my thesis, if accepted, to be available for photocopying and for inter-library loan, and for the title and summary to be made available to out side organisations.

Signed..... (Candidate)
Date.....

Nomenclature:		
Roman Symbols	Unit	Definition
u	m/s	Velocity of flow through a tube
L	M	Characteristic length
\bar{u}	m/s	Average velocity
q_{comb}	$kJ/mole$	The heat released by the combustion reaction
q_{wire}	$kJ/mole$	The heat needed to burn the wire
$n_{methane}$	moles	Number of moles for methane
a, b, c	-	constants
T	K	temperature
n	moles	Number of moles
R	$J/Kmole$	Ideal gas constant
V	m^3	volume
MW_{fuel}	Kg	Molecular weight of fuel
N	-	constant
U_{rms}	m/s	Turbulence strength
\dot{m}_{fuel}	Kg/s	Mass flow rate of fuel
\dot{m}_{air}	Kg/s	Mass flow rate of air
MW_{air}	Kg	Molecular weight of air
$v(t)$	m/s	Velocity on the y axis at certain time t
Re	-	Reynolds Number
$u(t)$	m/s	Velocity on the x axis at certain time t
t	s	time
u'	m/s	Velocity fluctuation on the x axis

\bar{u}_x	m/s	Average mean velocity on the x axis
u'_z	m/s	Velocity fluctuation on the z axis
u'_y	m/s	Velocity fluctuation on the y axis
u'_x	m/s	Velocity fluctuation on the x axis
S_u	m/s	Burning velocity after combustion wave
$H_{prod}(T_{ad}, P)$	kJ	absolute enthalpy of the products
S_b	m/s	Burning velocity before combustion wave
$H_{reac}(T_i, P)$	kJ	absolute enthalpy of the reactants
\dot{m}	Kg/s	Mass flow rate
P_u	bar	Pressure after the combustion wave
P_b	bar	Pressure before the combustion wave
Q	m^3/s	Volumetric flow rate
C_p	kJ/KgK	Specific heat capacity at constant pressure
$h_{prod}(T_{ad}, P)$	kJ/Kg	absolute enthalpy of the products per mass
$(C_p)_f$	kJ/KgK	The specific heat value at constant pressure for the flame
\bar{C}_p	kJ/KgK	The average specific heat value at constant pressure between T_0 and T_f .
$h_{reac}(T_i, P)$	kJ/Kg	absolute enthalpy of the reactants per mass
h	mm	Height of cone
U_n	m/s	Velocity of the fuel

T_0 K air mixture before
combustion T_i K Initial temperature of
the fuel air gas
mixture \dot{w} $mole/sec$ temperature of the
fuel air gas mixture
before the
combustion wave T_f K

Reaction rates

 T_{air} K

Flame temperature

 P_{air} bar

Air temperature

 P_{fuel} bar

Air pressure

 T_{fuel} K

Fuel pressure

 n_r $moles$

Fuel temperature

Number of moles of
reactants n_p $moles$ Number of moles for
products E $kJ / moles$

Activation energy

 D m^2 / sec

Thermal diffusivity

 R_{air} $J / Kmole$

Air gas constant

 Le

-

Lewis number

 R_{air} $J / Kmole$

Air gas constant

 R_{fuel} $J / Kmole$

Fuel gas constant

 S_L m / s Laminar burning
velocity Sc

-

Schmidt number

 Ka

-

Karlovitz number

 r_{air}

-

Air percentage in
mixture r_{fuel}

-

Fuel percentage in
mixture $f(t)$ Temperature
function with time r mm

Radius of cone

S_T	m/s	Turbulent burning velocity
$T(t)$	K	Fluctuation of temperature with time
\bar{T}	K	Average temperature
Re_T	-	Reynolds Turbulent number
a_0	$moles/m^3$	Initial concentration
$K(T)$	$mole/(m^3s)$	instantaneous-rate constant
$K(\bar{T})$	$mole/(m^3s)$	instantaneous-rate constant at mean temperature
z'	s^{-1}	Frequency factor
Re_{l_o}	-	Reynolds number for the integral scale
Re_{l_k}	-	Reynolds number for Taylor Microscale
Re_{l_λ}	-	Reynolds number for Kolmogorov Microscale
$R_x(r)$	-	correlation coefficient
S	mm^2	Cone slant height
$A_{conearea}$	mm^2	Cone area
$A_{cbasareaa}$	mm^2	Cone base area

Nomenclature:		
Greek Symbols	Unit	Definition
ΔH_{oxygen}^0	$kJ/mole$	Molar enthalpy of oxygen
$\Delta H_{fmethane}^0$	$kJ/mole$	Molar enthalpy of methane
ΔH_{fwater}^0	$kJ/mole$	Molar enthalpy of water
ΔH_{comb}	$kJ/mole$	The molar enthalpy of combustion
ΔE_{comb}	$kJ/mole$	internal energy of combustion
ϕ	-	Stoichiometric
ν	m^2/s	Kinematic viscosity
τ	s	Time interval
$v(t)$	m/s	Velocity on the y axis at certain time t
v'	m/s	Velocity fluctuation on the y axis
α	Kg_{fuel}/Kg_{air}	Fuel air ratio
α_{stoic}	$(Kg_{fuel}/Kg_{air})_{stoic}$	Fuel air ratio at Stoichiometric conditions
ρ_u	Kg/m^3	Density after combustion wave
ρ_b	Kg/m^3	Density before combustion wave
λ	J/mK	Thermal conductivity
δ	mm	Flame thickness
ρ_{air}	Kg/m^3	Air density
ρ_{fuel}	Kg/m^3	Fuel density
v_{mean}	m/s	Mean velocity
δ_{min}	mm	Minimum flame thickness
τ_m	s	Time needed for

τ_c ρ_0 δ_{ideal} δ_{max} v_{bulk} v'_{rms} ϵ_0 s Kg/m^3 mm mm m/s m/s m^2/sec^3

mixing

Time needed for
chemical reactionDensity of mixture
before combustion

Ideal flame thickness

Maximum flame
thickness

Bulk velocity

mean-square
fluctuating velocity

rate of dissipation

Table of Contents

Abstract	i
Acknowledgments.....	ii
DECLARATION.....	iii
Nomenclature.....	iv
Table of contents.....	x

1. Introduction and motivation.....	-1-
1.1. The environmental issue connected with combustion.....	-1 -
1.2. Design modifications on automotive engines.....	- 1-
1.3. Designers provided with accurate Data gives improved designs.....	- 2-
1.4. Aims and objectives.....	-4 -
2. Theory and Literature Overview.....	-5-
2.1. Fuel Chemistry.....	-5-
2.1.1. Some basic info.....	-5-
2.1.2. Methane Properties.....	-5-
2.1.3. The combustion of Methane.....	-6-
2.1.4. The Oxidation of Methane.....	-7-
2.2. Combustion Fundamentals.....	-11-
2.2.1. Introduction.....	-11-
2.2.2. The combustion equation of an arbitrary hydrocarbon.....	-11-
2.2.3. There are cases which are fundamental for conducting the lab-work.....	-12-
2.2.4. The implementation of the fundamentals on a lab methane case.....	-15-
2.2.5. The heat of combustion for Methane.....	-17-
2.3. A Study of Turbulence.....	-19-
2.3.1. Basics of Turbulent Flow	-19-
2.3.2. Turbulent flows are commonly characterized using statistical methods.....	-21-
2.4.1. Flames	-26-
2.4.2. Premixed Flames.....	-27-
2.4.3. Mass and energy conservation in premixed flames.....	-27-

2.4.4. Adiabatic Flame Temperature.....	-28-
2.4.5. Structure of the ideal, adiabatic, one dimensional, laminar, premixed flame.....	-29-
2.4.6. The Laminar Flame Speed	-31-
2.4.7. Laminar Flame Structure.....	-33-
2.4.8. The Theory of Mallard and Le Chatelier	-34-
2.4.9. Comments on the Mallard and Le Chatelier Theory	-36-
2.4.10. The Theory of Zeldovich Frank-Kamenetskii, and Semenov	-38-
2.5. Turbulent Reacting Flows and Turbulent Flames.....	-40-
2.5.1 The Rate of Reaction in a Turbulent Field.....	-40-
2.5.2. The Turbulent Flame Speed.....	-44-
2.6. Length Scales in Turbulent Flows.....	-50-
2.6.1. Characteristic Width of Flow or Microscale	-50-
2.6.2. Integral Scale or Turbulence Microscale	-50-
2.6.3. Taylor Microscale	-51-
2.6.4. Kolmogorov Microscale.....	-51-
2.6.5 Turbulence Reynolds Numbers.....	-52-
2.7. Flame Regimes and Governing Physical Phenomena.....	-52-
2.7.1. The turbulent Reynolds number	-52-
2.7.2. The Damköhler number	-53-
2.7.3. The Karlovitz number	-53-
2.7.4. Lewis Number (Le).....	-54-
2.7.5. Description of the Borghi/Peters chart.....	-56-
2.8. Flame Speed Measurements.....	-56-
3. Experimental setup	-57-
3.1. Atmospheric-pressure test facility.....	-57-
3.1.2. Dantec automated data collection module.....	-59-
4. Measuring Techniques.....	-62-
4-1. Introduction.....	-62-
4.2. Principles of Particle Image Velocimetry (PIV).....	-62-

4.3. Description of PIV	-63-
4.4. Principles of LDA	-66-
4.4.1 Laser Beam.....	-66-
4.4.2 The Doppler effect.....	-67-
4.4.3. Intersecting beams.....	-68-
4.4.4.The Doppler frequency.....	-69-
4.4.5.The fringe model.....	-70-
4.5. The Seeding.....	-70-
4.5.1. Aluminum Oxide seeding.....	-70-
4.5.2 Properties of the seeding material.....	70-
4.5.3. Seeding as flow field tracers.....	71-
4.5.4. Particle motion.....	-71-
4.6 Photron’s APX-RS high-speed system camera.....	-73-
5. Results and Discussion.....	-74-
5.1. Turbulence plates fluid dynamics data.....	-74-
5.1.1. Introduction.....	-74-
5.1.2.Clear factors affecting the velocity parameters in graphs.....	-74-
5.1.3. The graphs with a Turbulence plate.....	-76-
5.1.4. The graphs without a Turbulence plate.....	-81-
5.1.5. The summary chart of the data.....	-84-
5.2. The burning velocity calculation.....	-85-
5.2.1. Introduction.....	-85-
5.2.2. The Flow Chart of the calculation procedure for the calculation of the turbulent burning velocity.....	-85-
5.2.3. The first method is using 3dmax software to calculate the flame area.....	-86-
5.2.4. The second method used to calculate the flame surface.....	-86-
5.2.5. The third method assuming the flame area as a cone area.....	-87-
5.2.6. Flame thickness.....	-95-
5.3. Turbulence plate parameters.....	-96-

5.4. The factors affecting the Turbulent Burning velocity.....	-104-
5.5. The calculation of the Kolmogrov scales for the three turbulence discs.....	-107-
5.6. The use of the Borghi to specify where the turbulence discs are situated.....	-108-
6. Conclusion.....	-109-
References	-111-
Appendix A.....	-114 -
Appendix B.....	- 118 -
Appendix C.....	- 119 -
Appendix D.....	-120-

1. Introduction:

1.1. The environmental issue connected with combustion:

Due to the rise in fuel prices which has been the result of the growing demanding economies of the countries of the world especially China India, global warming, depletion of oil sources (the ones which are reachable and easy to get) and the race for space tourism has meant that more research is to be invested in the field of combustion .This research covers all aspects of the flame which include products of combustion the reactants, the type of oxidizer (air or oxygen) the fluid dynamics and the thermodynamics side of the process. A large portion of CO_2 emissions are emitted by the energy production sector and the Kyoto protocol has restricted countries in how much CO_2 they should emit (this has been one of the main drive for countries) and due to the CO_2 taxation on the CO_2 emissions exceeding there limits for ,each country countries has its own limits which it should not exceed, European countries have been trying to cut down on there CO_2 emissions either by CO_2 sequestration ,scrubbers , capturing CO_2 and later pumping it back into run out oil wells.

1.2. Design modifications on automotive engines:

On the motor vehicle side, installing emissions filters on there gas exhaust on cars has been one of the methods in tackling the problem. of the process Car companies have also been trying to solve the emissions problem either by improving the efficiency of the combustion process such as using the better efficiency atomizers (fuel sprays) or piston surface design modification .Accurate control of the spray timing of the fuel air mixture and controlling this process electronically results in better combustion efficiency not forgetting that having different running modes in a car (sport or economic mode) also improves the fuel economy .Due to the fast response that electronic equipment have ,less weight and also is much easy to replace and upgrade they have an advantage on mechanical mechanisms that means better burning.

1.3. Designers provided with accurate Data gives improved designs:

Knowing the conditions of the fuel that can make it burn at its best can speed up the design control modification up grade estimation of costs process. Turbulence in a combustion process is needed but the type of turbulence should be controlled, turbulence is used for flame stabilization because the creation of a circulation zone provides the gaseous mixture the appropriate time to burn completely (that's the purpose of what is called flame holders in jet engines).

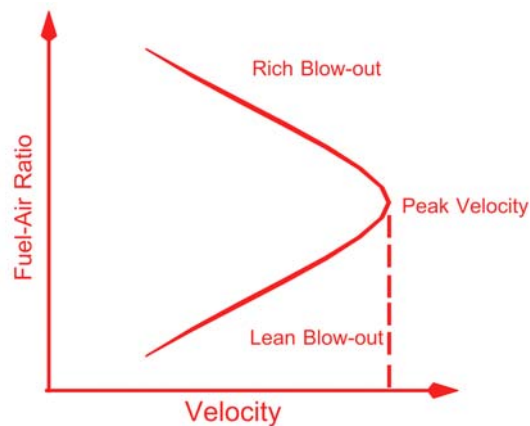


Figure1-1: Range of bumable fuel-air ratios versus combustor gas velocity.

Knowing the combustion flame temperature and pressure for a certain fuel helps out in the selection of combustors material. Having back ground info on fuel air ratio leads the designer to making the correct selection of flow rates volumes and size of the combustors as can be seen in the figure 1-1.

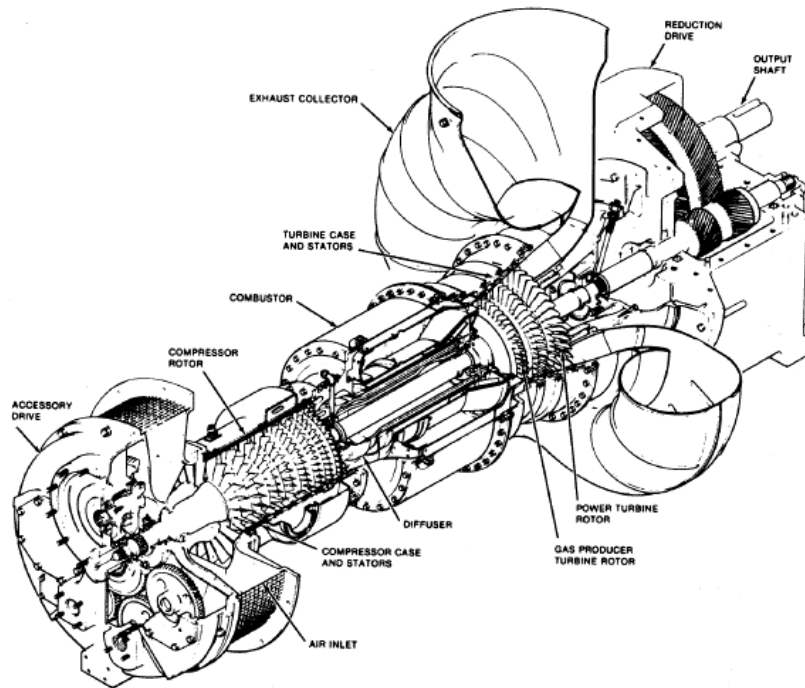


Figure 1-2: a gas turbine used to generate electricity with all its components excluding the Alternator shows how difficult it is for a designer to get all the components to work at its best [11].

The velocity profile in the combustion chamber helps out in knowing the residence time for the fuel charge as can be seen from the following figure 1-1, for the fuel charge to spend less time in the combustor means incomplete combustion and increasing the residence time means this will cause blow out of the flame and that can be hazardous for a jet plane and would cause severe knocking effect and vibrations in internal combustion engines. This is the case for a gaseous fuel air mixture in some other cases like in internal combustion engines droplets of the fuel need time to evaporate to turn into gas and then oxidize this will increase.

From figure 1-3 ,For a jet engine fuel droplets need to be atomized from the fuel nozzle to small particles so that the oxidize straight away then additional air is provided for dilution which means for the un burnt fuel. Cooling air is provided so that would prevent No_x from being produced and to cool the combustor surface and for reducing high gas temperature reaching the turbine blades.

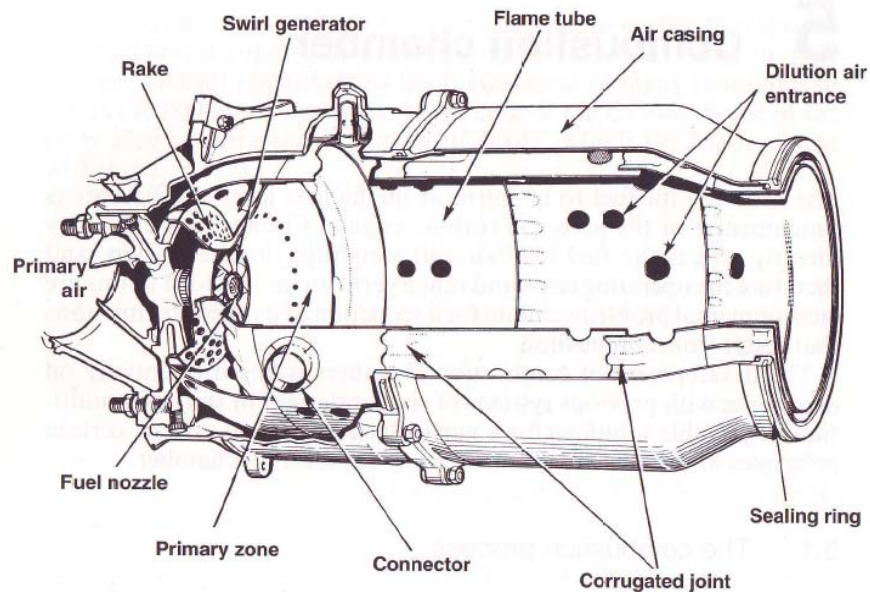


Figure1-3: A cross section in a combustor of an early model jet engine and how complicated it is for the designer to get every component running at its best [24].

1.4. Aims and objectives:

The objectives required to achieve the goal are:

- 1-The aim of the research is to provide understanding and interpretation of new data generated on a new stationary turbulent burning rate rig at Cardiff school of engineering, and the burn and interpretation of data from a new high pressure temperature optical rig at the new gas turbine research centre (The Centre, at Port Talbot South Wales).
- 2-To provide understanding of turbulent combustion.
- 3-Apply theory and practical methods to new data.
- 4-Analyse new data and the predict consequences and elevating ambient parameters.

2. Theory and Literature Overview

2.1. Fuel Chemistry:

2.1.1. Some basic info:

The various hydrocarbon families are differentiated by whether the fuel molecules consist entirely of single carbon-carbon bonds (c-c) or contain one double (c=c) or contain one triple (c≡c) bond, and whether the molecules are open chains (all chain ends are unconnected) or form rings.

The **Alkanes**, **Alkenes**, and **Alkynes** are all open-chain structures, while the **Cyclanes** and **Aromatic** exhibit ring structures.

For the open-chain families (Alkanes, Alkenes, and Alkynes), the following nomenclature is used to denote the number of carbon atoms contained in a particular family member:

1-meth	5-pent	9-non
2-eth	6-hex	10-dec
3-prop	7-hep	11-undec
4-but	8-oct	12-dodec

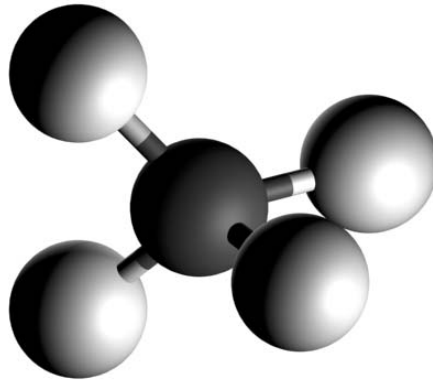
Table 2-1: A summary of hydro-carbons [3]:

Family Name	Other Designations	Molecular Formula	Carbon-Carbon Bonding	Primary Molecular Structure
Alkanes	Paraffines	$C_n H_{2n+2}$	Single bonds only	Straight or branched open chains
Alkenes	Olefines	$C_n H_{2n}$	One double bond, remainder single	Straight or branched open chains
Alkynes	Acetylene	$C_n H_{2n-2}$	One triple bond, remainder single	Straight or branched open chains
Cyclanes	Cycloalkanes, Cycloparaffines, Naphthenes	$C_n H_{2n}$ or $(CH_2)_n$	Single bonds only	Closed rings
Aromatics	Benzene family	$C_n H_{2n-6}$	Resonance hybrid bonds (Aromatic bonds)	closed rings

2.1.2. Methane Properties:

Methane is the major component of a natural gas, typically 97% by volume. At room temperature and standard pressure, Methane is a colourless, odourless gas; the smell characteristic of natural gas is an artificial safety measure caused by the addition of an odorant, often Methanethiol or Ethanethiol. It melts at -183°C and boils at -164°C . It is not very soluble in water. Methane is combustible, and mixtures of about 5 to 15 percent

in air are explosive. Methane is not toxic when inhaled, but it can produce suffocation by reducing the concentration of oxygen inhaled. Liquid methane does not burn unless subjected to high pressure (normally 4–5 atmospheres.)[12, 22].



Methane

Figure 2-1: Methane 3d balls.

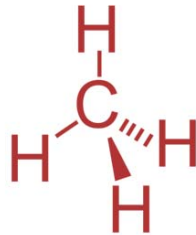


Figure 2-2: This shows the chemical structure of Methane.

Because it contains a carbon atom, when methane burns it creates carbon dioxide, which is a greenhouse gas. Therefore methane is not the perfect fuel [23].

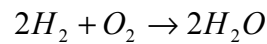
2.1.3. The combustion of Methane:

In the combustion of methane, several steps are involved:

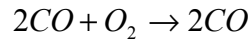
a-Methane is believed to form a formaldehyde (HCHO or H₂CO). The formaldehyde gives a formyl radical (HCO), which then forms carbon monoxide (CO). The process is called oxidative pyrolysis:



b-Following oxidative pyrolysis, the H₂ oxidizes, forming H₂O, replenishing the active species, and releasing heat. This occurs very quickly, usually in significantly less than a millisecond.



c-Finally, the CO oxidizes, forming CO₂ and releasing more heat. This process is generally slower than the other chemical steps, and typically requires a few to several milliseconds to occur [18].



2.1.4. The Oxidation of Methane:

The oxidation process of Methane either occurs at low temperature or at high temperature due to conducting the lab tests at $\phi = 1.43$ this has the result of low flame temperature as shown on figure, so the description of low temperature oxidation has only been described in this paragraph.

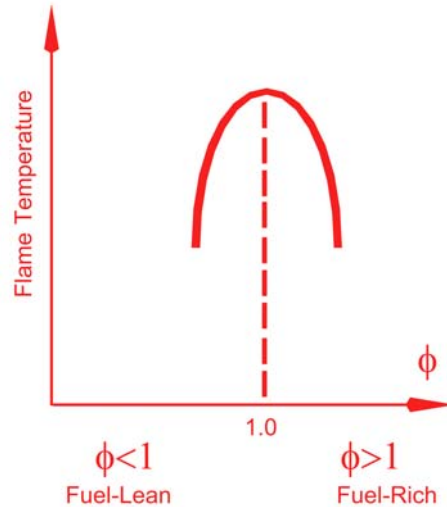


Figure 2-3: variation of flame temperature with the increase of equivalence ratio.

So in conclusion the flame temperature at the Stoichiometric condition is 2210 K which is taken from table on figure for methane air condition so this is the maximum burning temperature.

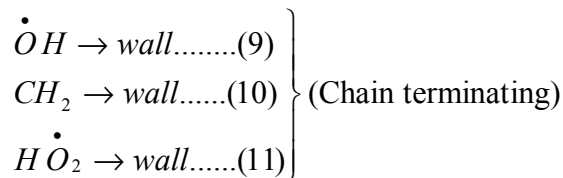
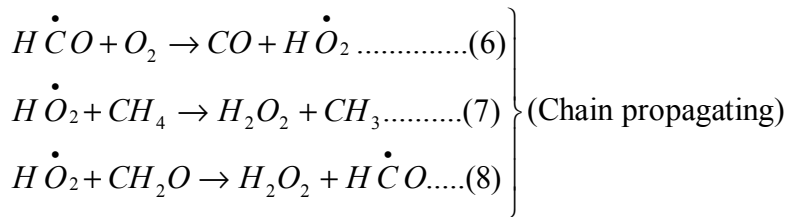
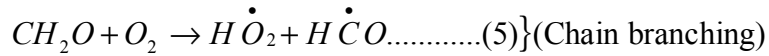
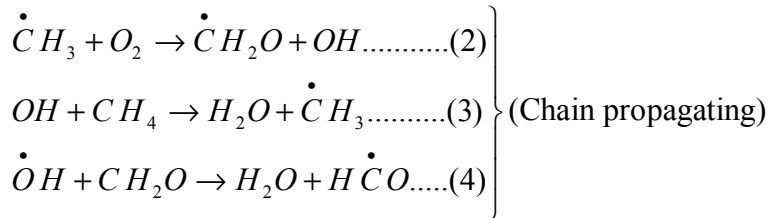
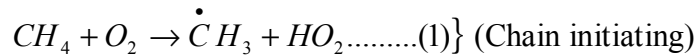
Table 2-2: Approximate flame temperatures of various Stoichiometric mixtures critical temperature 298(K).

Fuel	Oxidizer	Pressure(atm)	Temperature (K)
Acetylene	Air	1	2600 a
Acetylene	Oxygen	1	3410 b
Carbon monoxide	Air	1	2400
Carbon monoxide	Oxygen	1	3220
Heptane	Air	1	2290
Heptane	Oxygen	1	3100
Hydrogen	Air	1	2400
Hydrogen	Oxygen	1	3080
Methane	Air	1	2210
Methane	Air	20	2270
Methane	Oxygen	1	3030
Methane	Oxygen	20	3460

a: This maximum exists at $\phi = 1.3$.

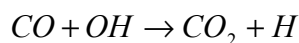
b: This maximum exists at $\phi = 1.7$.

Methane has certain oxidation characteristics that differentiate it from other hydrocarbons. The first bond ($C-H$) in Methane needs the largest portion of energy to break it in comparison with the other three bonds [12]. This is the reason why the ignition of methane at lower temperatures is harder to achieve in comparison with other hydrocarbons due to the fact the oxygen molecule attack would be slower at lower temperature than at high temperatures where it will have low kinetic energy. The simplest scheme that will explain the lower-temperature results of methane oxidation is the following:

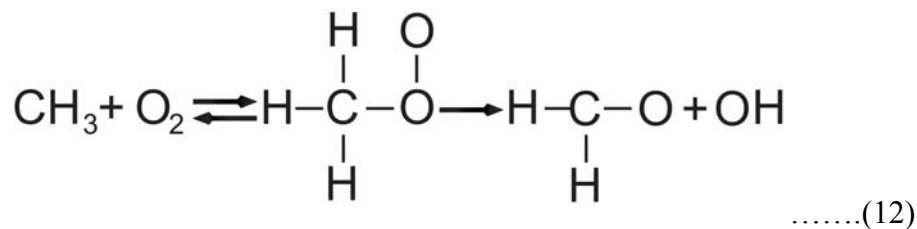


There is no H_2O_2 dissociation to OH radicals at low temperatures. H_2O_2 dissociation does not become effective until temperature reaches about 900K. As before, reaction 1 is slow. Reaction 2 and 3 are faster since they involve a radical and one of the initial reactants. The same is true for reactions 5, 6 and 7. Reaction 5 represents the necessary chain branching step. Reaction 4 and 8 introduce the formyl radical known to exist in the low temperature combustion scheme. Carbon monoxide is formed by reaction 6, and

water by reaction 3 and the subsequent decay of the peroxides formed. A conversion step of CO to CO_2 is not considered because the rate of conversion by reaction:



is too slow at the temperatures of concern here. It is important to examine more closely reaction 2, which proceeds through a metastable intermediate complex-the methyl peroxy radical-in the following manner:



At lower temperatures the equilibrium step is shifted strongly toward the complex, allowing the formaldehyde and hydroxyl radical formation. The structure of the complex represented in reaction 12 is well established. Recall that when O_2 adds to the carbon atom in a hydrocarbon radical, it forms about a 90deg bond angle.

Perhaps more important, however, is the suggestion Benson that at temperatures of the order of 1000k and above the equilibrium step in reaction 12 shifts strongly toward the reactants so that the overall reaction to form formaldehyde and hydroxyl cannot proceed[1].

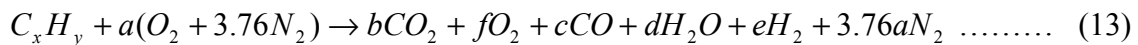
2. 2.Combustion Fundamentals:

2.2.1. Introduction:

This section will give the reader good back ground info on the fundamentals needed in this project study. Getting the equivalence ratio correctly will pave the way to make a comparison of the work that was found in the lab with other researchers work. Usually researchers illustrate the burning velocities as a function of the equivalence ratio. That's why this chapter has been given so much attention.

2.2.2. The combustion equation of an arbitrary hydrocarbon:

Here is the general equation [13] used for an arbitrary hydrocarbon by substituting the constants in x and y which are known once you know what fuel is used this will lead us to evaluate the constant (a) , (a) is easy to evaluate due to our knowledge of the equivalence ratio while conducting our experiment and x and y are known due to there relation with the fuel molecular formula.



$$\phi = \frac{x + 0.25y}{a} \dots\dots\dots(14)$$

The coefficients *b* *d* and *f* can be found by *C* – , *H* – and *O* – atom balances,

$$\begin{aligned} b &= x \\ c &= 0 \\ d &= y/2 \\ e &= 0 \\ b &= \frac{(1-\phi)}{\phi}(x + y/4) \end{aligned}$$

During Lab tests with the change of the air fuel ratio the constants change that's why for each given case to find the constants you have to solve the set of equations which can take a number of six equations with six unknowns.

2.2.3. There are cases which are fundamental for conducting the lab-work:

a-The Stoichiometric case:

Is the quantity of oxidizer which is just the amount needed to completely burn a quantity of fuel.

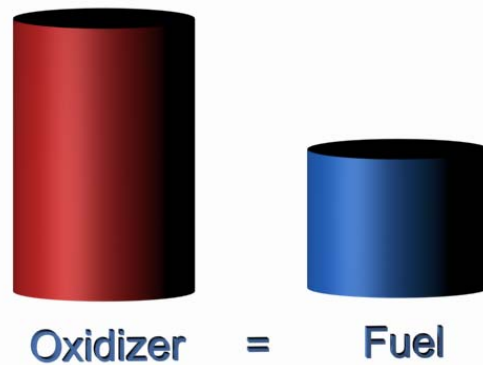
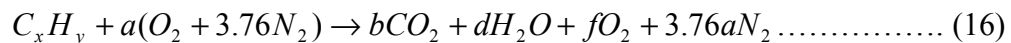


Figure 2-4: This shows the exact volume of oxidizer equals the exact volume of fuel which refers to the Stoichiometric ,but due to difference in density they don't have the same volume .

b- The Fuel Lean case:

If more than a Stoichiometric quantity of air is provided to the fuel.

$$\phi \leq 1 \dots\dots\dots(15)$$



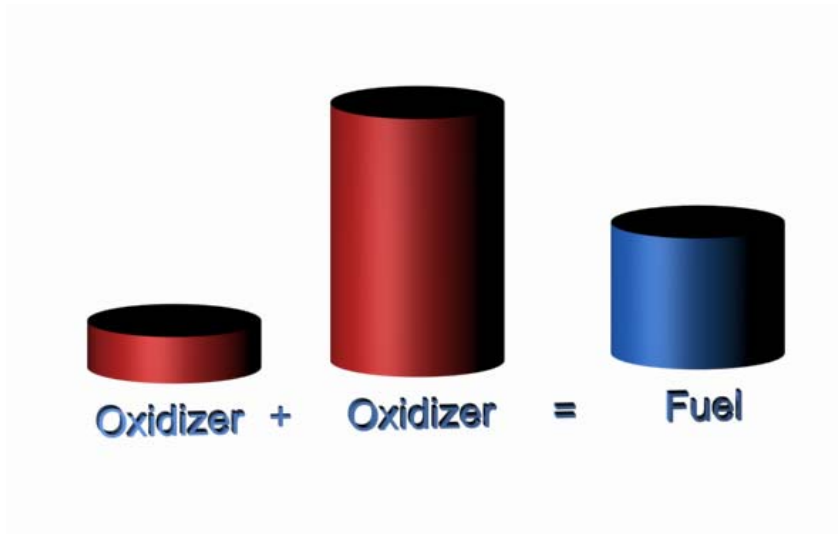


Figure 2-5: This shows the exact amount of fuel equals the excess amount of oxidizer which refers to the fuel lean case.

c- The Fuel Rich case:

Supplying less of the oxidizer to the fuel results in a fuel rich mixture.

$$\phi > 1 \dots\dots\dots(17)$$

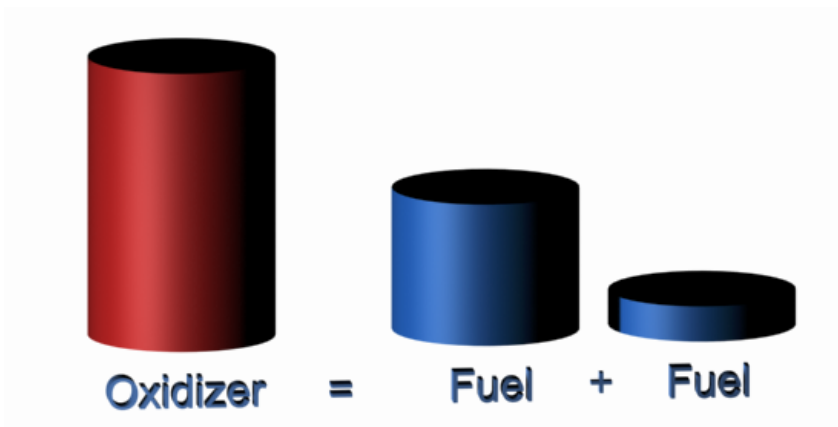
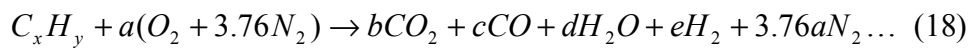


Figure 2-6: This shows the exact amount of oxidizer equals the exact amount of fuel in addition to it excess fuel this refers to the fuel rich case.

d- The Fuel Air Ratio:

Is the division of the mass of fuel over the mass of air in a certain condition

Where F is the mass of fuel (kg_{fuel}) and A is the mass of air (kg_{air}).

$$\alpha = (F / A) \dots\dots\dots (19)$$

So α unit should be (kg_{fuel} / kg_{air}).

e- The Stoichiometric Fuel Air Ratio:

Is the division of the exact mass of fuel over the exact amount of air needed for a the combustion of a fuel.

$$\alpha_{stoic} = (F / A)_{stoic} \dots\dots\dots(20)$$

So α unit should be (kg_{fuel} / kg_{air})_{stoic}.

f- The Equivalence Ratio:

Is used to indicate quantitatively whether a fuel-oxidizer mixture is rich ,lean ,or Stoichiometric.

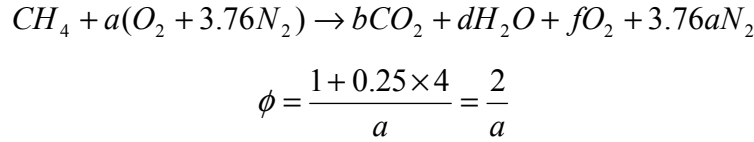
$$\phi = \frac{(A / F)_{stoic}}{(A / F)} = \frac{(F / A)}{(F / A)_{stoic}} = \frac{\alpha}{\alpha_{stoic}} \dots\dots\dots(21)$$

$$\% \text{ The Stoichiometric Air} = \frac{100\%}{\phi} \dots\dots\dots (22)$$

$$\% \text{ The Percent of Excess Air} = \frac{(1 - \phi)}{\phi} 100\% \dots\dots\dots (23)$$

2.2.4. The implementation of the fundamentals on a lab methane case:

The use of methane leads us to substitute $x = 1$ and $y = 4$ in the molecular form equation



So that means once a reading is made from the flow meters of the fuel (\dot{m}_{fuel}) and the air (\dot{m}_{air}) the value of a can be calculated starting from the fuel air ratio:

$$\alpha = (A/F) = \frac{\dot{m}_{air}}{\dot{m}_{fuel}}$$

Then using the equivalence ratio that is a function of the fuel air ratio for both the lab case and the Stoichiometric case:

$$\phi = \frac{(A/F)_{stoic}}{(A/F)} = \frac{(F/A)}{(F/A)_{stoic}}$$

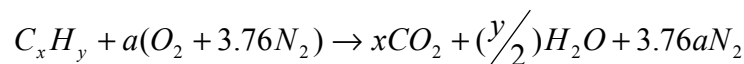
The problem has two unknowns for one equation that leads to the following step of finding the Stoichiometric fuel air ratio.

For a Stoichiometric case and ease of calculation we assume the simplified composition for air is 21% O_2 and 79% N_2 (by volume) i.e., that for each mole of O_2 in air, there are 3.76 moles of N_2 .

$$\alpha_{stoic} = (F/A)_{stoic} = \frac{4.76a}{1} \frac{MW_{air}}{MW_{fuel}}$$

Where MW_{air} and MW_{fuel} are the molecular weights of the air and fuel.

So for our case Methane is CH_4 so for a hydrocarbon given by the following equation



Where:

$$a = x + y/4 = 2$$

And:

$$MW_{air} = 29$$

$$MW_{fuel} = 16$$

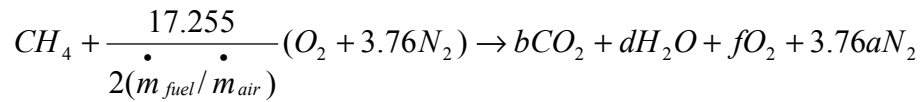
$$(F/A)_{stoic} = \frac{4.76a}{1} \frac{MW_{air}}{MW_{fuel}} = \frac{9.52 \times 29}{1 \cdot 16}$$

$$(F/A)_{stoic} = 17.255 \text{ (kg}_{fuel} / \text{kg}_{air} \text{)}$$

$$\phi = \frac{2}{a} = \frac{(F/A)}{(F/A)_{stoic}}$$

$$a = \frac{(F/A)_{stoic}}{2(F/A)}$$

So for the studied case the final equation should be:



By solving the four equations with the four unknown the studied case chemical equation can be found .

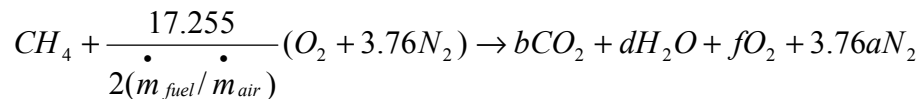
$$\frac{17.255}{2(\dot{m}_{fuel} / \dot{m}_{air})} = 2b + d + f$$

$$3.76 \frac{17.255}{2(\dot{m}_{fuel} / \dot{m}_{air})} = 2 \times 3.76a$$

$$1 = b$$

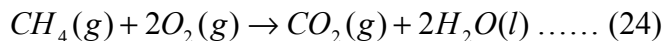
$$4 = 2d$$

Then we would substitute them into the equation:



2.2.5. The heat of combustion for Methane:

The heat of combustion is the difference in enthalpy. The method used to measure it is measured by pressurizing a strong metal reaction vessel (called a bomb) with a mixture of methane and oxygen gas.



The vessel is immersed in a calorimeter filled with water. An ignition source is used, which is an electrical wire. A current is passed through the wire (a fine iron wire), which ignites the wire and the fuel air mixture.

The heat balance for the experiment is as follows:

$$0 = q_{cal} + q_{wire} + q_{comb} \dots\dots (25)$$

The heat flow through the calorimeter q_{cal} can be calculated by multiplying the heat capacity of the calorimeter with temperature difference between the initial and the final temperature after the experiment had been conducted and the whole fuel mixture has been burnt, The amount of water in the calorimeter stays the same; that means that C_{cal} is the combination of the heat capacities of the calorimeter, the water, and the bomb itself.

The ignition wire burns and releases heat this heat should not be neglected in the calculations. Note: this heat is treated separately for each time the experiment is conducted due to the fact that the amount of wire used changes from each experiment.

The heat released by the combustion reaction is q_{comb} which is also connected to the molar internal energy of the combustion process:

$$\Delta E_{comb} = \frac{q_{comb}}{n_{methane}}$$

Large amounts of oxygen are used in the Combustion experiments, because methane is the limiting reactant. Once the methane is finished there is no more heat release not forgetting that the whole process occurs at constant pressure.

The molar enthalpy of combustion (ΔH_{comb}) is related to the molar internal energy of combustion (ΔE_{comb}) by the equation 26. (Note: that $H = E + PV$ and the volume is constant when the experiment is conducted.)

$$\Delta H_{comb} = \Delta E_{comb} + V\Delta P = \Delta E_{comb} + R\Delta(nT) \dots\dots\dots (26)$$

The total moles of gas-phase specie is n. *(The assumption implicit in this analysis is that the volume occupied by solids and liquids is negligible compared to the volume of the bomb and thus condensed phases do not contribute significantly to changes in pressure.)* The term $R\Delta(nT)$ is small compared with ΔE_{comb} , and that's why ΔH_{comb} is usually very close to ΔE_{comb} .

For example," suppose the bomb has a volume of 271 mL and initially contains 10. mmole of methane and excess oxygen at 25.0 °C. Further suppose that after combustion the system reaches a temperature of 27.0 °C, at which time 10.0 mmole of methane and 20.0 mmole oxygen have reacted to form 10.0 mmole of carbon dioxide and 20.0 mmole of liquid water. The initial $n T$ for gaseous species is 8.94 K mole and the final value is 3.00 K mole. The term $R \Delta(n T)$ is thus -49.4 J per 10.0 mmole methane or -4.94 kJ mole⁻¹ [20]. Compare this quantity with the molar heat of combustion as determined in the experiment described below.

Combustion reactions are often used to calculate the molar enthalpies of formation. For the methane case, the standard molar enthalpy of combustion for methane can be expressed in terms of the standard molar enthalpies of formation of the reactants and products equation 27:

$$\Delta H_{comb}^0 = 2\Delta H_{fwater}^0 + \Delta H_{f\text{methane}}^0 - 2\Delta H_{foxygen}^0 \dots\dots\dots(27)$$

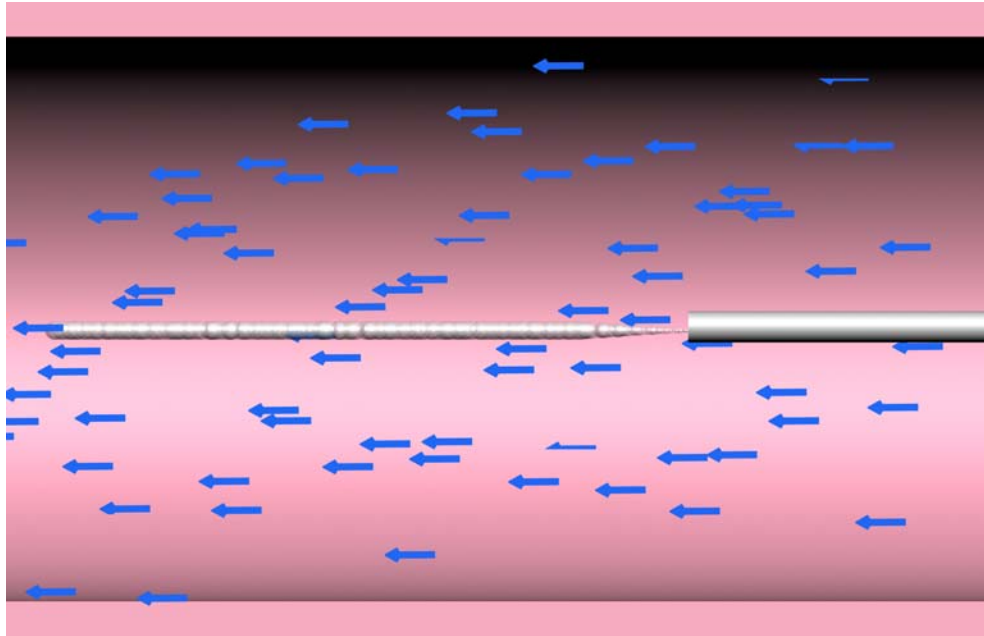
ΔH_{comb}^0 : is measured experimentally.

$\Delta H_{foxygen}^0 = 0$, because oxygen is a pure element.

2.3. The Study of Turbulence:

2.3.1. Basics of Turbulent Flow:

Whether a flow is laminar or turbulent depends of the relative importance of fluid friction (Viscosity) and flow inertia. The ratio of inertial to viscous forces is the Reynolds number. Given the characteristic velocity scale, U , and length scale, L , for a system, the Reynolds number is $Re = uL/\nu$, where ν is the kinematic viscosity of the fluid.



Laminar Flow

Figure 2-7: Tracer transport in laminar flow.

From figure we can see the straight, parallel blue arrows which are streamlines, which are everywhere parallel to the mean flow. In laminar flow the fluid particles follow the streamlines, as shown by the linear white dye trace in the laminar tube region injected by the white tube on the right hand side.

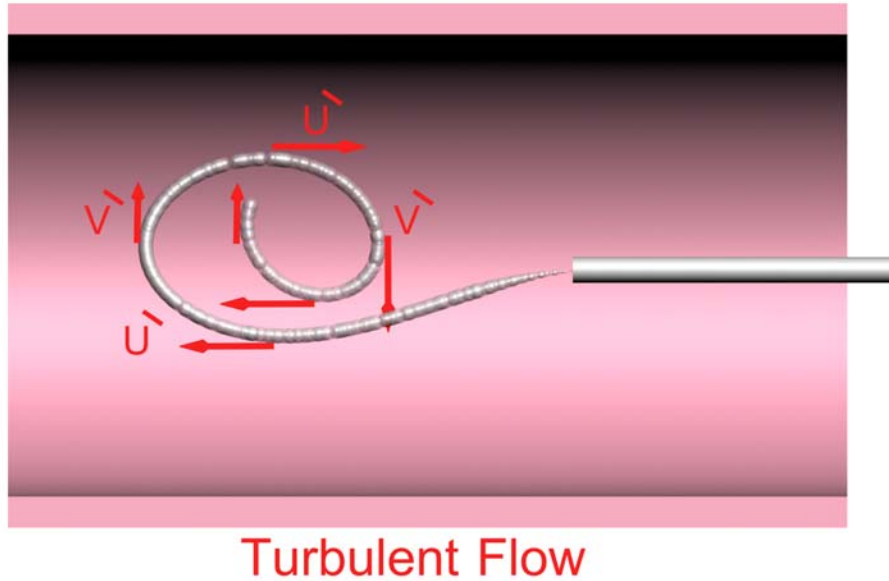


Figure 2-8: Tracer transport in turbulent flow.

Figure 2-8 shows the velocity vectors for velocity fluctuations for an eddie in a turbulent flow. In turbulent flow eddies of many sizes are superimposed onto the mean flow. When dye enters the turbulent region it traces a path dictated by both the mean flow (streamlines) and the eddies. Larger eddies carry the dye laterally across streamlines. Smaller eddies create smaller scale stirring that causes the dye filament to spread (diffuse) [10, 25].

The turbulent flow can be characterized qualitatively by

- 1- Irregularity in space and time (chaotic behavior with coherent structures)
- 2- Continuous spectrum of time and length scales
- 3- Large Reynolds numbers
- 4- Three-dimensionality
- 5- Domination of vortical motion
- 6- Intermittency
- 7- Enhanced mass and heat transfer

2.3.2. Turbulent flows are commonly characterized using statistical methods:

Characterizing Turbulence:

Turbulent eddies create fluctuations in velocity. As an example, the longitudinal (u) and vertical (v) velocity measured at point A in figure 2-8. Both velocities varying in time due to turbulent fluctuations. If the flow were steady ($u' = v' = 0$) and laminar then $u(t) = \bar{u}$ and $v(t) = \bar{v}$ for all time t, where the over-bar denotes a time average. For turbulent flow, however the velocity record includes both mean and turbulent component.

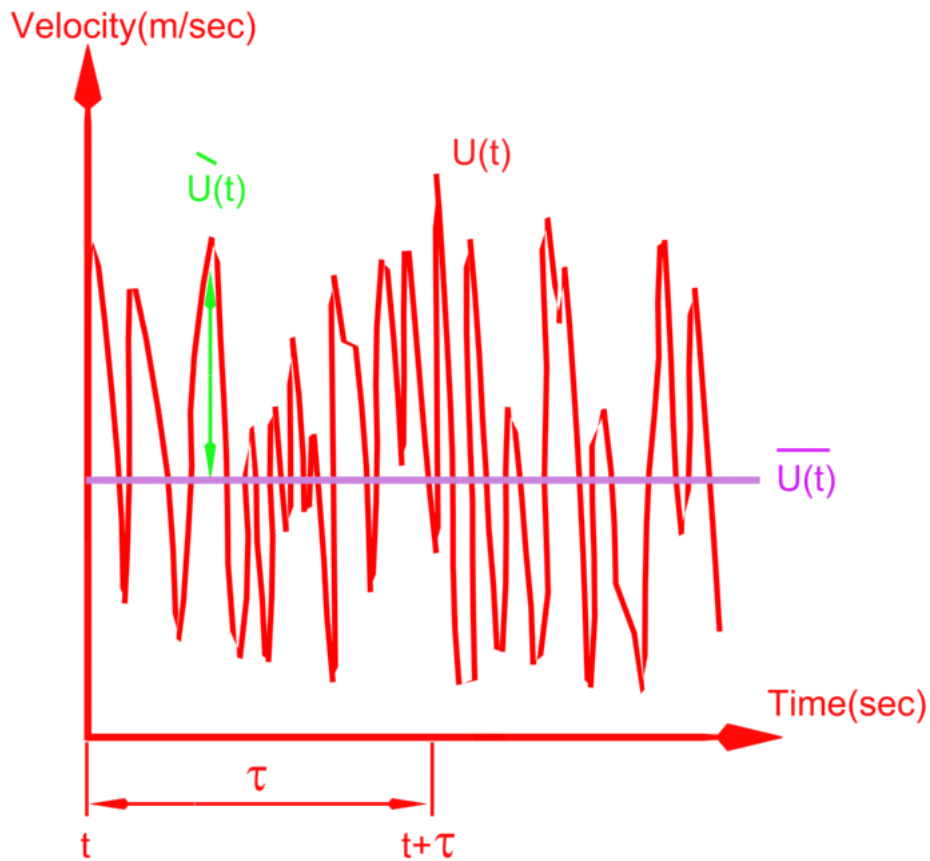


Figure 2-9: Velocity recorded at random point in figure 2-8.

The flow is decomposed as follows.

$$\begin{aligned}
 u(t) &= \bar{u} + u'(t) \\
 v(t) &= \bar{v} + v'(t) \quad \dots\dots\dots(28)
 \end{aligned}$$

Where \bar{u}, \bar{v} are the mean velocity value and $u'(t), v'(t)$ are the turbulent fluctuation.

This is commonly called a Reynolds decomposition.

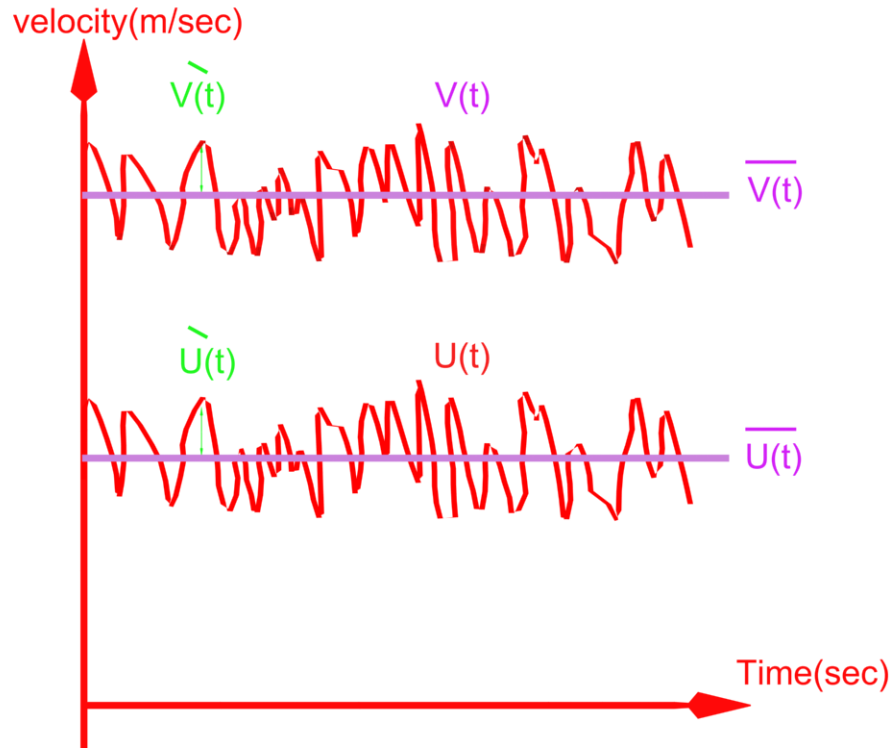


Figure 2-10: Velocity recorded at random point which has turbulence effects on both the x and y axis.

Because the turbulent motions associated with the eddies are approximately random, it is characterized using statistical concepts. In theory the velocity record is continuous and the mean can be evaluated through integration. However, in practice the measured velocity records are a series of discrete points, u_i . Below an over bar is used to denote a time average over the time interval t to $(t + T)$ as shown on figure 2-9, where T is much longer than any turbulence time scale, but much shorter than the time-scale for mean flow unsteadiness, e.g. water hammer.

Mean velocity:

The mean velocity is given using equation (29).

$$\bar{u} = \int_t^{t+T} u(t) dt = \frac{1}{N} \sum_1^N u_{(t)} \dots\dots\dots(29)$$

Where: $\int_t^{t+T} u(t)dt$ is a continuous record and $U = \frac{1}{N} \sum_1^N u_{(t)}$ is a discrete, equally-spaced parts.

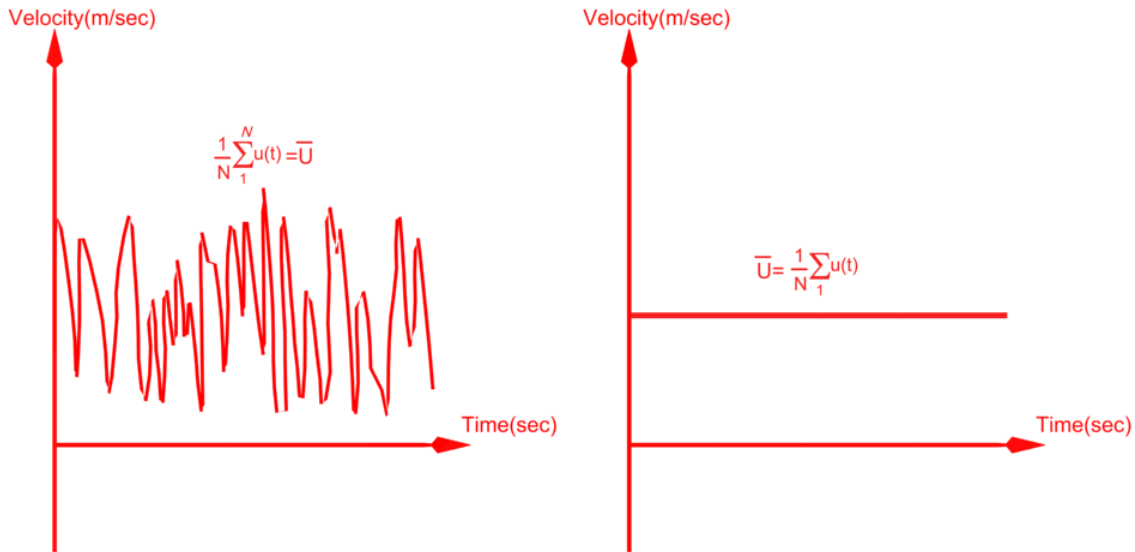


Figure 2-11: The transfer of data from a none uniform structure(graph shown on the left) to a uniform structure(graph on the left).

Turbulent Fluctuation:

Turbulence fluctuation is given by equation (28) where $u'(t)$ is a continuous record is.

$$u'(t) = u(t) - \bar{u} \dots\dots\dots(30)$$

Turbulence Strength:

Turbulence strength is given by equation (2-4):

$$U_{rms} = \sqrt{(u'(t)^2)} = \left[\frac{1}{N-1} \sum_1^N (u'_{(t)})^2 \right]^{\frac{1}{2}} \dots\dots\dots(31)$$

The turbulence strength is obtained using the equation above.

Turbulence Intensity:

Turbulent flow is often described in terms of intensity, which is a measure of the importance of the fluctuating velocity relative to the mean velocity.

For parallel flow intensity, or level of turbulence, is defined quantitatively by the expression:

$$T = \frac{\sqrt{1/3((u'_x)^2 + (u'_y)^2 + (u'_z)^2)}}{\bar{u}_x} \dots\dots\dots (32)$$

In the special case called isotropic turbulence, the three mean-fluctuating velocities are equal so that the equation is simplified to:

$$T = \frac{\sqrt{(u'_x)^2}}{\bar{u}_x} \dots\dots\dots (34)$$

Is the ratio between the turbulence strength and the mean velocity.

$$T = \frac{u_{rms}}{u} \dots\dots\dots (35)$$

The subscript .rms. stands for .root-mean-square... You should recognize the definition of u_{rms} given in (31) as the standard deviation of the set of random velocity fluctuations, $u'(t)$. Similar definitions apply to the lateral and vertical velocities, $v(t)$ and $w(t)$. A larger u_{rms} indicates a higher level turbulence. In the figure (2-12), both records have the same mean velocity, but the record on the left has a higher level of turbulence [6].

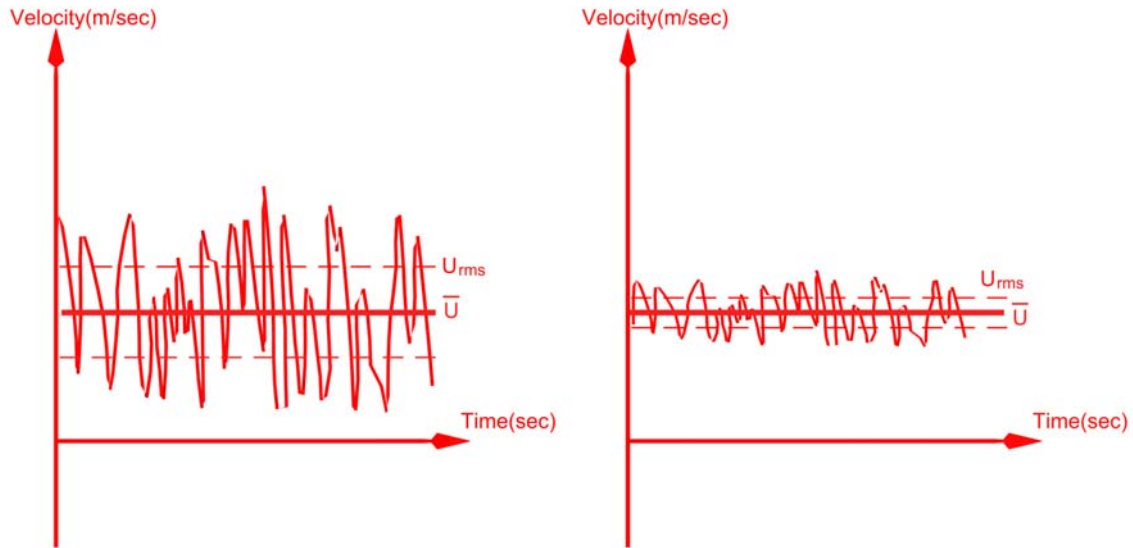


Figure 2-12: The effects of turbulence intensity and how it is shown graphically. The study of turbulence has been given a priority due to the need to understand the lab data measurements were fluid dynamics data is provided.

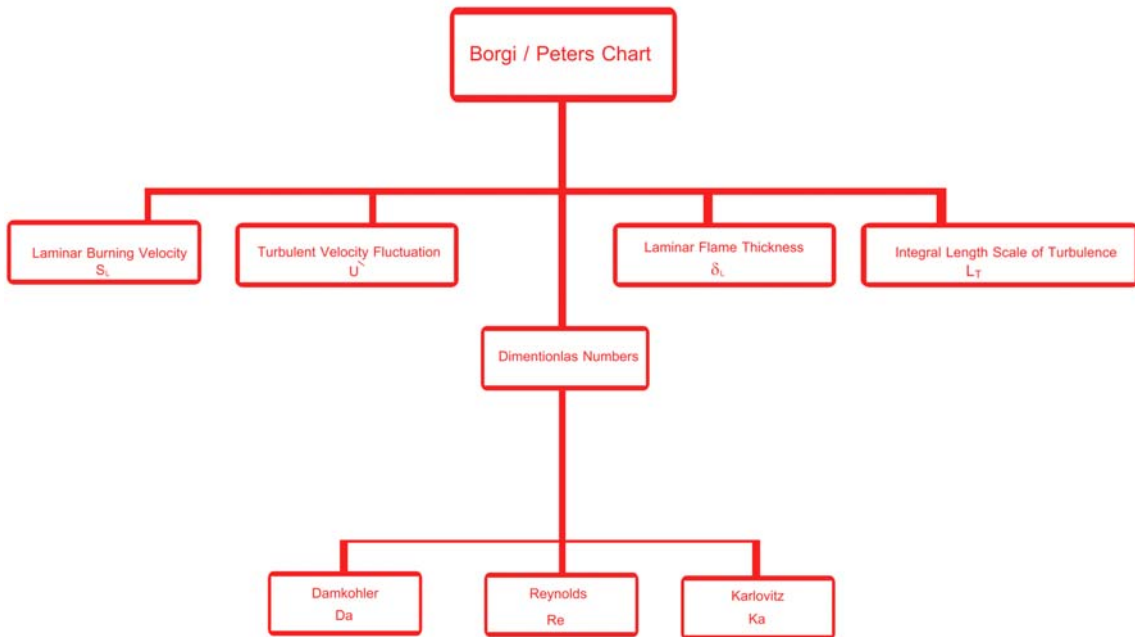


Figure 2-13: The turbulence fluctuating plays a vital role in the Borgi /Peters chart.

2.4.1. Flames:

Since the time man was on earth fire has been some thing that interested humans due to his motivation to satisfy his daily needs such as for cooking heatingetc, by time his knowledge and understanding of flames grew more and more when the industrial revolution happened and the use of steam engines came and into use scientists became more aware of the need to quantify parameters related to fuel and burning.

It is important due to that flames burn all in a very similar way once we can understand one we can understand the rest as can be shown the similarity of the flames.



Figure 2-14: The image of a number of flames which illustrate the similarity of flames in the way they burn and there flame structure similarity [19].

Due to the importance and relationship of the laminar burning velocity with the Borghi chart it is crucial to know what parameters have an effect on the laminar burning velocity Not forgetting having the basic knowledge and understanding of the flame structure.

2.4.2. Premixed Flames:

Premixing air and fuel and providing an ignition source will result in an exothermic flame (exothermic describes a process or reaction that releases energy in the form of heat), this flame will burn continuously on the condition (self-propagate) of providing it with the right conditions of temperature and temperature and a continues source of air-fuel mixture.

2.4.3. Mass and energy conservation in premixed flames:

To describe this case some assumptions have to be taken in account, the effect of the reaction tube with regard to loss of heat or reactive species or viscous drag on the flowing gas may be neglected in an ideal propagation of a premixed flame in a tube. The fuel air mixture is considered to be laminar and uniform across the diameter so that the flame front is planner and perpendicular to the flow.

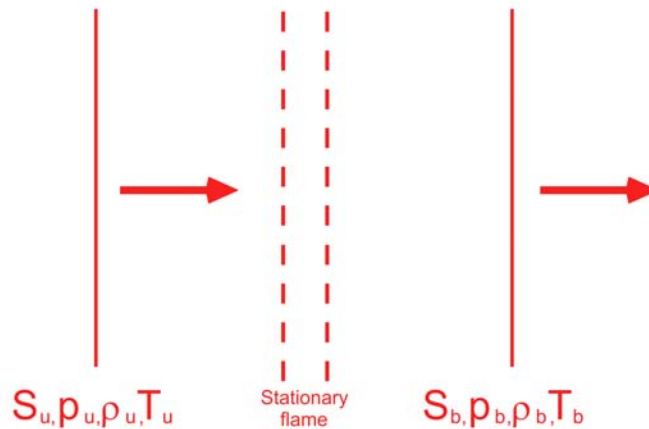


Figure 2-15: the description of a stationary shock wave, subscripts 1 and 2 refer to the pre-and post-shock gases respectively.

The flow rate is equal to in a magnitude but opposite in sign to the burning the burning velocity, so that the flame is stationary.

Conservation of mass:

$$\rho_u S_U = \rho_b S_b = \dot{m} \dots\dots\dots(36)$$

Where \dot{m} is the (constant) mass flow rate per unit area through the transition ,S is the velocity of the gas stream and ρ is its density .The subscript U and b refer to unburned

and burned and burned gas ,respectively. This terminology follows convention in which S_U is defined as the burning velocity.

Conservation of momentum (expressed as flux):

The pressure and density must change in the same direction.

$$p_u + \rho_u S_U^2 = p_b + \rho_b S_b^2 \dots\dots\dots (37)$$

$$m = \frac{(p_u - p_b)}{(S_b - S_u)} \dots\dots\dots (38)$$

As a result there are two types of process possible, the first is called detonations, in which both pressure and density increase across the transition, the second is called deflagrations (i.e. combustion waves and flames), in which pressure and density decrease across the transition. Deflagrations are low-velocity expansion waves in which chemical reaction is brought about by heat and mass transport [5].

2.4.4. Adiabatic Flame Temperature:

In the study of combustion, there are two types of adiabatic flame temperature depending on how the process is completed: constant volume and constant pressure. The constant pressure adiabatic flame temperature (this is the case that reflects the lab conditions) is the temperature that results from a complete combustion process that occurs without any heat transfer or changes in kinetic or potential energy. Its temperature is lower than the constant volume process because some of the energy is utilized to change the volume of the system (i.e., generate work in internal combustion engines). The constant volume adiabatic flame temperature is the temperature that results from a complete combustion process that occurs without any work, heat transfer or changes in kinetic or potential energy. This is the maximum temperature that can be achieved for given reactants because any heat transfer from the reacting substances and/or any incomplete combustion would tend to lower the temperature of the products.[13]

If a fuel-air mixture burns adiabatically at constant pressure, the absolute enthalpy of the products at the final state ($T = T_{ad}$, $P = 1atm$)

$$H_{reac}(T_i, P) = H_{prod}(T_{ad}, p) \dots\dots (39)$$

Or, equivalently, on a per-mass-of mixture basis:

$$h_{reac}(T_i, P) = h_{prod}(T_{ad}, p) \dots\dots (40)$$

The first-law statement the top equation what is called the constant pressure adiabatic flame temperature. Conceptually, the adiabatic flame temperature is simple: however, evaluating this quantity requires knowledge of the composition of the combustion products. At typical flame temperature, the products dissociate and the mixture comprises many species [3].

2.4.5. Structure of the ideal, adiabatic, one dimensional, laminar, premixed flame:

In the detailed structure of the flame is composed of four zones as follows cold reactants, preflame, reaction and product zone. The temperature (illustrated in orange) increases smoothly from the initial to the final state. The intermediate (shown in red) and product (shown in pink) concentrations will increase through the first to two zones and later becomes steady, whereas the concentrations of the fuel air mixture (shown in green) must show a corresponding decrease.

The hatched region (reaction zone) on the figure shows the visible part of the flame. The emission is due largely to electronically excited species, such as CH , CN , C_2 , CHO , and also CO_2 emitting light, as they return to their ground state.

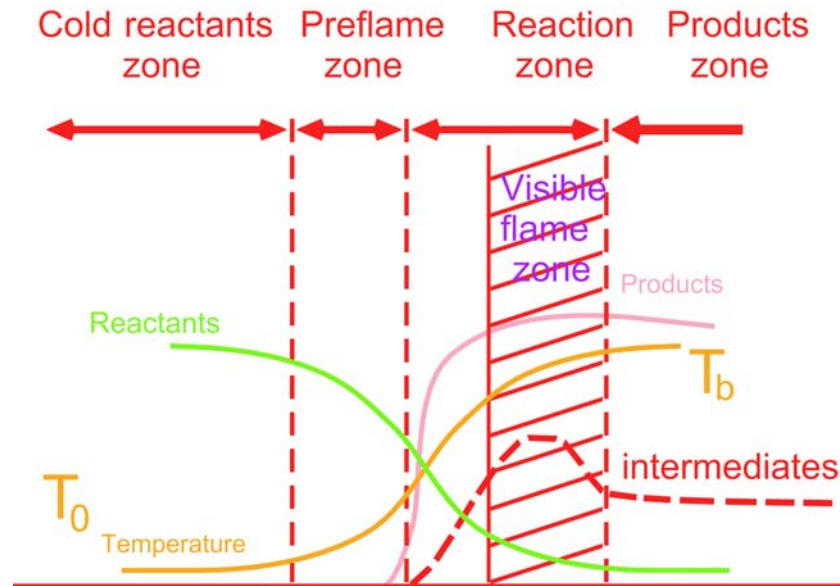


Figure 2-16: concentration and temperature profiles associated with a one dimensional, premixed, adiabatic flame.

An element of the flowing gas mixture can receive heat in two ways, either from chemical reactions occurring within it or by conduction from the hotter gas ahead of it.

Two distinct regions can be recognised, which are attributed to these processes.

Beginning at low temperature T_0 , for any given cross-section, the heat flow into the cooler region owing to conduction is greater than the corresponding heat loss because the gradient is steeper on the high temperature side T_b . Beyond the point of inflexion what happens is the reverse; the heat loss rate exceeds the heat gain rate. However, at this higher temperature the reaction rate has increased sufficiently for a significant amount of heat to be produced by chemical reaction. The temperature therefore continues to increase through the flame although at a progressively slower rate. It eventually reaches a constant value when all the fuel has been consumed and reaction has ceased. Parallel behaviour also occurs in the reactant concentration profile, the major loss initially being diffusion of fuel into the flame but subsequently being consumption by chemical reaction. The concentration of all species in the post-flame zone must approach that defined by thermodynamic equilibrium at the prevailing temperature. The difficulty in the reaction zone is that species may not reside there for a sufficiently long period for thermodynamic equilibrium to be established. Since the predominant termination

reactions are termolecular processes, and therefore they are relatively slow, the species most affected and, by implication, held at concentrations above those at thermodynamic equilibrium, are the propagating free radicals. Since bimolecular interactions tend to be equilibrated, all other intermediate species tend to be enhanced to super-equilibrium concentrations [5].

2.4.6. The Laminar Flame Speed:

The laminar flame speed (Laminar burning velocity) S_L : is defined as the velocity at which unburned gases move through the combustion wave in the direction normal to the wave surface as can be seen on figure 2-16.

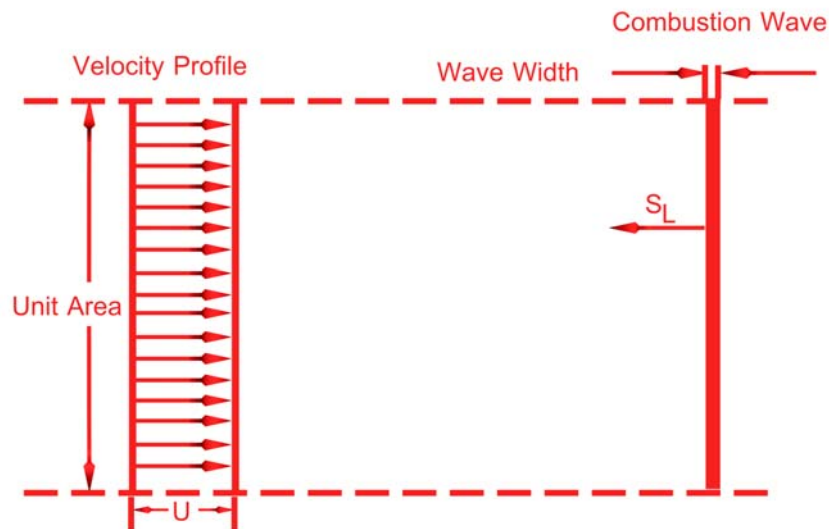
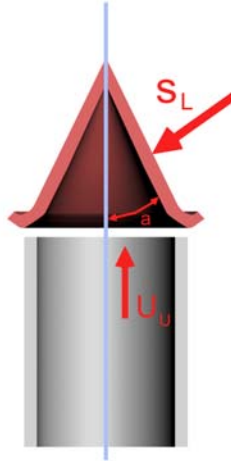


Figure 2-17: shows the burning velocity vector which is normal to the wave surface.



Velocity vectors in a bunsen core flame

Figure 2-18: velocity vectors in a Bunsen core flame.

By taking a picture of the burning flame, the angle α can be found out and by reading the flow meter (Q is also known) and using the continuity equation we can find the speed U_u and using equation (42) we can find the laminar burning velocity.

$$Q = U_u A \dots\dots\dots(41)$$

$$S_L = U_u \sin \alpha \dots\dots\dots(42)$$

This is some thing similar students are taught in fluid mechanics, laminar and turbulent flows is the flow that can be characterized by using a Reynolds number which we can also use in flame characterization with the assistance with other Dimensionless numbers such as the Damköhler Lewis..... etc with the help of the Borghi chart which is described in detail later .

2.4.7. Laminar Flame Structure

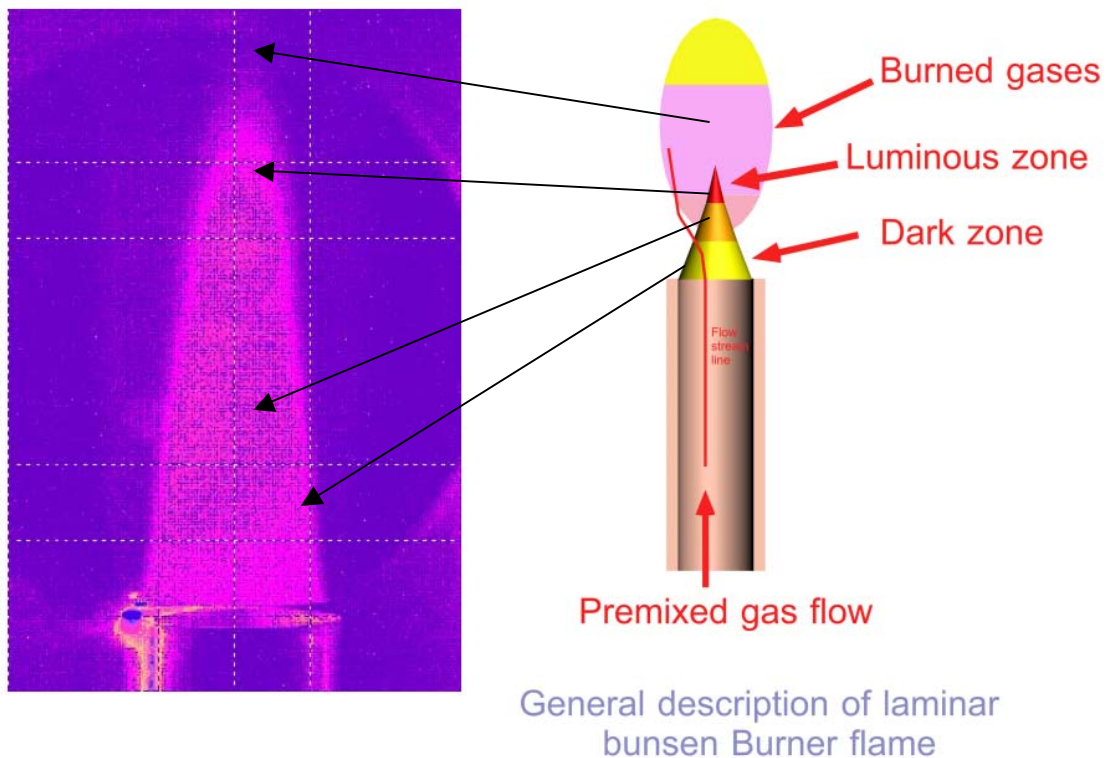


Figure 2-19: General description of laminar Bunsen burner flame.

What we can see is that the fuel gas entering the burner induces air into the tube surroundings. As the fuel and air flow up the tube, they mix and before the top of the tube is reached, the mixture is completely homogeneous. The flow velocity in the tube is considered to be laminar and the velocity across the tube is parabolic nature. Thus the flow velocity near the tube wall is very low. This low flow velocity is a major factor, together with heat losses to the burner rim, in stabilizing the flame at the top. The yellow zone designated in the figure 2-18 is the unburned premixed gases before they enter the area of the luminous zone where reaction and heat release take place. The luminous zone is less than 1mm thick. More specifically, the luminous zone (which looks like a purple cap on the top of the flame on the left hand picture on figure 2-18) is that portion of the reacting zone in which the temperature is the highest: indeed, much of the reacting and heat release takes place in this zone. The colour of the luminous zone changes with fuel-air ratio. For hydrocarbon-air mixtures that are fuel-lean, a deep violet radiation due to excited CH radicals appears.

2.4.8. The Theory of Mallard and Le Chatelier:

Both scientists stated that the heat conducted from zone II in the figure shown below is equal to that necessary to raise the unburned gases to the ignition temperature (the boundary zones I and II) .

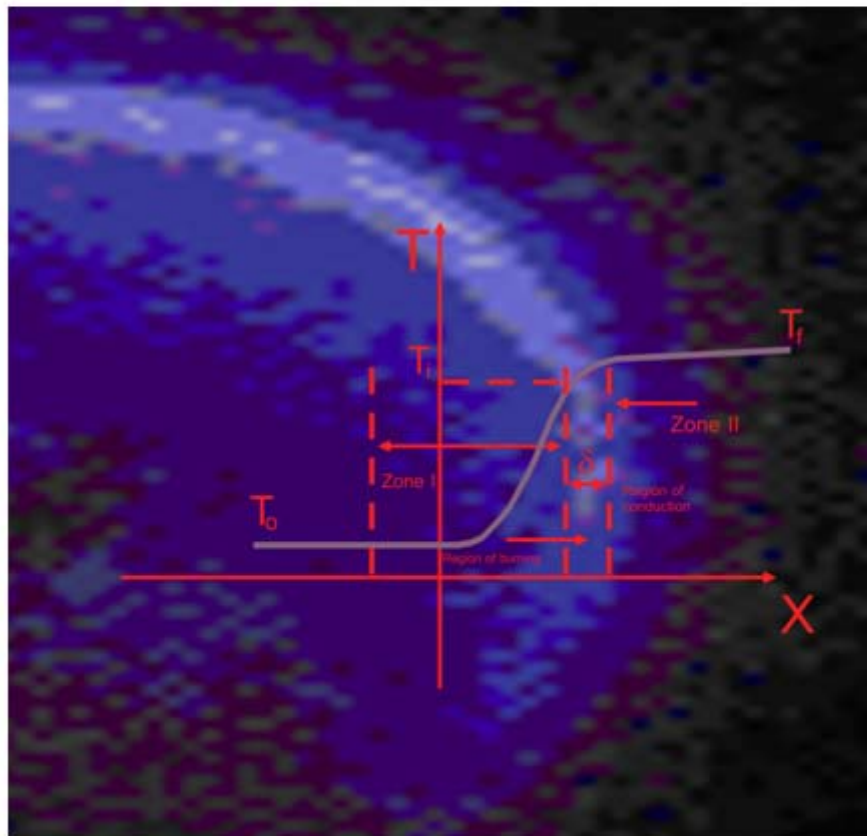
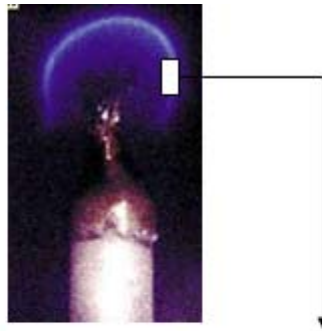


Figure 2-20: A small slice is taken from the flame to be studied.

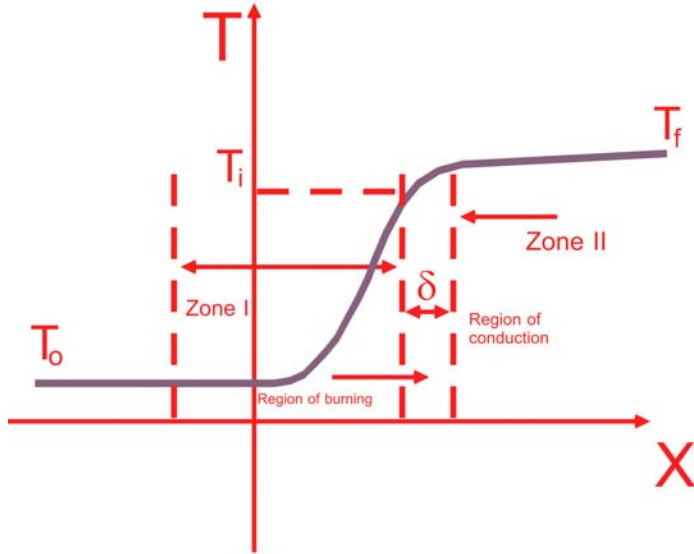


Figure 2-21: The balance between zone I and zone II.
 From balancing the Energy on both zones we have:

$$Q_{zoneI} = Q_{zoneII} \dots\dots\dots (43)$$

So from the enthalpy balance then becomes:

$$\dot{m} C_p (T_i - T_0) = \lambda \frac{(T_i - T_0)}{\delta} A \dots\dots\dots (44)$$

Since the problem is considered one-dimensional we use the following continuity equation:

$$\dot{m} = \rho A u = \rho S_L A \dots\dots\dots (45)$$

Because the unburned gases enter normal to the wave by definition

$$S_L = u \dots\dots\dots (46)$$

- T_f : Flame temperature
- T_i : Mixture temperature before the burning layer
- T_0 : The temperature of the gas mixture
- λ : The thermal conductivity of t
- ρ : Flame density mixture
- c_p : Specific heat capacity at constant pressure.
- δ : Flame thickness
- S_L : Laminar burning velocity
- \dot{w} : Reaction rate in terms of concentration

$$\rho u = \rho S_L = \dot{w} \delta \dots\dots\dots (47)$$

$$S_L = \left[\left(\frac{\lambda(T_f - T_i)}{\rho c_p (T_i - T_0)} \frac{1}{\delta} \right) \right] \dots\dots\dots(48)$$

$$S_L = \left[\left(\frac{\lambda(T_f - T_i)}{\rho c_p (T_i - T_0)} \frac{\dot{w}}{\rho} \right) \right]^{1/2} \dots\dots\dots(49)$$

The derivation process is expressed in more detail in reference [1]

2.4.9. Comments on the Mallard and Le Chatelier Theory:

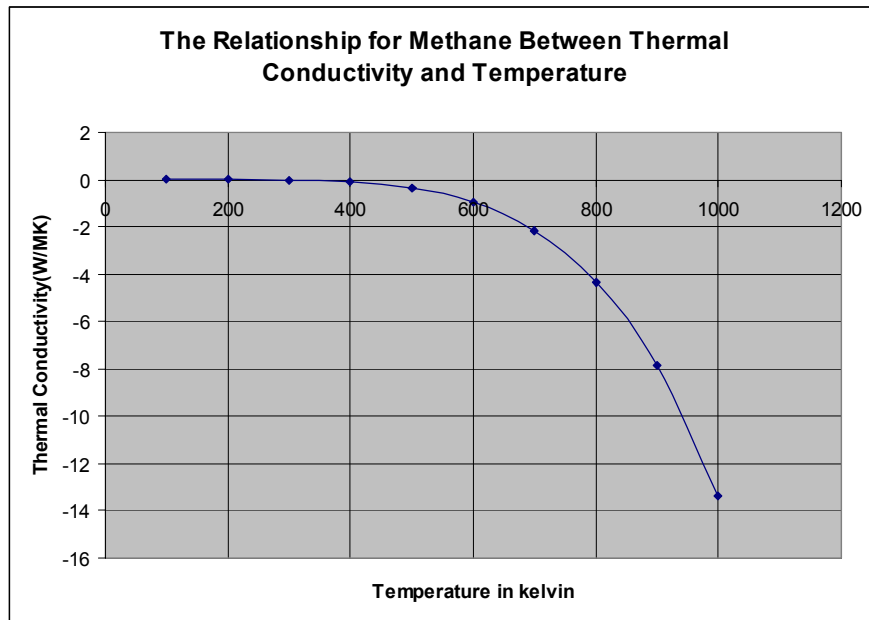
Comment 1: If a thorough look is taken at equation (48) on this ratio $\frac{T_f - T_i}{T_i - T_0}$ what is know is that usually $T_f = T_i$ so the bigger $T_i - T_0$ the smaller $T_f - T_i$ that leads us to the conclusion pre-heating the air-fuel mixture speeds up the laminar burning velocity and this is a practical method and its proof is that its been used in various aspects in combustion engines and In the energy production sector.

Comment 2: The flame thickness is some thing not easy to control were $\delta = \frac{\rho u}{\dot{w}}$ because controlling the reaction rate means change the amount of fuel and oxidizer our even change the type of fuel used which is an impractical idea. This thickness should be in an ideal range $\delta_{min} < \delta_{ideal} < \delta_{max}$ where if it is too small the flame will burnout and where it gets to thick it will also cause the chemical reactions to stop.

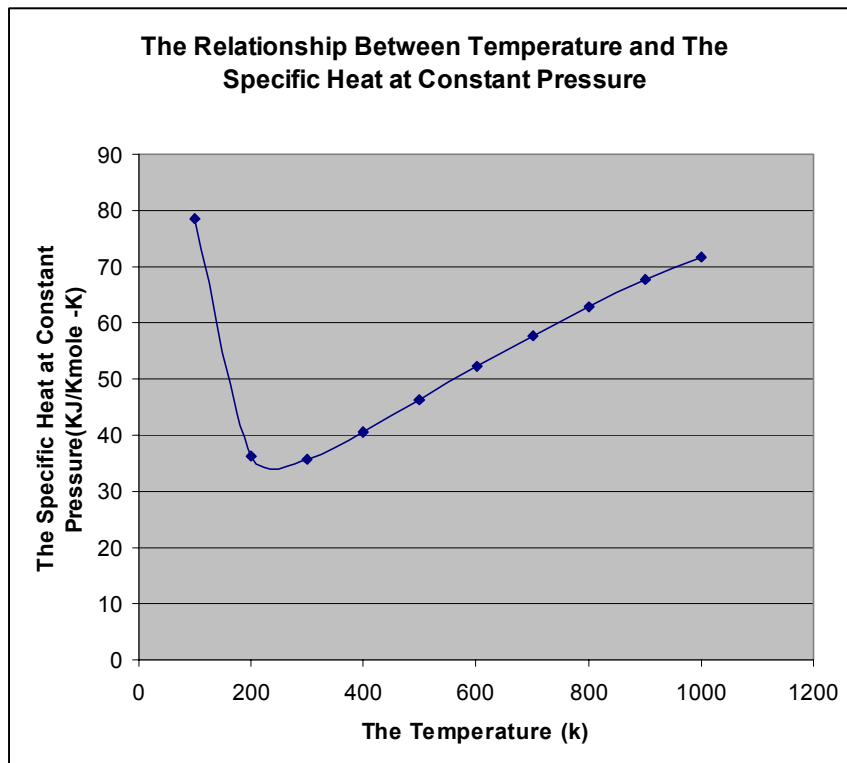
Comment 3: Another parameter is the gas mixture density $\rho = \rho_{air} r_{air} + \rho_{fuel} r_{fuel}$ which should be as as small as possible and this can be accomplished be raising the pressure which in return decreases the mixture density as can be seen in this

equation $\rho = \frac{T_{air}}{P_{air}} R_{air} r_{air} + \frac{T_{fuel}}{P_{fuel}} R_{fuel} r_{fuel}$.

Comment 4: The thermal conductivity of methane decreases with the rise in temperature until it starts to become an insulator at high temperatures.



Comment 5: The Heat Capacity at Constant Pressure of methane decreases till 200(K) then with the rise in temperature there is a rise in its heat capacity starts.



2.4.10. The Theory of Zeldovich Frank-Kamenetskii, and Semenov:

The three Russian scientists derived an expression for laminar flame speed by an important extension of the very simplified Mallard-Le Chatelier approach.

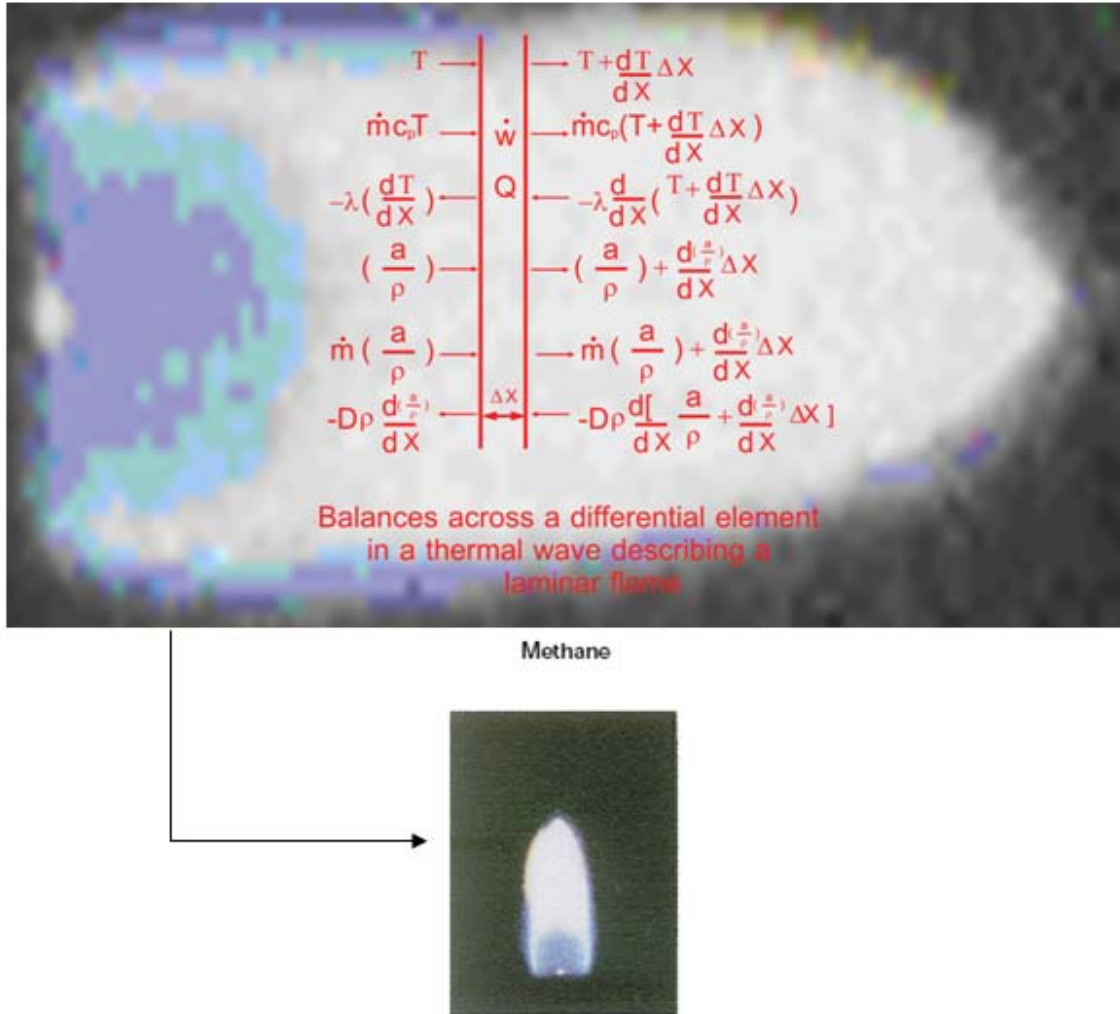


Figure 2-22: The balance across a methane flame differential element.

ρ_0 : The initial fuel air density before combustion.

λ : The thermal conductivity of the flame

T_f : The flame temperature.

T_0 : The initial temperature of the fuel air mixture before combustion

n_r : The number of moles of reactants

n_p : The number of moles of the products of reaction

R : Gas constant

E : Activation Energy

$(c_p)_f$: The specific heat value at constant pressure for the flame.

\bar{c}_p : The average specific heat value at constant pressure between T_0 and T_f .

D : Thermal diffusivity.

A: Constant.

B: Constant.

$$-(D\rho)\frac{d^2(T/\rho)}{dx^2} + m\frac{d(T/\rho)}{dx} + \dot{w} = 0 \dots\dots (50)$$

From the energy equation:

$$\frac{d^2T}{dx^2} + \frac{\dot{w}Q}{\lambda} = 0 \dots\dots\dots (51)$$

From solving this equation and relying on the boundary conditions that would lead us to the two equations:

$$\frac{dT}{dx} = \left(2 \frac{Q}{\lambda} \int_{T_i}^{T_f} \dot{w} dT \right)^{1/2} \dots\dots\dots (52)$$

$$\frac{dT}{dx} = \frac{\dot{m}c_p}{\lambda} (T_i - T_0) \dots\dots\dots (53)$$

We know that the temperature before the flame thickness is nearly the same as the flame temperature:

$$T_i \approx T_f$$

$$\frac{dT}{dx} = \frac{\dot{m}c_p}{\lambda} (T_f - T_0) \dots\dots\dots (54)$$

So we will get to this equation:

$$\frac{\dot{m}c_p}{\lambda} (T_f - T_0) = \left(2 \frac{Q}{\lambda} \int_{T_i}^{T_f} \dot{w} dT \right)^{1/2} \dots\dots\dots (55)$$

With the reliance on the three equation and the substitution of them in the top equation

$$\dot{w} = Z'e^{-E/RT} \dots\dots\dots (56)$$

$$\dot{m} = S_L \rho_0 \dots\dots\dots (57)$$

$$Q = c_p (T_f - T_0) \dots\dots\dots (58)$$

$$S_L = \left[\frac{2}{a_0} \left(\frac{\lambda}{\rho_0 c_p} \right) (Z'e^{-E/RT_f}) \left(\frac{ET_f^2}{E(T_f - T_0)} \right) \right]^{1/2} \dots\dots\dots (59)$$

$$\text{were } \frac{A}{B} = D\rho \left(\frac{\lambda}{c_p} \right)$$

First order equation:

$$S_L = \left(\frac{2\lambda(c_p)_f Z'}{\rho_0 \overline{c_p}^2} \left(\frac{T_0}{T_f} \right) \left(\frac{n_r}{n_p} \right) \left(\frac{A}{B} \right) \left(\frac{RT_f^2}{E} \right) \left(\frac{e^{-E/RT_f}}{(T_f - T_0)^2} \right) \right)^{1/2} \dots\dots\dots (60)$$

Second order equation:

$$S_L = \left(\frac{2\lambda(c_{p_f})^2 Z' \alpha_0}{\rho_0 \overline{c_p}^3} \left(\frac{T_0}{T_f} \right)^2 \left(\frac{n_r}{n_p} \right) \left(\frac{A}{B} \right)^2 \left(\frac{RT_f^2}{E} \right)^3 \left(\frac{e^{-E/RT_f}}{(T_f - T_0)^3} \right) \right)^{1/2} \dots\dots\dots (61)$$

The derivation process is expressed in more detail in reference [1]

2.5. Turbulent Reacting Flows and Turbulent Flames:

2.5.1. The Rate of Reaction in a Turbulent Field:

A very good example of how fluctuating parameters can have a big affect on a reacting system, one can examine how the mean rate of a reaction would differ from the rate evaluated at the mean properties when there are no corrections among these properties. in flow reactors ,time averaged concentrations and temperatures are usually measured ,and then rates are determined from these quantities .Only by optical techniques or very fast response sensors (Thermo couples are the proper instantaneous rate values could be measured, and these would fluctuate with time).The fractional rate of change of a reactant can be written as

$$\dot{w} = -k\rho^{n-1}Y_i^n = -Ae^{-E/RT} \left(\frac{P}{R} \right)^{n-1} T^{1-n} Y_i^n \dots\dots\dots (62)$$

Where the Y_i 's is the mass fractions of the reactants. The instantaneous change in rate is given by

$$dw = -A \left(\frac{P}{R} \right)^{n-1} \left[\left(\frac{E}{RT^2} \right) e^{-E/RT} T^{1-n} Y_i^n dT + (1-n) T^{-n} e^{-E/RT} Y_i^n dT + n e^{-E/RT} T^{1-n} Y_i^{n-1} dY \right]$$

$$d \dot{w} = \left(\frac{E}{RT} \right) \dot{w} \left(\frac{dT}{T} \right) + (1-n) \dot{w} \left(\frac{dT}{T} \right) + \dot{w} n \left(\frac{dY_i}{Y_i} \right)$$

or

$$\frac{d \dot{w}}{\dot{w}} = \left[\frac{E}{RT} + (1-n) \right] \left(\frac{dT}{T} \right) + n \left(\frac{dY_i}{Y_i} \right) \dots\dots\dots (63)$$

For nearly all hydrocarbons flame or reacting systems the overall order of reaction is about 2, E/R is some where 20,000K, and the flame temperature comes to about 2000K, that leads us to equation 64,

$$\left(\frac{E}{RT}\right) + (1 - n) \cong 9 \dots \dots \dots (64)$$

it is noticeable that the temperature variation is the dominant factor in turbulent reacting flows. The temperature effect comes into this situation having a relation with the specific reaction rate that is constant, the problem can be simplified by whether to consider the mean rate constant. This can be represented by the rate constant evaluated at the mean temperature.

In this hypothetical simplified problem one assumes further that the temperature T fluctuates with time around some mean represented by the form shown on equation 65:

$$\frac{T(t)}{\bar{T}} = 1 + a_n f(t) \dots \dots \dots (65)$$

where a_n is the amplitude of the fluctuation and $f(t)$ is some time-varying function in which

$$-1 \leq f(t) \leq +1 \dots \dots \dots (66)$$

And

$$\bar{T} = \frac{1}{\tau} \int_0^\tau T(t) dt \dots \dots \dots (67)$$

Over some time interval τ in conclusion $T(t)$ can be considered to be composed of $\bar{T} + T'(t)$, where T' is the fluctuating component around the mean temperature as can be seen on figure 2-22.

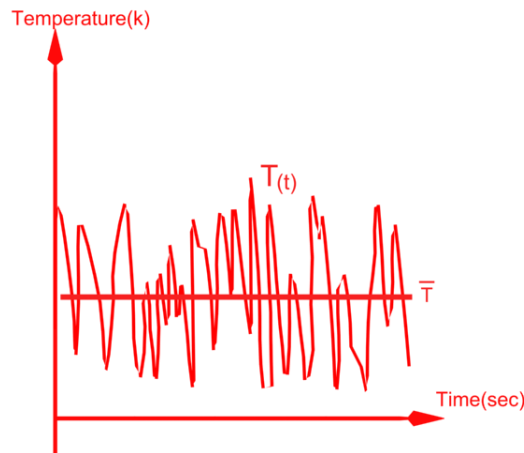


Figure 2-23: The temperature at different time intervals.

By ignoring the temperature dependence in the pre-exponential, one writes the instantaneous-rate constant as

$$K(T) = A \exp(-E/RT) \dots\dots\dots (68)$$

and the rate constant evaluated at the mean temperature as:

$$K(\bar{T}) = A \exp(-E/R\bar{T}) \dots\dots\dots (69)$$

Dividing the two expressions, one obtains:

$$K(T)/K(\bar{T}) = \exp\left[\frac{E}{R\bar{T}}\left[1 - \frac{\bar{T}}{T}\right]\right] \dots\dots\dots (70)$$

Obviously, then, for small fluctuations:

$$1 - \frac{\bar{T}}{T} = [a_n f(t)]/[1 + a_n f(t)] \approx a_n f(t) \dots\dots\dots (71)$$

The expression for the mean rate is written as:

$$\frac{\overline{K(T)}}{K(\bar{T})} = \frac{1}{\tau} \int_0^\tau \frac{k(T)}{K\bar{T}} dt = \frac{1}{\tau} \int_0^\tau \exp\left(\frac{E}{R\bar{T}} a_n f(t)\right) dt \dots\dots\dots (72)$$

$$\frac{\overline{K(T)}}{K(\bar{T})} = \frac{1}{\tau} \int_0^\tau \left[1 + \frac{E}{R\bar{T}} a_n f(t) + \frac{1}{2} \left(\frac{E}{R\bar{T}} a_n f(t)\right)^2 + \dots \right] dt \dots\dots\dots (73)$$

But recall

$$\int_0^\tau f(t) dt = 0 \text{ And } 0 \leq f^2(t) \leq 1 \dots\dots\dots (74)$$

Examining the third term in equation 73, it is apparent that

$$\frac{1}{\tau} \int_0^\tau a_n^2 f^2(t) dt \leq a_n^2 \dots\dots\dots (75)$$

Since the integral of the function can never be greater than 1. thus,

$$\frac{\overline{K(T)}}{K(\bar{T})} \leq 1 + \frac{1}{2} \left(\frac{E}{R\bar{T}} a_n\right)^2 \text{ Or } \Delta = \frac{\overline{K(T)} - K(\bar{T})}{K(\bar{T})} \leq \frac{1}{2} \left(\frac{E}{R\bar{T}} a_n\right)^2 \dots\dots\dots (76)$$

If the amplitude of the temperature fluctuations is of the order of 10% of the mean temperature, one can take $a_n \approx 0.1$; and if the fluctuations are considered sinusoidal, then

$$\frac{1}{\tau} \int_0^\tau \sin^2 t dt = \frac{1}{2} \dots\dots\dots (77)$$

Thus for the example being discussed,

$$\Delta = \frac{1}{4} \left(\frac{E}{RT} a_n \right)^2 = \frac{1}{4} \left(\frac{40000 \times 0.1}{2 \times 2000} \right)^2, \Delta \cong \frac{1}{4} \dots \dots \dots (78)$$

Or a 25% difference in the two rate constants.

This result could be improved by assuming a more appropriate distribution function of T' instead of a simple sinusoidal fluctuation as can be seen on figure 2-23; however, this example-even with its assumptions-usefully illustrates the problem. Normally, probability distribution functions are chosen. If the concentrations and temperatures are correlated, the rate expression becomes very complicated and therefore needs very powerful computers to conduct the calculations [1].

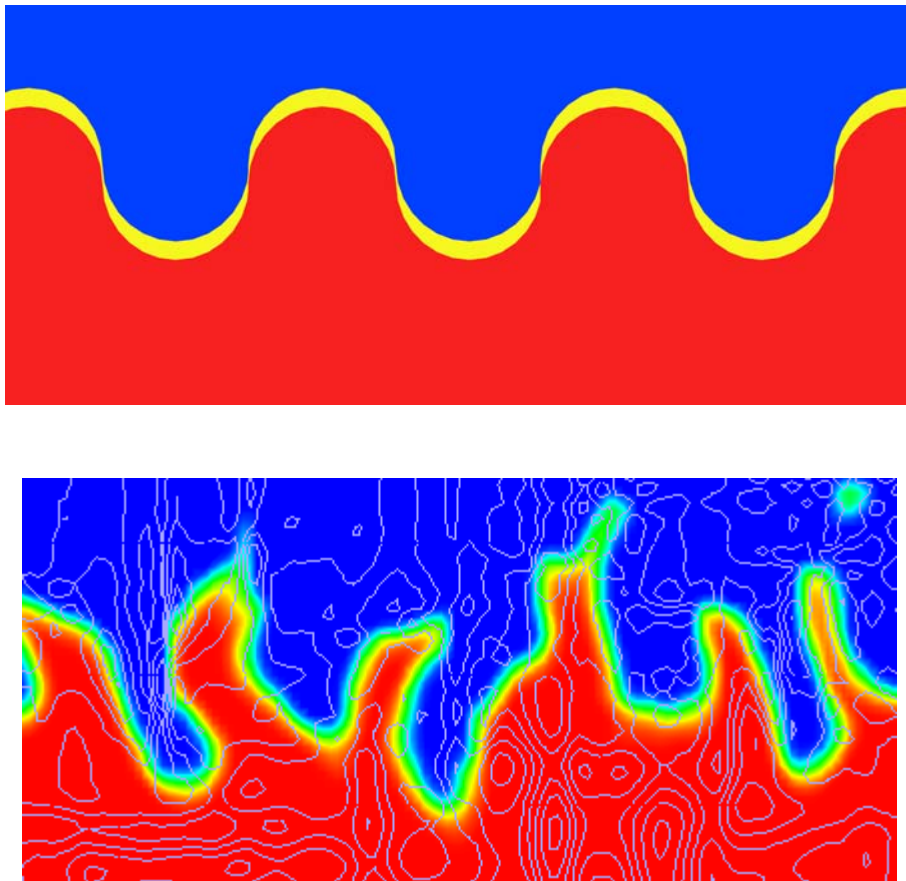


Figure 2-24: a comparison between a sinusoidal combustion wave at the top and a real combustion wave at the bottom [17].

Regimes of Turbulent Flame Speed: The previous section 2-5-1 epitomizes and gives a better understanding of how reacting mixtures can be affected by a turbulent field. To understand the detailed effect, one must understand the elements of the field of turbulence. When considering turbulent combustion systems in this regard a suitable starting point is the consideration of the quantities (fuel rich or a fuel lean case) that determines the fluid characteristics of the system.

2.5.2. The Turbulent Flame Speed:

Although a laminar flame speed S_L is a physicochemical and chemical kinetic property of the unburned gas mixture that can be assigned, a turbulent flame speed S_T is, in reality, the mass consumption rate per unit area divided by the unburned gas mixture density. This means, S_T must be a function of the properties of the turbulent field in which it exists and the method by which the flame is stabilized.

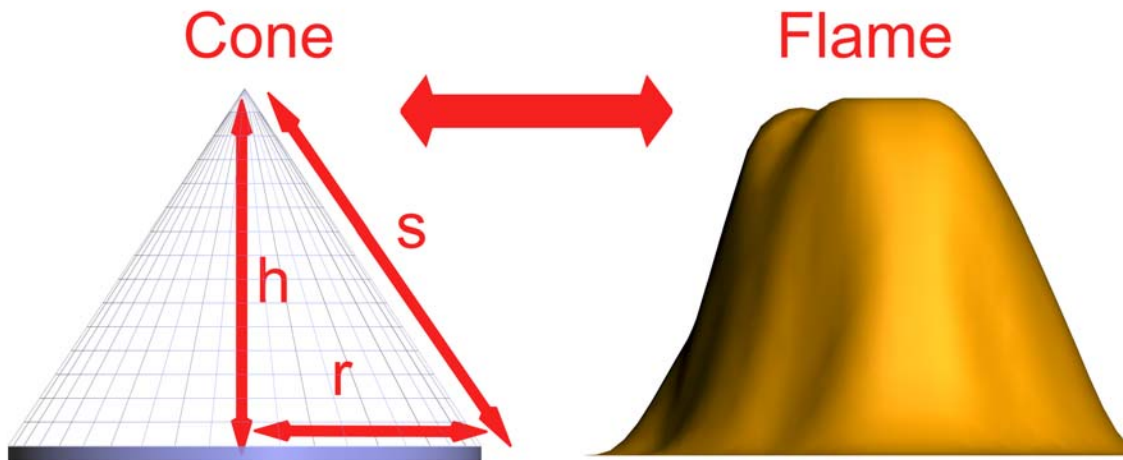


Figure 2-25: The approximation of the turbulent flame to a cone shape.

Area of the cone is:

$$A_{\text{conearea}} = r\pi s \dots\dots\dots (79)$$

Area of the base is:

The base area is neglected in the calculation because we are only interested in the cone area.

$$A_{\text{basearea}} = \pi r^2 \dots\dots\dots (80)$$

There for the formula is :

$$SA = r\pi s + \pi r^2 \dots\dots\dots (81)$$

u' : Turbulence intensity

t : Time

l_0 : The flame base diameter

h : Cone height

A_c : Cone area

A_b : Cone base area

S_L : Laminar burning velocity

S_T : Turbulent burning velocity

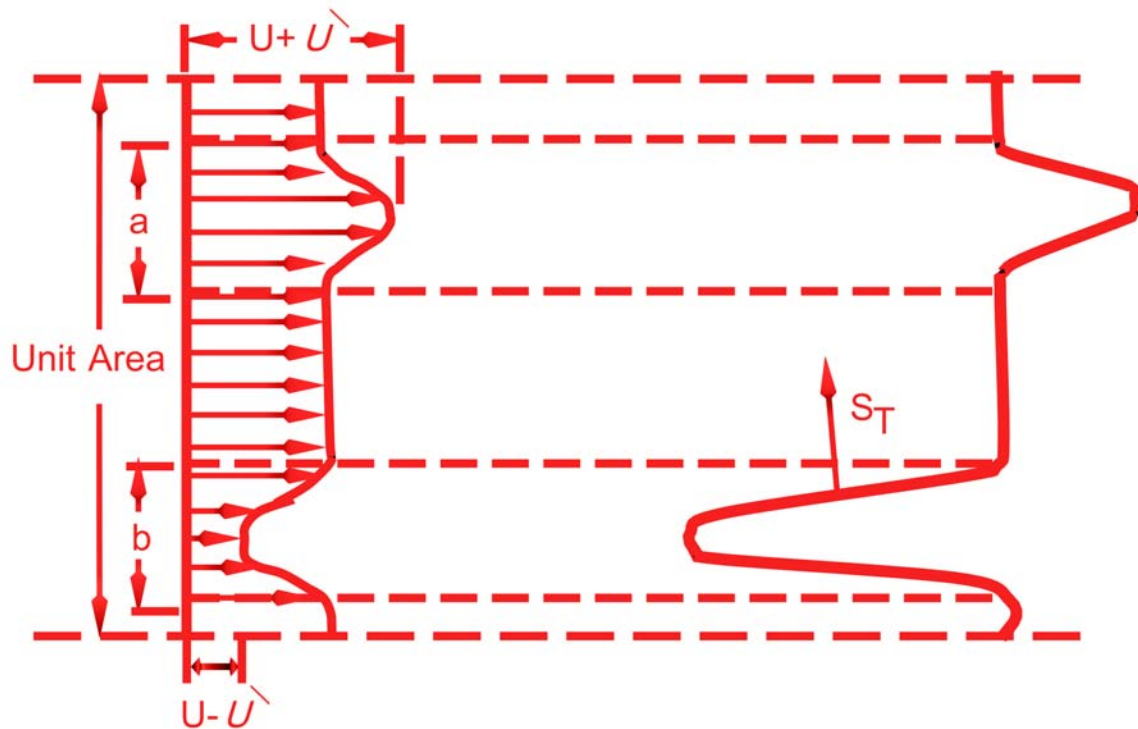


Figure 2-26: Model of combustion wave in a turbulent flow.

The turbulence intensity is the change of the height of the flame with time, This is shown in figure 2-26.

:

$$u' = \frac{h_2 - h_1}{t_2 - t_1} = \frac{h}{t} \dots\dots\dots (82)$$

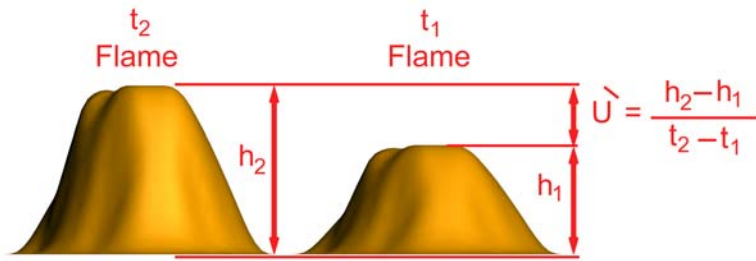


Figure 2-27: The difference with height at time intervals gives us the turbulence fluctuation.

$$S_L = \frac{\pi(l_0)^2}{4t} \dots\dots\dots (83)$$

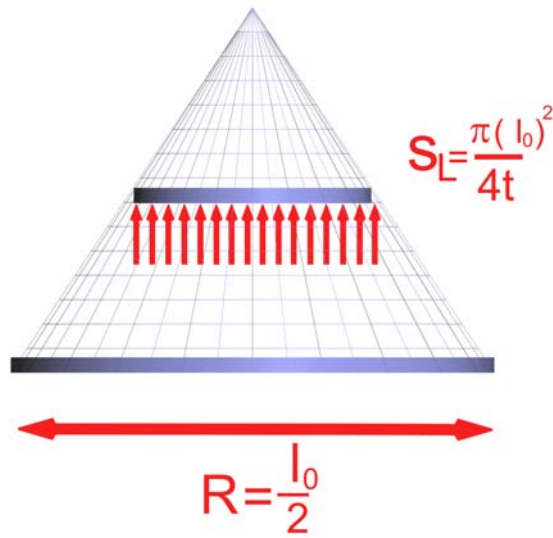


Figure 2-28: shows the laminar burning velocity at one of the cross sections of the flame.

To begin the deriving process:

Surface area=area of the cone

$$A_c = r\pi S$$

$$A_c = \pi \frac{l_0}{2} S$$

$$A_c = \pi \frac{l_0}{2} \sqrt{(h^2 + R^2)}$$

$$A_c = \pi \frac{l_0}{2} \sqrt{(h^2 + \frac{l_0^2}{4})}$$

$$A_c = \pi \frac{l_0^2}{4} \sqrt{(\frac{4h^2}{l_0^2} + 1)}$$

$$A_c = A_B (1 + (4h/l_0)^2)^{1/2}$$

By the division of both sides of the equation with t:

$$\frac{A_c}{t} = \frac{A_B}{t} (1 + (\frac{2h}{t} / \frac{l_0}{t})^2)^{1/2}$$

This leads us to the final shape of the equation:

$$S_T = S_L (1 + (2u'/S_L)^2)^{1/2} \dots \dots \dots (84)$$

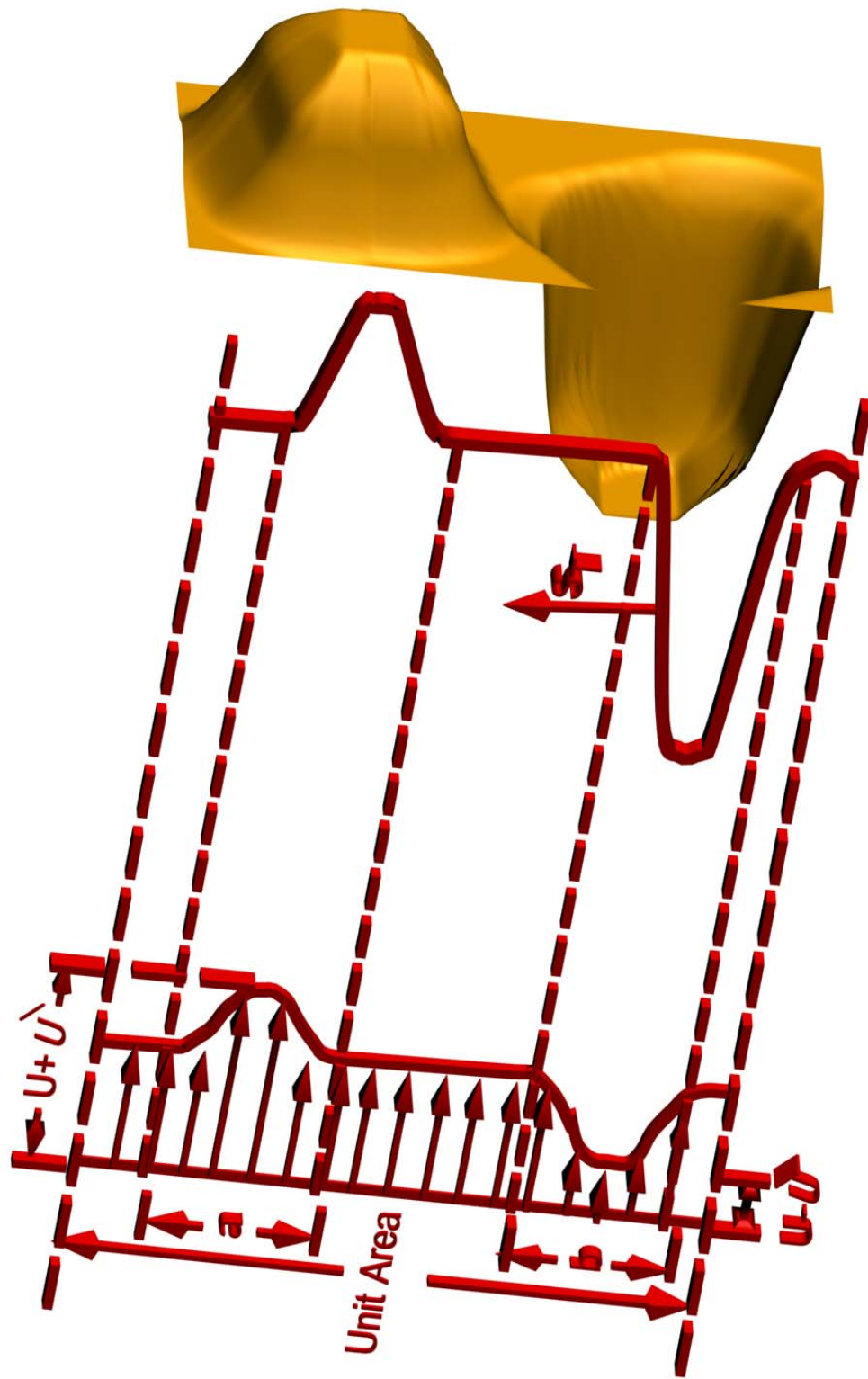


Figure 2-29: A 3D look on a combustion wave in a turbulent flow with a slice of a flame profile taken from a larger flame.

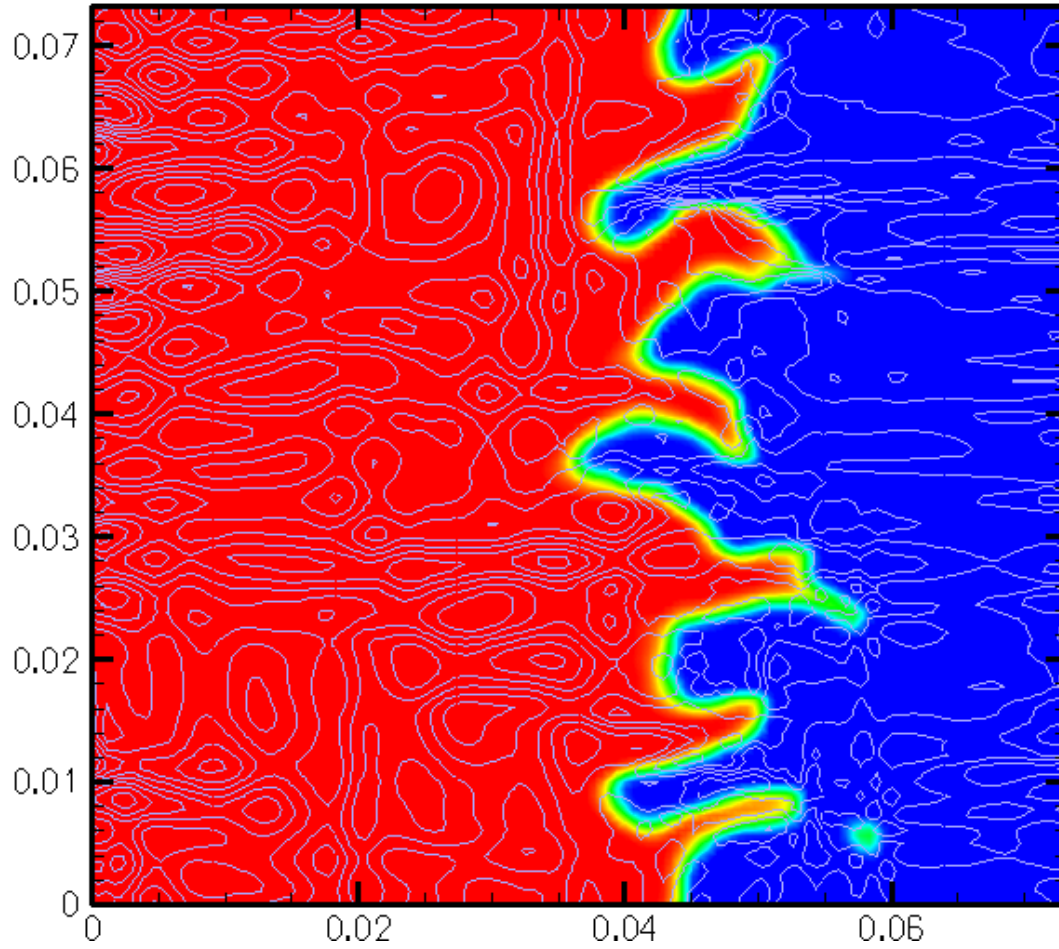


Figure 2-30 : LES predictions of a free-propagating turbulent premixed methane-air flame using thickened flame with power-law flame wrinkling subfilter scale models[17]

2.6. Length Scales in Turbulent Flows

2.6.1 Characteristic Width of Flow or Microscale L:

This is the largest length scale in the system and is the upper bound for the largest possible eddies. Example 1: in a pipe flow the largest eddy would be equal to the pipe diameter. Example 2: in a jet flow L would be the local width of the jet at any axial location. Example 3: in a reciprocating internal combustion engine might be taken as the time-varying clearance between the piston top and the head, or perhaps the cylinder bore. Conclusion: In general this length scale is defined by the actual hardware or device being considered. This length scale is frequently used to define a Reynolds number based on the mean flow velocity, but is not used to define turbulence Reynolds number, as are the other three length scales.

2.6.2 Integral Scale or Turbulence Microscale, l_0 The integral scale:

Physically represents the mean size of the larger eddies in a turbulent flow those eddies with low frequency and large wave length.



Figure 2-31: shows due in a flow which illustrates large eddies with low frequency and large wave length.

The integral scale is always smaller than L, but is of the same order of magnitude.

Operationally, the integral scale can be measured by integrating the correlation coefficient for the fluctuating velocities obtained as a function of the distance between two points

$$l_0 = \int_0^{\infty} R(x) dr \dots\dots\dots (85)$$

Where :

$$R_x(r) \equiv \frac{\overline{v'_x(0)v'_x(r)}}{\overline{v'_{x,rms}(0)v'_{x,rms}(r)}} \dots\dots\dots (86)$$

In less precise terms, l_0 represents the distance between two points in a flow where these ceases to be a correlation between the fluctuating velocities at the two locations.

2.6.3 Taylor Microscale l_λ :

The Taylor Microscale is an intermediate length scale between l_0 and l_k ,but is weighted more towards the smaller scales. This scale is related to the mean rate of strain and can be formally expressed as

$$l_\lambda = \frac{v'_{x,rms}}{\left[\left(\frac{\partial v_x}{\partial x} \right)^2 \right]^{1/2}} \dots\dots\dots (87)$$

Where the denominator represents the mean strain rate.

2.6.4 Kolmogrov Microscale l_k :

The Kolmogorov micro scale is the smallest length scale associated with a turbulent flow and as such, is representative of the dimension at which the dissipation of turbulent kinetic energy to fluid internal energy occurs.

Thus, the Kolmogrov scale is the scale at which molecular effects (kinematic viscosity) are significant. Dimensional arguments show that l_k can be related to the rate of dissipation, ϵ_0 as

$$l_k \approx (\nu^3 / \epsilon_0)^{1/4} \dots\dots\dots (88)$$

where ν is the molecular kinematic viscosity, and the dissipation rate is approximately expressed as

$$\epsilon_0 \equiv \frac{\delta(kl_{turb})}{\partial t} \approx \frac{3v'^2_{rms}/2}{l_0/v'_{rms}} \dots\dots\dots (89)$$

Note that the integral length scale l_0 appears in the approximation for the dissipation rate, thereby linking the two scales.

2.6.5 Turbulence Reynolds Numbers:

Three of the four length scales discussed above are used to define three turbulence Reynolds numbers. In all of the Reynolds numbers, the characteristic velocity is the root-mean-square fluctuating velocity, v'_{rms} . Thus, we define

$$Re_{l_0} \equiv v'_{rms} l_0 / \nu \dots\dots\dots (90)$$

$$Re_{l_\lambda} \equiv v'_{rms} l_\lambda / \nu \dots\dots\dots (91)$$

And

$$Re_{l_k} \equiv v'_{rms} l_k / \nu \dots\dots\dots (92)$$

Equations 90 and 91 defining l_k and the dissipation rate ϵ_0 can be used to relate the largest (the integral) and the smallest (the Kolmogorov) turbulence length scales:

$$l_0 / l_k = Re_{l_0}^{3/4} \dots\dots\dots (93)$$

The Taylor micro scale, l_λ , also can be related to Re_{l_0} as follows :

$$l_0 / l_\lambda = Re_{l_0}^{1/2} \dots\dots\dots (94)$$

Equation 93, expresses, in a semi quantitative way, the wide separation of length scales in high-Re flows discussed earlier in this chapter. For example, with $Re_{l_0}=1000$, the ratio l_0 / l_k is about 178; but when Re_{l_0} is increased to 10000, by increasing the mean flow velocity, say, the ratio becomes 1000:1.

2.7. Flame Regimes and Governing Physical Phenomena:

The interaction between the turbulent flow field and the flame front is described by means of characteristic dimensionless numbers.

The most commonly used are the:

2.7.1. The turbulent Reynolds number (Re_T):

The Reynolds number describes the ratio of the momentum forces (destabilizing effects) to the viscous forces (stabilizing effect). Reacting flows at high turbulence Reynolds numbers are characterized by highly fluctuating flames.

$$\text{Re}_T = \frac{u' L_T}{S_L \delta_L} \dots\dots\dots(95)$$

2.7.2. The Damköhler number (Da):

Is a number that relates the time scale of the turbulent mixing defined as L_T/u' to the time scale of the chemical reaction defined as δ_L/S_L .

There are two distinguishable cases for Damköhler number:

A-Large Damköhler numbers (Da >> 1):

Refers to a flame where the chemistry is fast and thus the combustion is controlled by mixing processes. As a result these flames form structures of a sheet type.

B-Flame at small Damköhler numbers (Da < 1) :

Are characterized by intense mixing. The reaction of combustion is controlled by chemical kinetics and flames referred to as well-stirred reactor are formed.

$$Da = \frac{\tau_m}{\tau_c} = \frac{L_T S_L}{u' \delta_L} \dots\dots\dots(96)$$

2.7.3. Karlovitz number (Ka):

Defined as in Equation (97). The Karlovitz number relates the thickness of the reaction zone represented by the laminar flame thickness δ_L to the smallest scales of the turbulent flow represented by the Kolmogorov microscale η . Thus the Karlovitz number can be used as a measure of the flame front stretch.

Note: The relations have been derived with the assumption that the thermal diffusivity is equal to the mass diffusivity (Schmidt number $Sc \equiv 1$).

$$Ka = \left(\frac{L_T}{\delta_L} \right)^{\frac{1}{2}} \left(\frac{u'}{S_L} \right)^{\frac{3}{2}} \dots\dots\dots(97)$$

Using these three characteristic numbers (Re_T, Da and Ka) it is possible to classify the turbulent premixed flames into groups (flame regimes) as already been classified by the scientist Borghi and later extended by Peters.

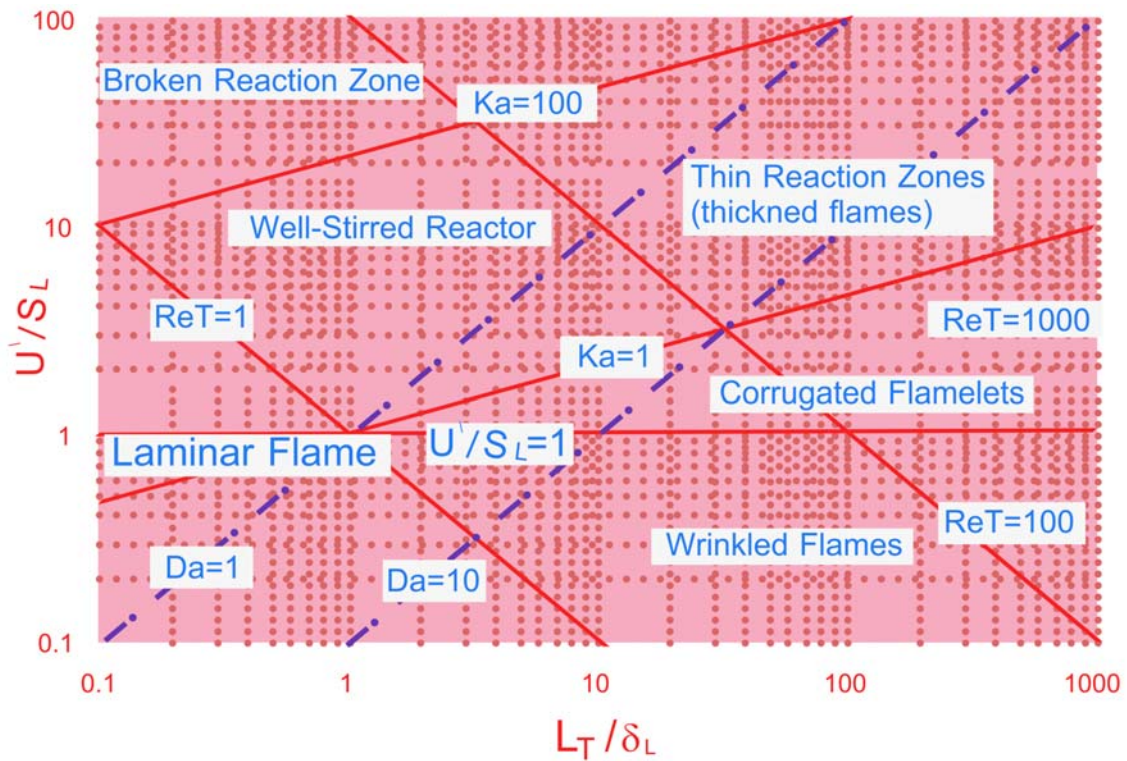


Figure 2-32: Borghi /Peters chart illustrating different types of burning regimes.

2.7.4. Lewis Number (Le):

Lewis number is a dimensionless number defined as the ratio of thermal diffusivity to mass diffusivity. It is used to characterize fluid flows where there is simultaneous heat and mass transfer by convection.

$$Le = \frac{\alpha}{D} \dots\dots\dots(98)$$

where α is the thermal diffusivity and D is the mass diffusivity.

2.7.5. Description of the Borghi chart:

1-The L_T/δ_L -axis in Figure characterizes the size of the flame structures by means of the ratio of the characteristic length scales (Integral Length Scale of turbulence L_T to the laminar flame thickness δ_L). The characteristic size of the turbulent flow (e.g. vortices) in comparison to the laminar flame thickness grows along the x-axis.

2- The u'/S_L -axis refers to the ratio of characteristic velocities represented by an intensity of the flow field fluctuation (turbulence intensity u') to the laminar flame speed S_L . The flame regimes of turbulent premixed flames ($Re_T > 1$) and their characteristics are summarized in (figure 2-33).

All of the flame regimes listed in (figure 2-33) except the well stirred reactor are characterized by a Damköhler number on the order or larger than 1 which refers to “fast chemistry” i.e. the reaction zone is relatively thin (fraction of a millimeter for $p > p_{atm}$) and the flame front can be treated as a discontinuity. The characterization of the flame front is in the focus of most of investigations of the turbulent premixed flames. The pictures presented in the last column of figure (2-33) illustrate the main characteristic properties of the flame fronts. The grey color represents the fresh gas mixture (unburned reactants) and the white color the exhaust gases (burned products). The black thick line which separates products and reactants represents the flame front which propagates from right to left in a stagnant fluid [21].





Flame Regime	Re	Da	Ka	\bar{u}/s_L	δ/η	Graphical Illustration of the Flame Front
Wrinkled Flame	>1	>1	<1	<1	<1	
Corrugated Flame	>1	>1	<1	>1	<1	
Thickened Flame (Thin reaction zones)	>>1	>=1	>1	>>1	>1	
Distributed Flame (well stirred reactor)	>1	<1	>1	>1	>1	

Figure 2-33: the classification of flame regimes based on three characteristic numbers [21].

2.8. Flame Speed Measurements

The Various Experimental Configurations used for flame speed may be classified under the following headings:

A-conical stationary flames on cylindrical tubes and nozzles

B-flames in tubes

C-Soap bubble method

D-constant volume explosion in spherical vessel

E-Flat Flame methods

The methods are listed in order of decreasing complexity of flame surface and corresponds to an increasing complexity of experimental arrangement. Each has certain advantages that attend its usage.

1-burner method

2-cylindrical tube method

3-soap bubble method

3. Experimental setup

3.1. Atmospheric-pressure test facility

All combustion experiments were performed in a generic, cylindrical combustor shown in figure 3-1. High pressure air is passed through the seeder and then mixed with methane the later mixture is then passed through the different types of turbulence plates. Then data is collected and stored on the computer hard drive to be analyzed later.

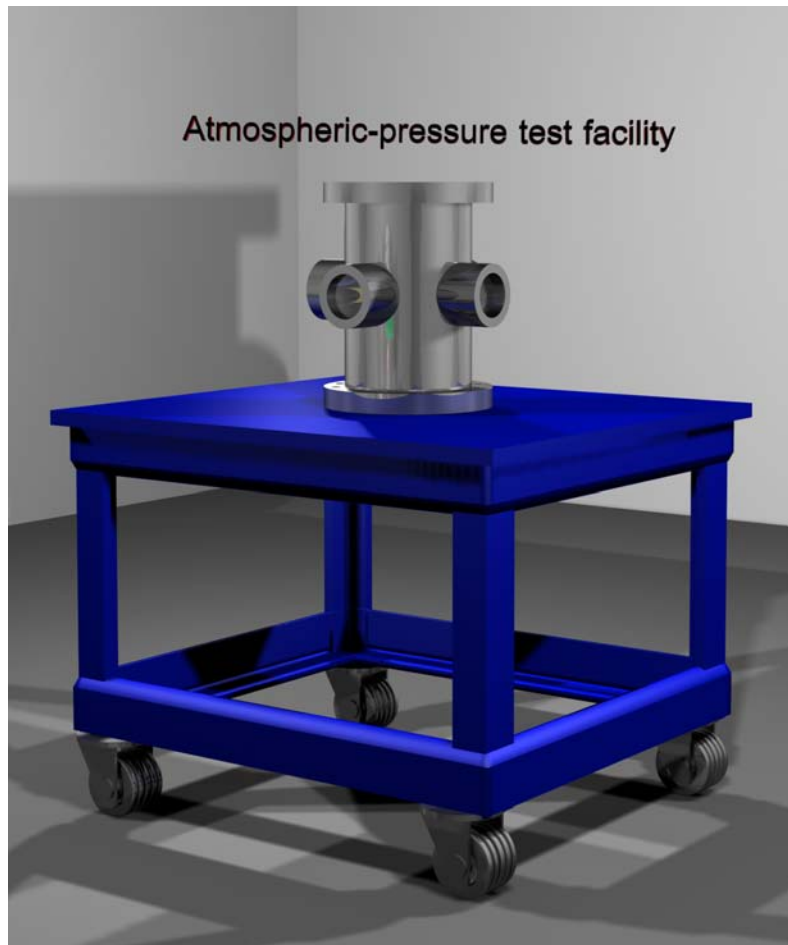


Figure 3-1: Shows the cylindrical atmospheric test facility.

The liner consists of two coaxial quartz glass tubes (inner quartz glass tube diameter $D = 75$ mm) which are cooled by natural draft free convection with air.

The combustor inlet diameter d is 25 mm. The flame is stabilized aerodynamically via the recirculation of hot flue gases, induced by the combustor geometry and different installed turbulence plates.

A methane torch igniter (pilot) is used to ignite the homogeneously premixed methane/air mixture. The high level of optical access required for non-intrusive laser diagnostics is provided by the four circular windows.

The turbulence intensity u' and the integral length scale L_T in the inlet are varied by using different turbulence grids (different hole diameters and blockage ratios) or by mounting these grids at different axial positions within the combustor inlet section. The nomenclature of the grids is explained in Figure 3-2.

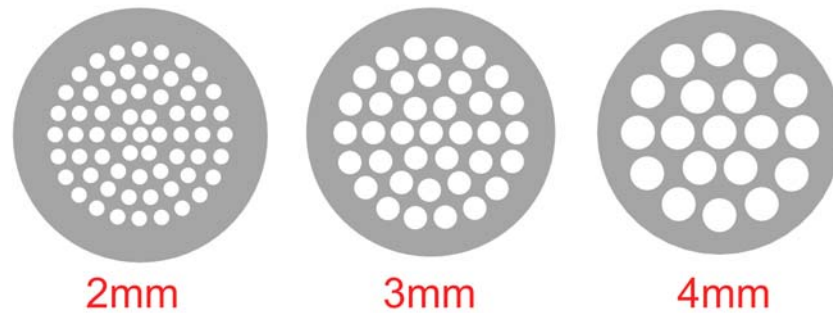


Figure 3-2: shows different types of blockage plates.

Table 3-1 : The Turbulence Plates characteristics :

Diameter of Blank(mm)	Hole Diameter(mm)	Number of Holes	Blockage Ratio%
25	2	61	61
25	3	37	47
25	4	19	51

The grid name consists of information about the diameter of the hole in millimeters followed by the blockage ratio (as shown on table 3-1). The position of the grid in the inlet section of the combustor is normalized by the grid-hole diameter. For example

g350xg10 refers to a grid with a hole diameter ($d_g = 3 \text{ mm}$) and a blockage ratio (bg) of 50% is mounted at $10 \times d_g = 30 \text{ mm}$ upstream in the inlet channel (Figure 3-4).

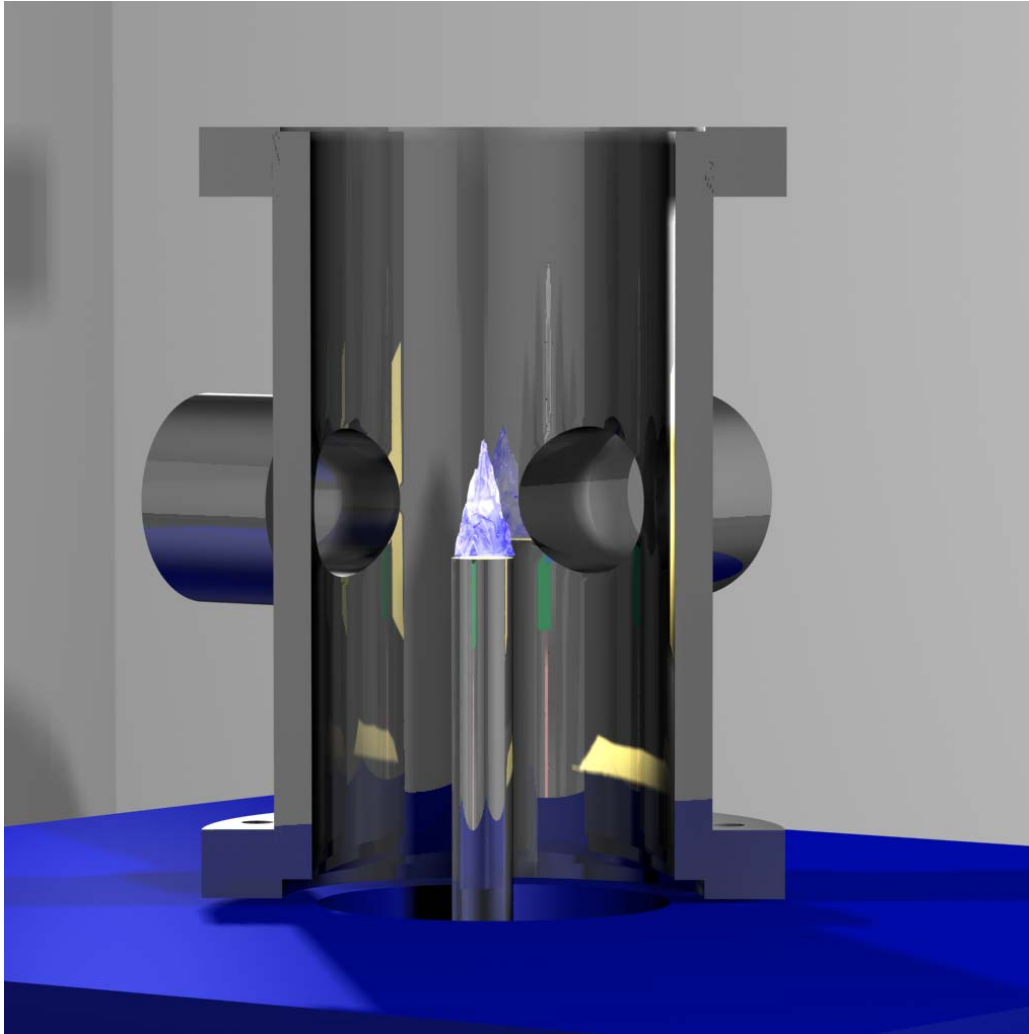


Figure 3-3: a cross section through the cylindrical atmospheric test bench.

3.2. Dantec automated data collection module:

It is connected up with a pc and is given the orders to take samples at certain points and these points are predetermined by the researchers, the hole points form the grid the more points you have the more time is needed to take the samples but you will have more accurate data .for the lab case there was no interest to move the rig on the z axis. So the movement was restricted on the x and y axis.

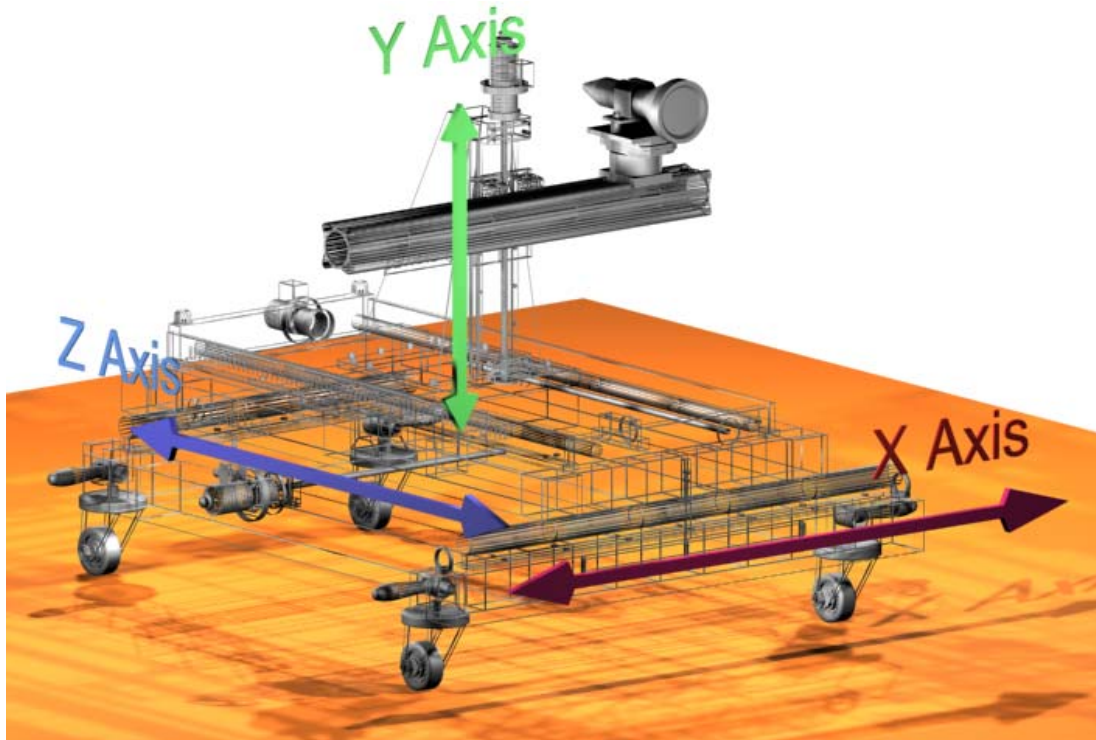


Figure 3-4: is a clear diagram of the Dantec module showing the x, y and z axis of movement.

The pressurized air is supplied from a high-pressure compressor near the lab building and methane is from the city gas supply. The camera with the test-rig operation is controlled from a PC using the data acquisition software. The schematic of the control and supply system is presented in Figure 3-5.

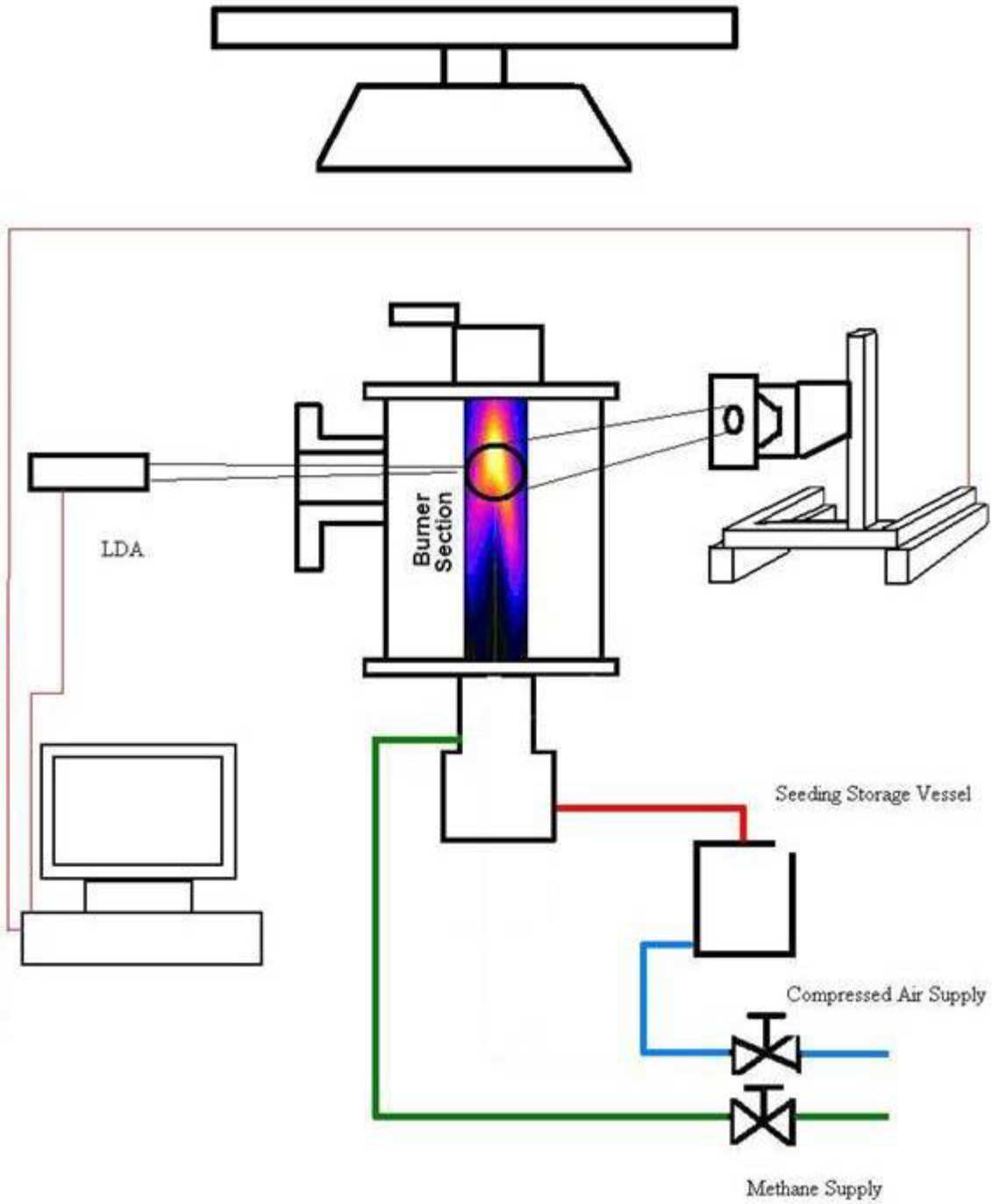


Figure 3-5: The whole test apparatus with all of its secondary circuits.

4. Measuring Techniques

4.1. Introduction:

In the first part of this chapter Principles of Particle Image Velocimetry (PIV) are briefly described. The next part describes Principles Laser Doppler Anemometry (LDA). The third part is devoted to aluminum oxide seeding. Finally in the fourth part is about the high speed imagery camera used.

4.2. Principles of Particle Image Velocimetry (PIV)

Particle Image Velocimetry (PIV) is an optical non-intrusive technique for measurements of instantaneous velocity field.

The main topics in a PIV system are

- 1-Seeding
- 2-Camera
- 3-Laser
- 4-Correlation

Validation and further analysis

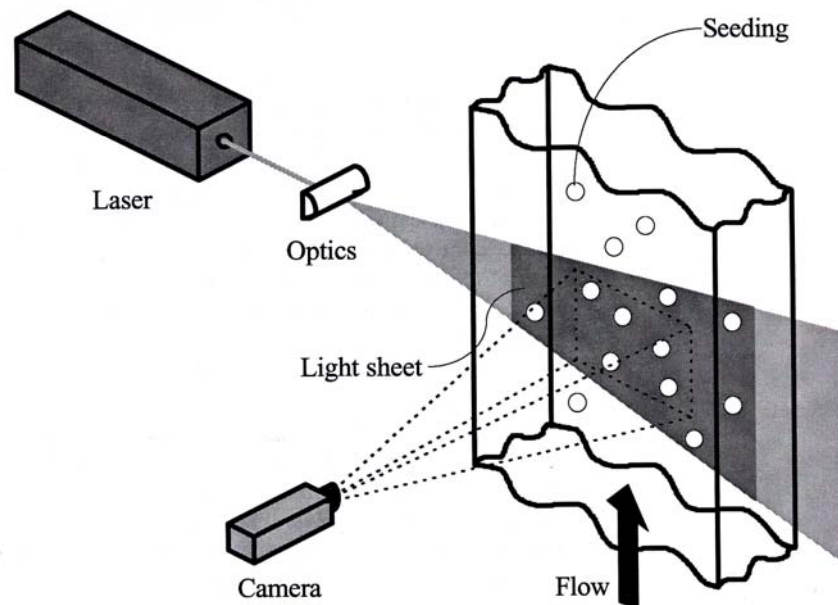


Figure 4-1: Particle Image Velocimetry [16]

4.3. Description of PIV:

Particle Image Velocimetry (PIV) is a measurement technique for obtaining instantaneous whole field velocities. It is based on the well-known equation in PIV, the property actually measured is the distance traveled by particles in the flow within a known interval of time. These particles are added to the flow and are known as seeding. 10µm silver coated glass particles are used as the seeding particles in this set up.

$$u = \frac{\Delta x}{\Delta t} \dots\dots\dots (99)$$

A light sheet produced by the laser is used to illuminate the particles. A high-speed imaging system (camera) detects the position of the particles. It takes two pictures separated in time and the distance moved by the particles in this time is used to determine their velocities figure 4-2.

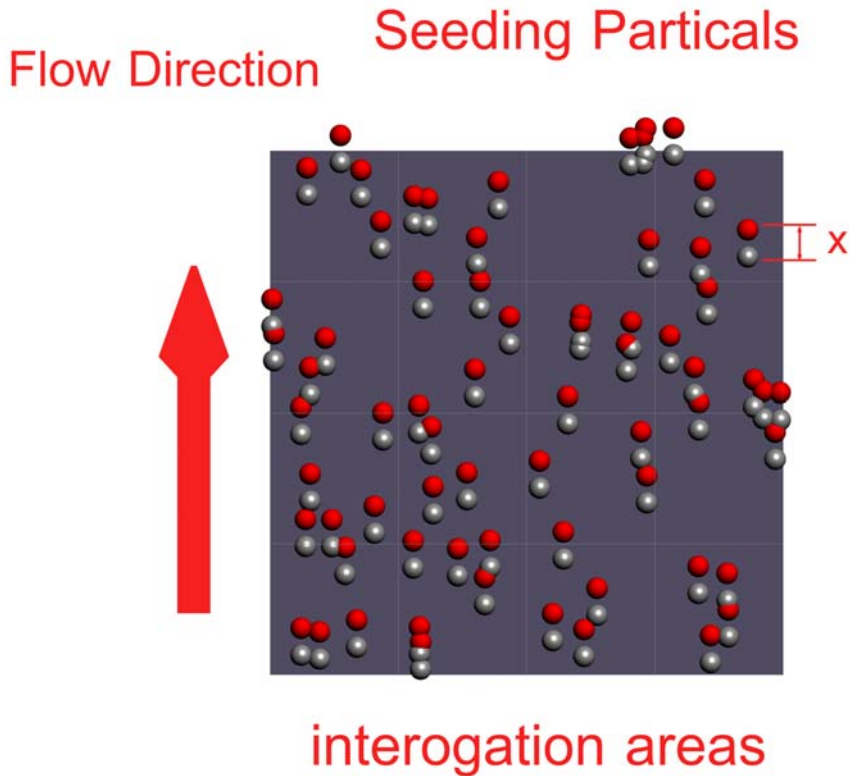


Figure 4-2: Interrogation areas the seeding particles where the grey particles were taken at time t1 and the red particles taken at t2.

The camera images are divided into rectangular regions called the interrogation areas, and for each of these interrogation areas the image from the first and the second pulse of the light sheet are correlated to produce an average particle displacement vector. Doing this for all the interrogation areas produce a vector map of average particle displacements figure 4-4. The calculation of the particle displacement is based on an analysis of the PIV images. Consequently the calculation yields one vector per every pair of the interrogation windows. From figure 4-2 dividing with the known time between the two images captured the displacement vectors are converted into a map of so-called raw velocity vectors. Applying validation algorithms to the raw vector maps, the erroneous vectors are detected and removed. Further analysis of these validated vectors will produce streamlines, vorticity, and turbulence as can be seen on figure 4-4 [16].

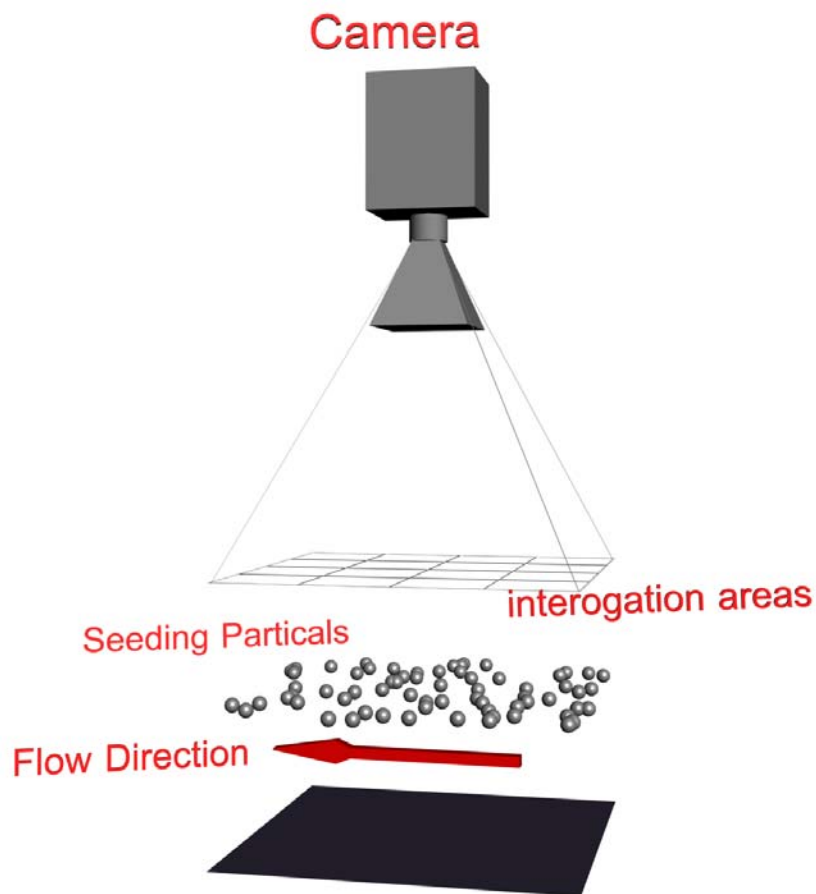


Figure 4-3: showing the camera and the particles and the interrogation areas.

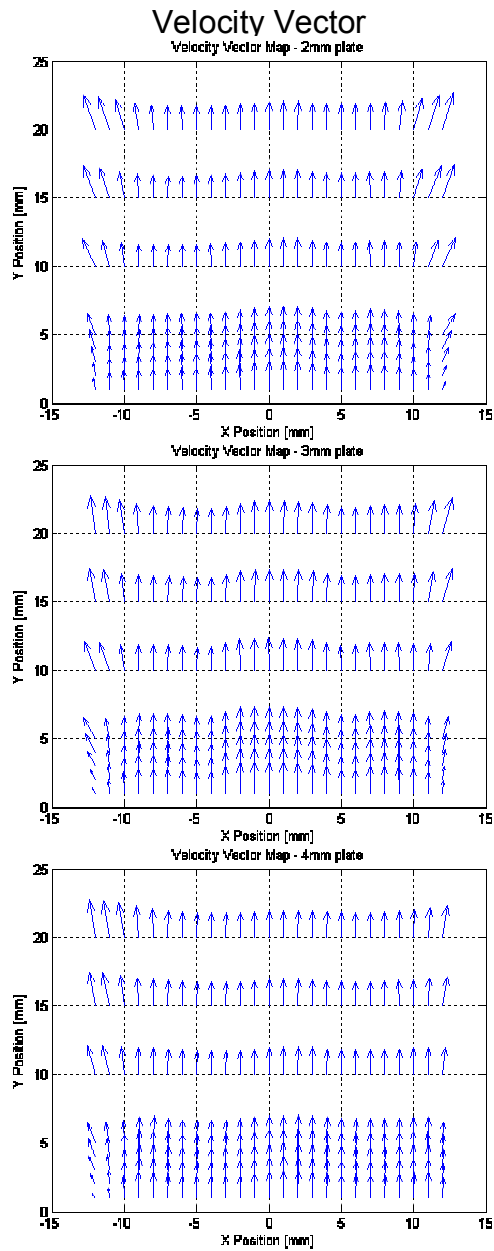


Figure 4-4: shows the vectors plotted by the soft wear after the collection of data and its analysis been conducted.

4.4. Principles of LDA:

Back scatter LDA is shown on figure 4-1 back scatter is the light collected after being reflected from the moving particles. The distance f refers to the distance from the laser lens to the point of laser beam concentration.

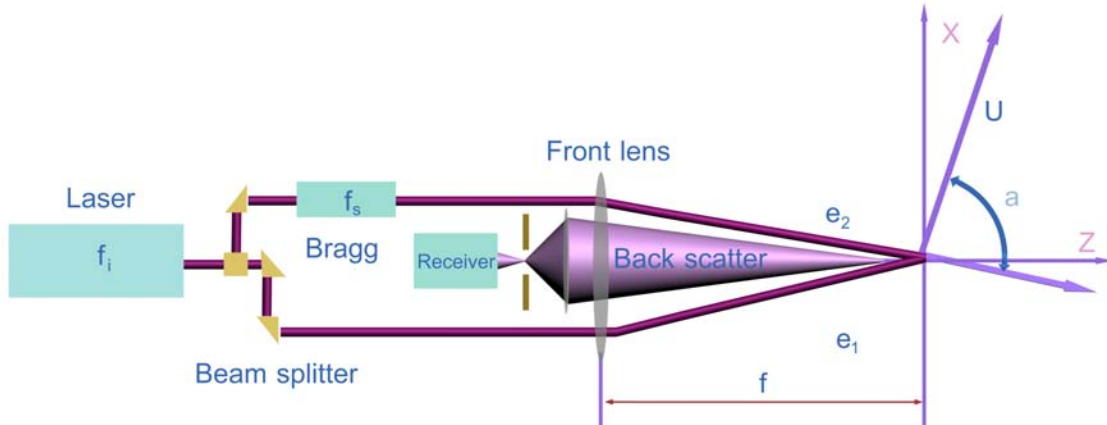


Figure 4-5: Principles of backscatter LDA.

4.4.1. Laser beam:

Gas lasers are very powerful tools to be used to measure mechanical properties, At one point the cross section attains its smallest value, and the laser beam is uniquely described by the size and position of this so called beam waist. With a known wave length λ of the laser light, the laser beam is uniquely described by the size d_0 , and the position of the beam waist as shown on figure 4-1.

With z describing the distance from the beam waist, the following formulas apply:

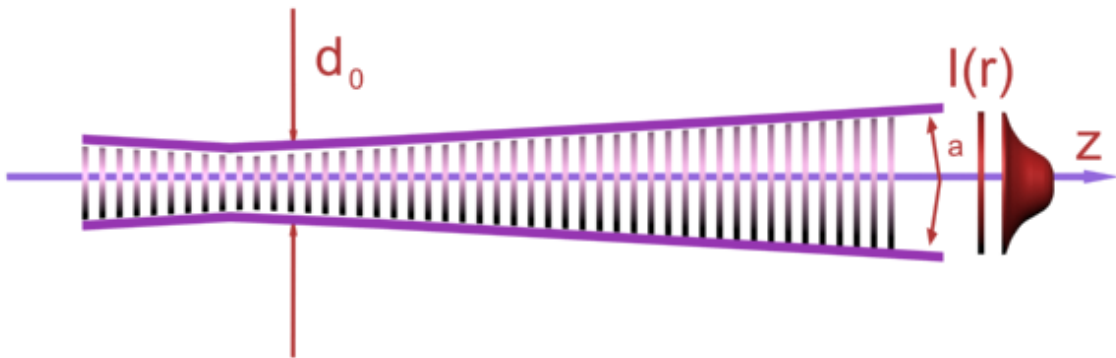


Figure 4-6: laser beam with Gaussian intensity distribution

With z describing the distance from the beam waist, the following formulas apply:

$$\text{Beam divergence } \alpha = \frac{4\lambda}{\pi d_0} \dots\dots\dots (100)$$

$$\text{Beam diameter } d(z) = d_0 \sqrt{1 + \left(\frac{4\lambda z}{\pi d_0^2}\right)^2} \dots\dots\dots (101)$$

$$\text{Wave front radius } R(z) = z \left[1 + \left(\frac{\pi d_0^2}{4\lambda z}\right)^2\right] \dots\dots\dots (102)$$

The beam divergence α is much smaller than indicated in figure 4-2 , and visually the laser beam appear to be straight and of constant thickness. it is important however to understand, that this is not the case, since measurements should take place in the beam In the beam waist to get optimal performance of any LDA-equipment. This is due to the wave fronts being straight in the beam waist, and curved elsewhere, and will be explained in the next part.

The wave front radius approach infinity for z approaching zero, meaning that the wave fronts are approximately straight in the immediate vicinity of the beam waist. This means that the theory of plane waves can be used here, greatly simplifying calculations.

4.4.2 Doppler Effect:

The Doppler Effect plays an important role in LDA, since the technique is based on Doppler shift of the light reflected (and /or refracted) from a moving seeding particle.

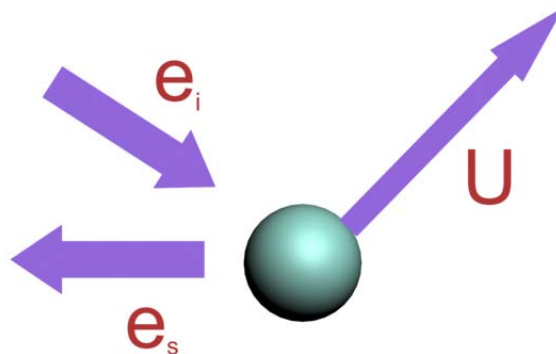


Figure 4-7: Light scattering from a moving seeding particle.

Based on the Lorenz-Mie scattering theory, light is scattered in all directions instantaneously, but due to our interest we only take into consideration the light reflected towards the receiver.

The illustration in figure 4-3 where the vector U represents the particle velocity, and the unit vectors e_i and e_s describe the direction of incoming and scattered light respectively.

The incoming light has the velocity c and the frequency f_i , but due to the particle movement, the seeding particle “sees a different frequency f_p , which is scattered towards the receiver. From the receiver's point of view, the seeding particle acts as a moving transmitter, and the movement introduces additional Doppler shift in the frequency of the light reaching the receiver.

Using Doppler-theory, the frequency of the light reaching the receiver can be calculated as:

$$f_s = f_i \frac{1 - e_i(U/c)}{1 - e_s(U/c)} \dots\dots\dots (103)$$

Even for supersonic flows the seeding particle velocity $|U|$ is much lower than the speed of light, meaning that $\|U/c\| \ll 1$.

Taking advantage of this, the above expression can be linearized to:

$$f_s \cong f_i [1 + \frac{U}{c}(e_s - e_i)] = f_i + \frac{f_i}{c} U(e_s - e_i) = f_i + \Delta f \dots\dots\dots (104)$$

With the particle velocity U being the only unknown parameter, in principle the particle velocity can be determined from measurements of the Doppler shift Δf .

4.4.3. Intersecting beams:

In practice this frequency change can only be measured directly for very high particle velocities (Fabry-Perot interferometer). More commonly the light scattered from two intersecting laser beams is mixed as illustrated in figure 4-3.

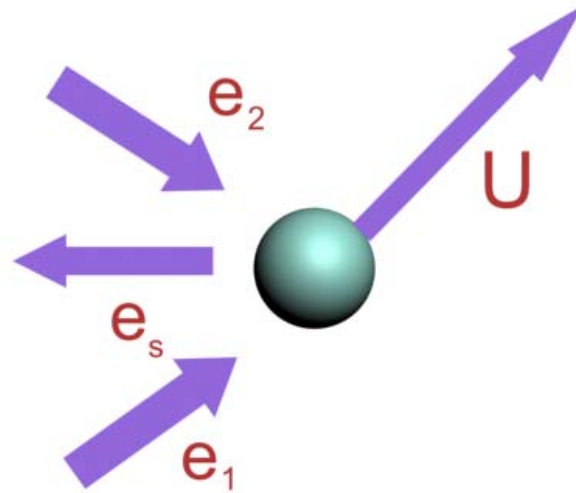


Figure 4-8: Light scattering from a moving seeding particle.

In this way both incoming laser beams are scattered towards the receiver, but with slightly different angles of the two laser beams.

$$f_{s,1} = f_1 \left(1 + \frac{U}{C} (e_s - e_1) \right) \dots\dots\dots (105)$$

$$f_{s,2} = f_2 \left(1 + \frac{U}{C} (e_s - e_2) \right) \dots\dots\dots (106)$$

4.4.4 Doppler frequency:

When two wave's trains of slightly different frequency are super-imposed, we get the well-known phenomenon of a beat frequency due to the waves intermittently interfering with each other constructively and destructively. The beat frequencies correspond to difference between two wave-frequencies, and since the two incoming waves originate from the same laser, they also have the same frequency, $f_1 = f_2 = f_i$ where subscript 1 refer to incident light:

$$f_D = f_{s,2} - f_{s,1} \dots\dots\dots (107)$$

4.4.5. The Fringe model:

Although the above description of LDA is accurate, it may be intuitively difficult to quantify. To handle this, the fringe model is commonly used in LDA as a reasonably simple visualization.

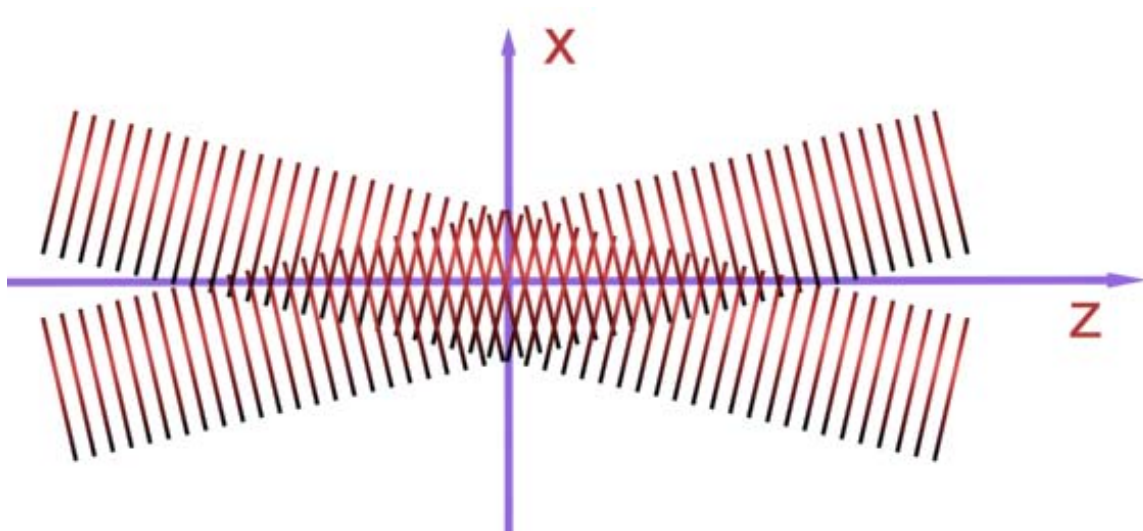


Figure 4-9 :Fringes from where two coherent laser beams cross.

4.5. The seeding:

4.5.1 Aluminum oxide seeding:

Aluminum is known to produce several molecular band systems. Two in particular, arising from AlO^+ , should be seen at 435–500 nm and 508–518 nm, the most intense emission centered at 484 nm. The atomic line emission of aluminum should occur at 396.2 nm when flame temperatures are hot enough to allow aluminum to exist in the atomic form. The relative intensities of the atomic line versus molecular bands will vary depending on flame temperature. Higher temperatures will produce more atomic species as the molecules are dissociated. The atomic line emission intensities should rise as the molecular band emissions decrease.

4.5.2 Properties of the seeding material:

The optimal seeding is characterized by:

1. Particles small enough to follow the flow(able to follow the flow).
2. Particles big enough to scatter sufficient amount of light(Good light scatters).
3. Particles homogenously distributed within the flow
4. Particles chemically inactive (in combustion experiments).
5. Non-volatile,or slow evaporate.
6. Chemically inactive.
7. Clean.
8. Cheap.

4.5.3 Seeding as flow field tracers:

In general the motion of particles suspended in a field is affected by

- 1- Particle shape.
- 2- Particle size.
- 3- Relative density of a particle and fluid.
- 4- Concentration of particles in the fluid.
- 5- Body forces.

The shape of the seeding particles affect the drag exerted on the particle by the surrounding fluid, and the size of particles along with their relative density influence their response to velocity change of the surrounding fluid.

The concentrations of particles affect particle motion through interaction between different particles .in practice the concentrations used normally so low, that particle interaction can be neglected.

Also body forces, such as gravity, can normally be ignored, except in very slow flows, where buoyancy of the seeding particles may be in an issue. Also in experiments including for example electrostatic fields, body forces may be of importance, but in such cases they can not really be considered a disturbance.

4.5.4 Particle motion:

Since the analysis of particle motion is rather complicated even for spherical particles and real particles can't be modelled properly any way, only spherical particles in an infinite fluid have been analysed. It is assumed, that the results apply qualitatively also for

particles of more irregular shape. This assumption is a good for liquid particles and fair for monodisperse particles, but poor for other solid particles, such as agglomerates.

$$\underbrace{\frac{\pi}{6} d_p^3 \rho_p \frac{dU_p}{dt}}_{\text{Accelerating force}} = \underbrace{-3\pi\mu d_p V}_{\text{Stokes viscous drag}} + \underbrace{\frac{\pi}{6} d_p^3 \rho_f \frac{dU_f}{dt}}_{\text{pressure gradient force on fluid}} - \underbrace{\frac{\pi}{12} d_p^3 \rho_f \frac{dV}{dt}}_{\text{fluid resistance to accelerating sphere}} - \underbrace{\frac{3}{2} d_p^2 \sqrt{\pi\mu\rho_f} \int_{t_0}^t \frac{dV}{d\xi} \frac{d\xi}{\sqrt{(t-\xi)}}}_{\text{drag force associated with unsteady motion}} \dots (108)$$

Where subscript p refer to the seeding particle and subscript f refer to the fluid.

The first term in this equation represents the

Note that when the first, third and fourth terms are combined, the accelerating force is equivalent to that of a sphere whose mass is increased by an additional “virtual mass” equal to half the mass of the displaced fluid.

The above equation is valid within the following assumption

- 1-the turbulence is homogeneous and time –invariant.
- 2-particles are smaller than the turbulence micro scale.
- 3-stokes drag law applies (particles are spherical)
- 4-there is no interaction between particles.

Furthermore external forces, such as gravitational, centrifugal and electrostatic forces have been ignored.

4.6. Photron’s APX-RS high-speed system camera:

The **Ultima APX-RS** provides full mega pixel resolution images at frame rates up to 3,000 frames per second (fps), 512 x 512-pixels resolution at 10,000fps and at reduced frame rates to an unrivaled frame rate of 250,000fps. Utilizing Photron’s advanced CMOS sensor technology, the **APX-RS** provides the higher light sensitivity than any other comparable high-speed imaging system [14].



Figure 4-10: shows the high imagery used in the experiments [14].

5. Results and Discussion

5.1. Turbulence plates fluid dynamics data:

5.1.1. Introduction:

This data is very useful because it illustrates what are the velocity conditions in the chosen section of the flame while at the same time comparing this velocity with the bulk velocity, so it's like comparing the kinetic energy of the oxide seeding before and after the combustion process. Fluid dynamic data should be presented in terms carefully chosen non dimensional parameters sensitive to major variables of the flow to obtain reliable information. Note that v/v_{bulk} is the same as v_{mean}/v_{bulk} in graphs (1, 3, 5, and 7).

It is assumed that:

- That the graphs (1, 2, 3, 4, 5, 6, 7, 8) are asymmetric around the y axis.
- Steady state process occurs where no change in mass flow and no change in mixture ratios, constant Stoichiometric ratio.
- Constant atmospheric parameters surrounding the flame.

5.1.2. Clear factors affecting the velocity parameters in graphs (1, 2, 3, 4, 5, 6, 7, and 8):

- looking at the tips of the curves, the wall shear stress has an effect on slowing down the gaseous mixture and in return v_{mean} will be affected while v_{rms} will be less affected and that is clear in cross sections from $y=1$ to 4. point of inflexion occurs in cross section $y=5$ mm. where there is an increase in v_{mean} and v_{rms} that is due to the chemical reaction and combustion where the aluminium oxide particles gain kinetic energy and move faster in y axis direction, at the burning of the flame at the outer tips, a suction effect is created by the reaction zone.

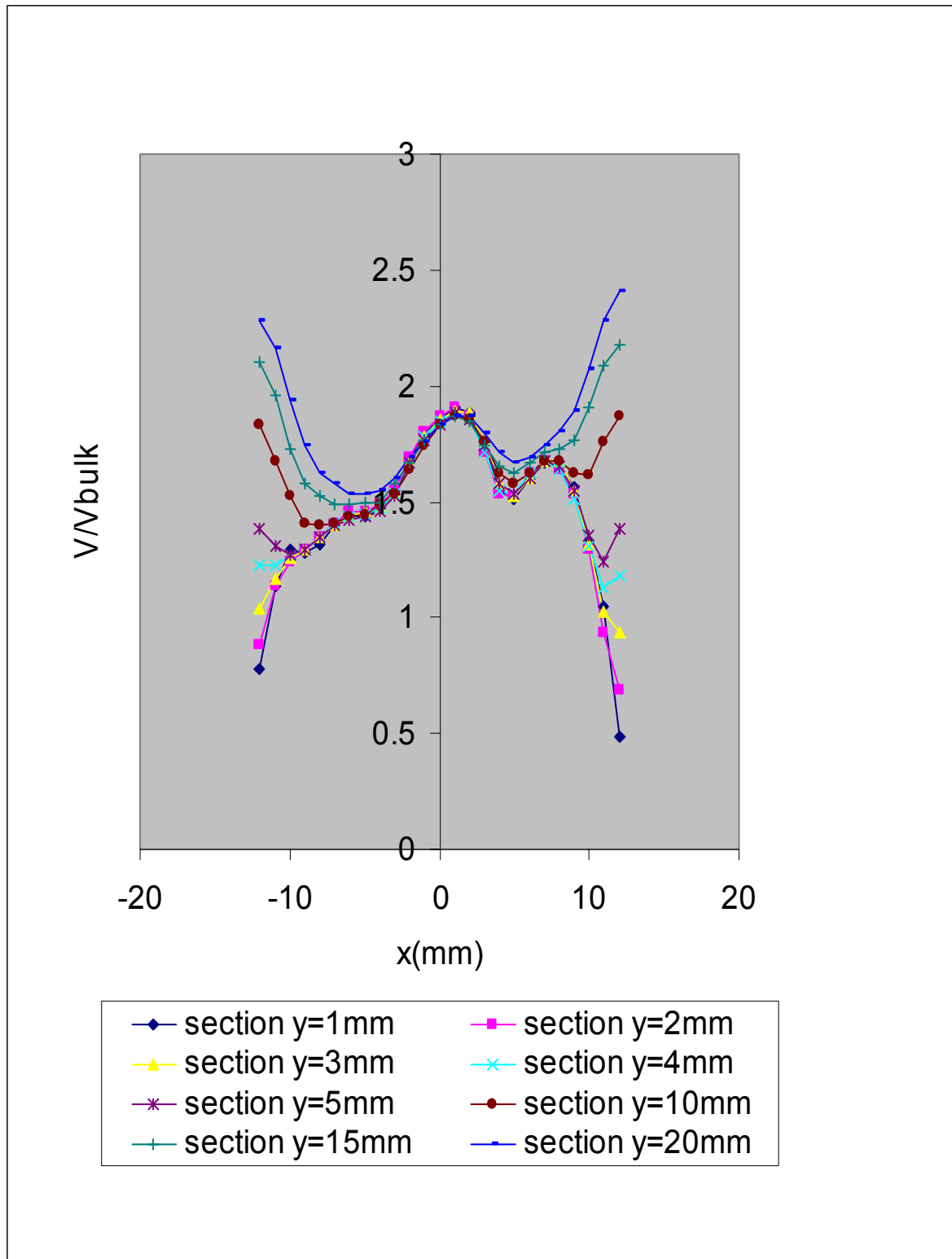
- Graph (1, 3, 5, and 7) have the same profile layout for all cross sections where the core has parabolic profile which is similar to $V_{mean} = V_{meanmax} (1 - (\frac{r}{R})^2)$ and the tips have a jump in velocity. The only difference between graph (1, 3, 4) and (7) is that the velocity

ration v_{mean} / v_{bulk} in the core for (1, 3, 5) is more well uniformly distributed out compared with graph (7) which shows a clear difference between having a turbulence plate and not having one.

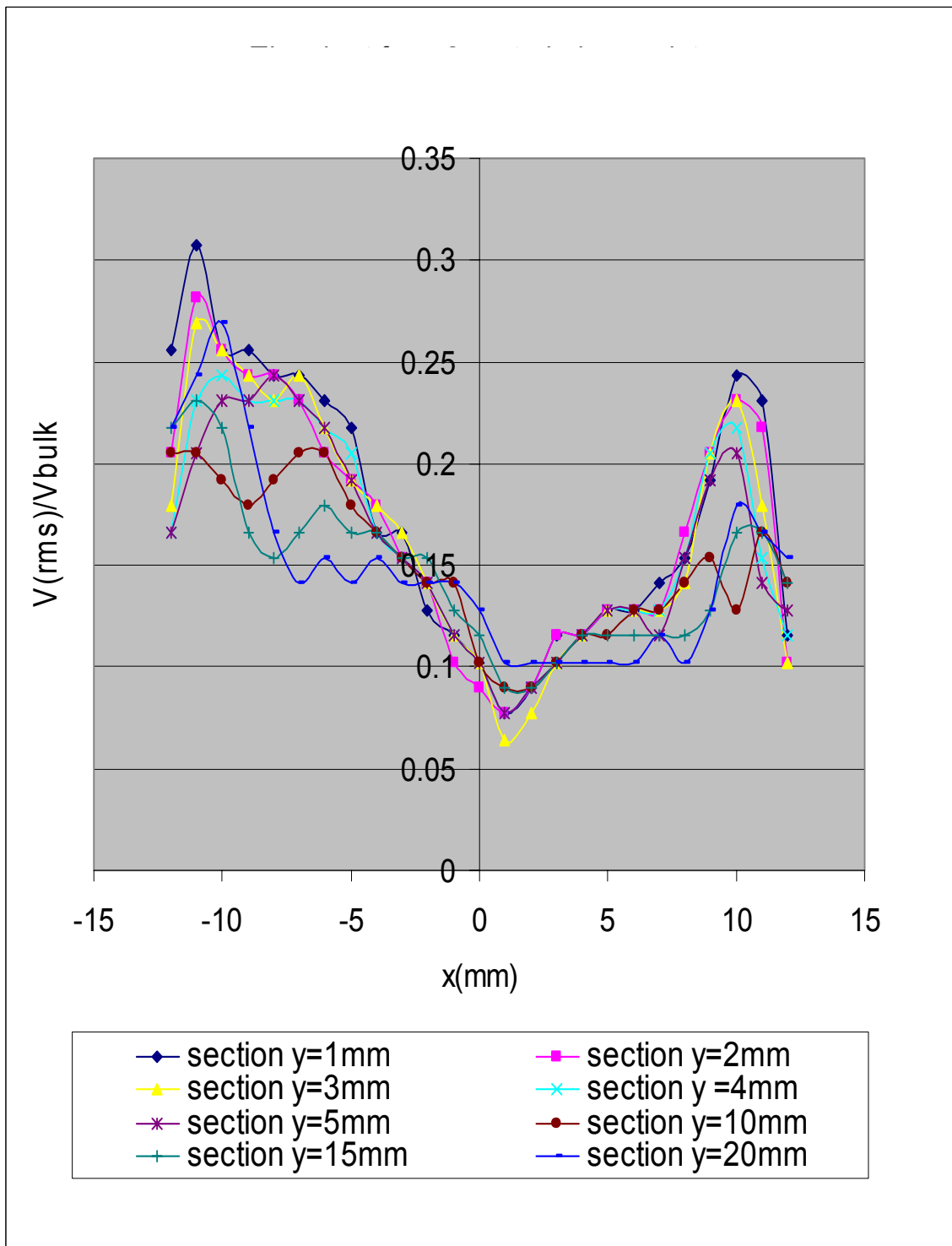
- There is a similarity between graph (1, 2) and graph (7, 8) in velocity ratio profiles except one has a turbulence disc (the first) and one does not (the second). The uniformity of the first is better than the second.
- There is a different velocity ratio profile for each of the three graphs (2, 4, 6) with totally different profiles.
- From graph (1, 3, 5, 7) what is quiet clear the velocity ratio v_{mean} / v_{bulk} at $x = 0$ for all y values is in the range of $1.5 < v_{mean} / v_{bulk} < 2$.
- looking in depth at (1, 3, 5) graphs the inflection point at $x = \pm 9$ is about $1.4 < v_{mean} / v_{bulk} < 1.6$.
- it is noted that in graph 4 is how v_{rms} / v_{bulk} is the range $0.05 < v_{rms} / v_{bulk} < 0.1$ at all y values and then there is a sudden jump in the velocity ratio at $x = \pm 9$ to a value of in the range of $0.125 < v_{rms} / v_{bulk} < 0.2$.
- One of the very clear velocity ratio profiles v_{rms} / v_{bulk} on graph 4 which was not clear in any of the other graphs concerned with 2mm and 4mm plate of all the diagrams is that the velocity profile of 7 parabolic profiles (there are 5 small peaks in the core and 2 large peaks at the tips).
- In graph 6 you can count the number of holes by pointing out the peaks which count to 5 where the core peak is the largest while the 2 peaks on the left and on the right are smaller.
- Considering at graph 2 very closely can only show 5 holes profiles out of 9 due to the unification of the profiles at the core.
- The velocity ratio v_{mean} / v_{bulk} from graph (1, 3, 5, and 7) at $x = \pm 12.5$ for different y values is in the ranges $0.5 < v_{mean} / v_{bulk} < 2.5$.

5.1.3. The Graphs with a turbulence plate:

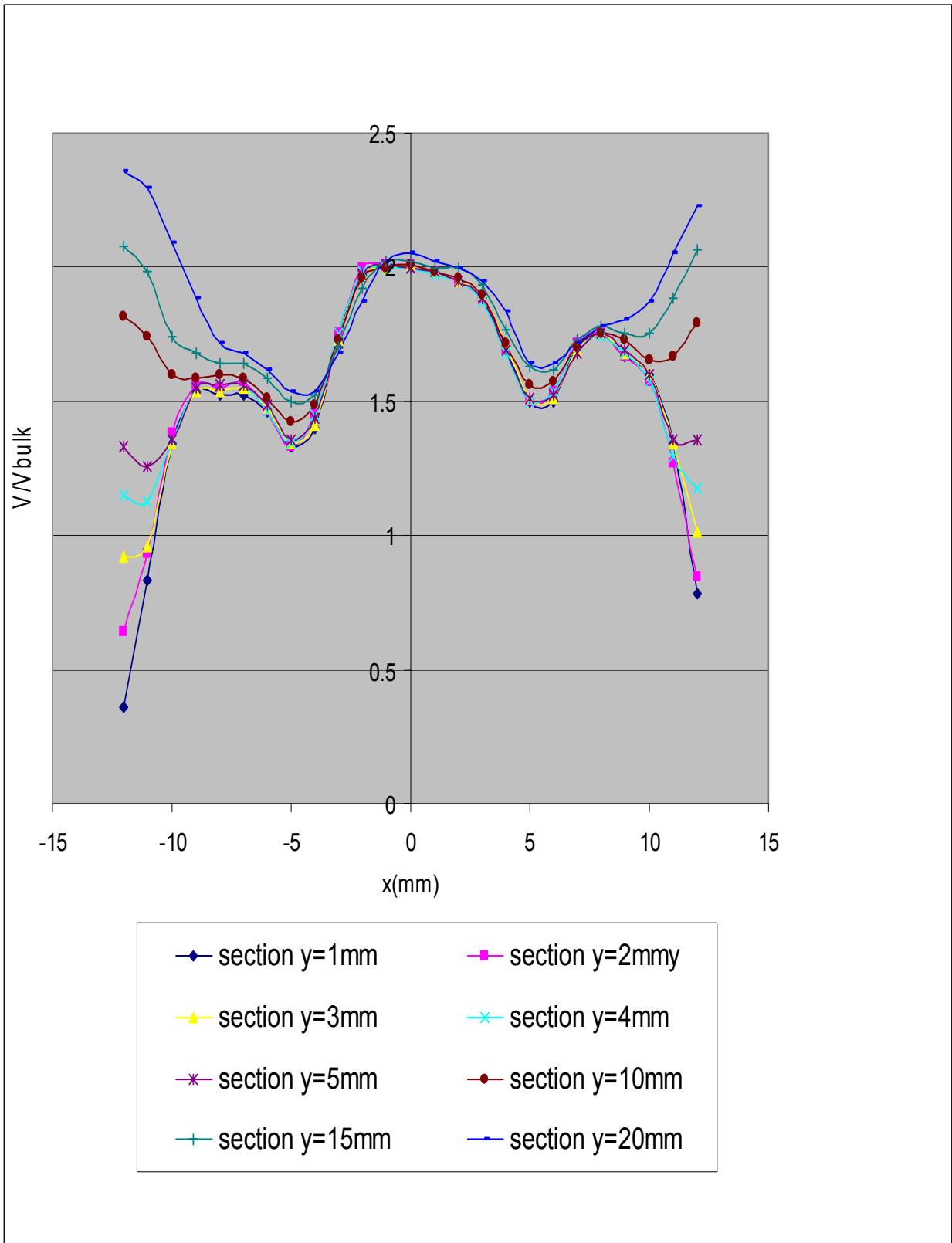
Graph 1: The v/v_{bulk} relation with x and y coordinates for 2 mm disc.



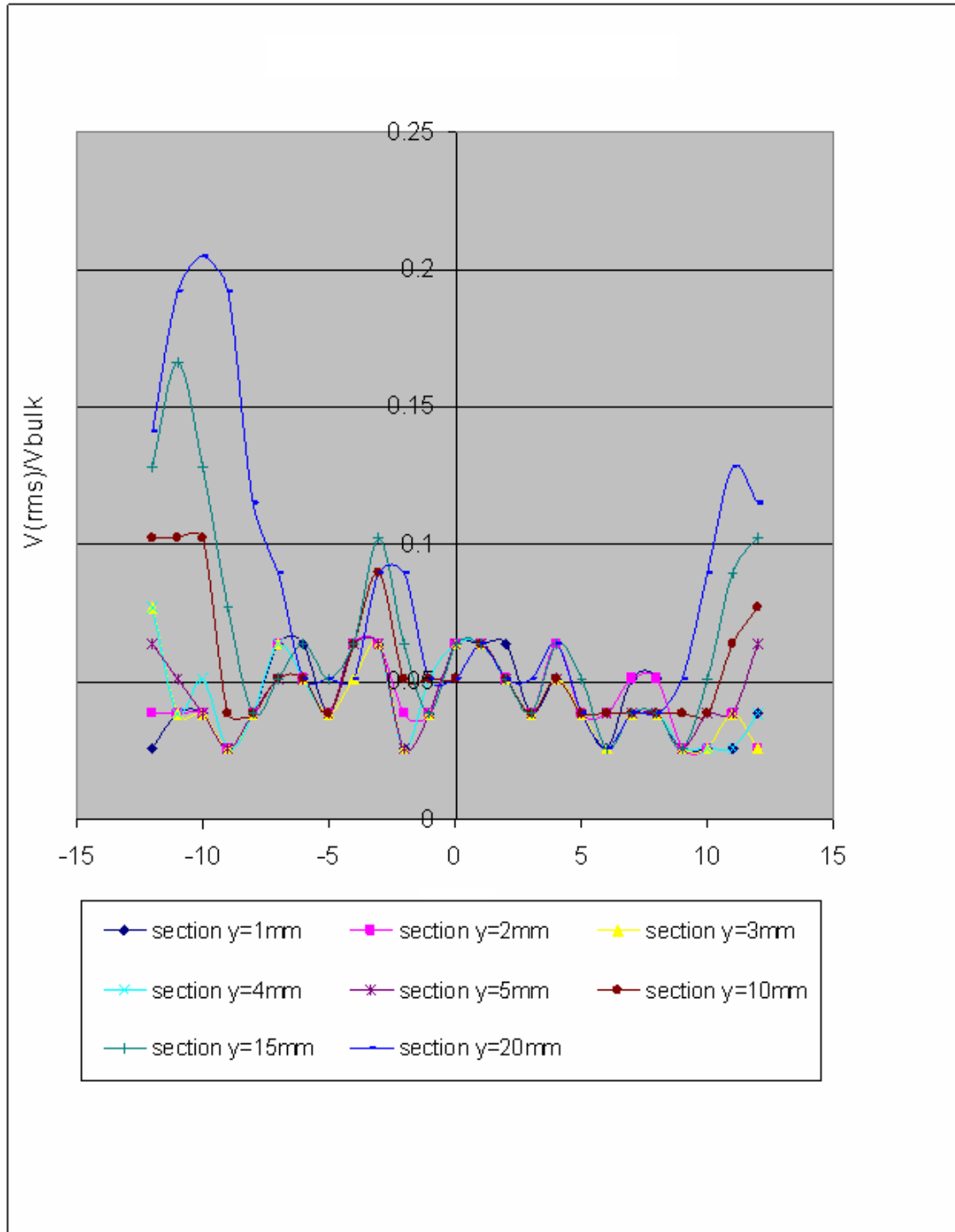
Graph 2: The v_{rms}/v_{bulk} relation with x and y coordinates for 2 mm disc.



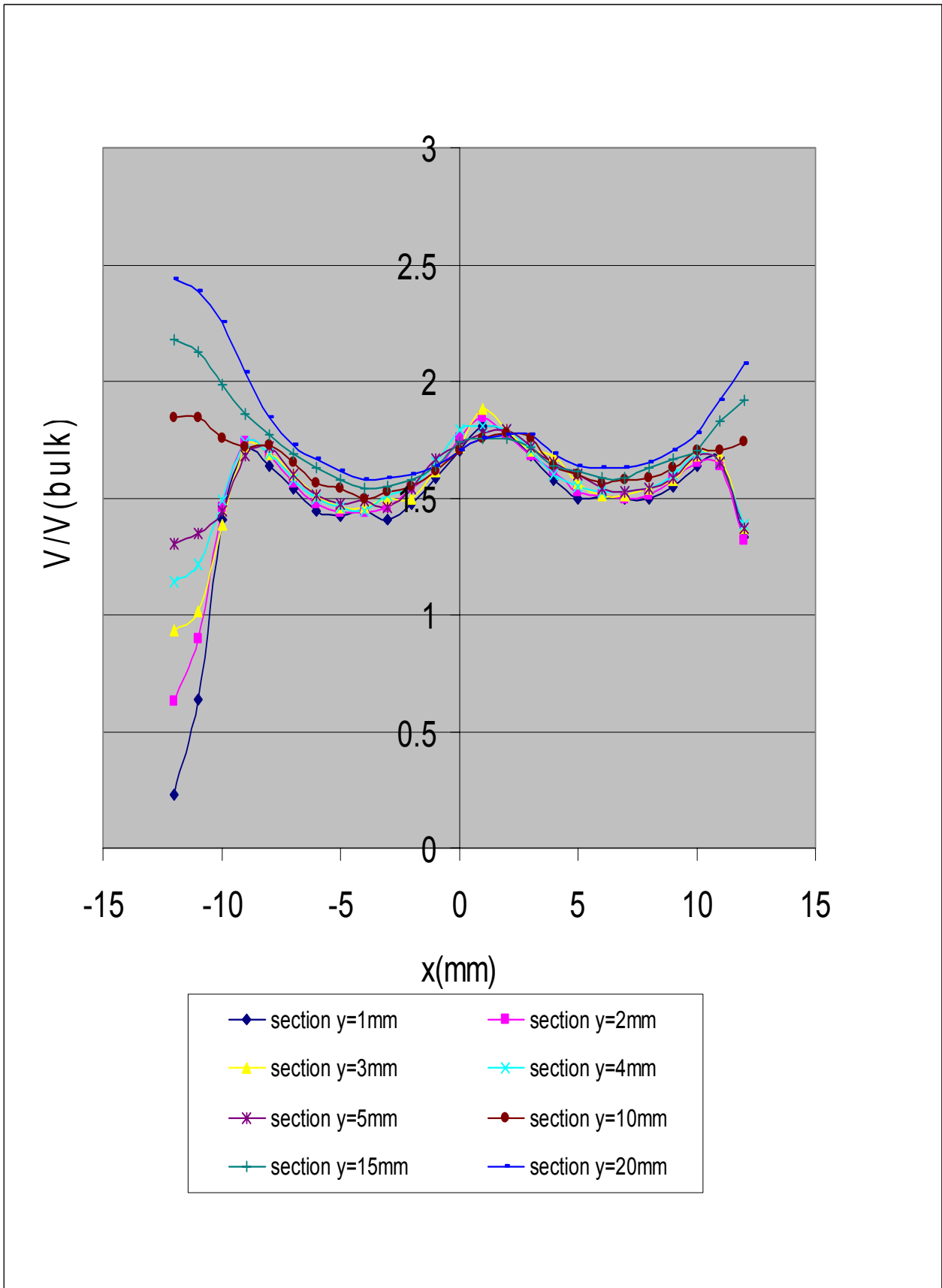
Graph 3: The v/v_{bulk} relation with x and y coordinates for 3 mm disc.



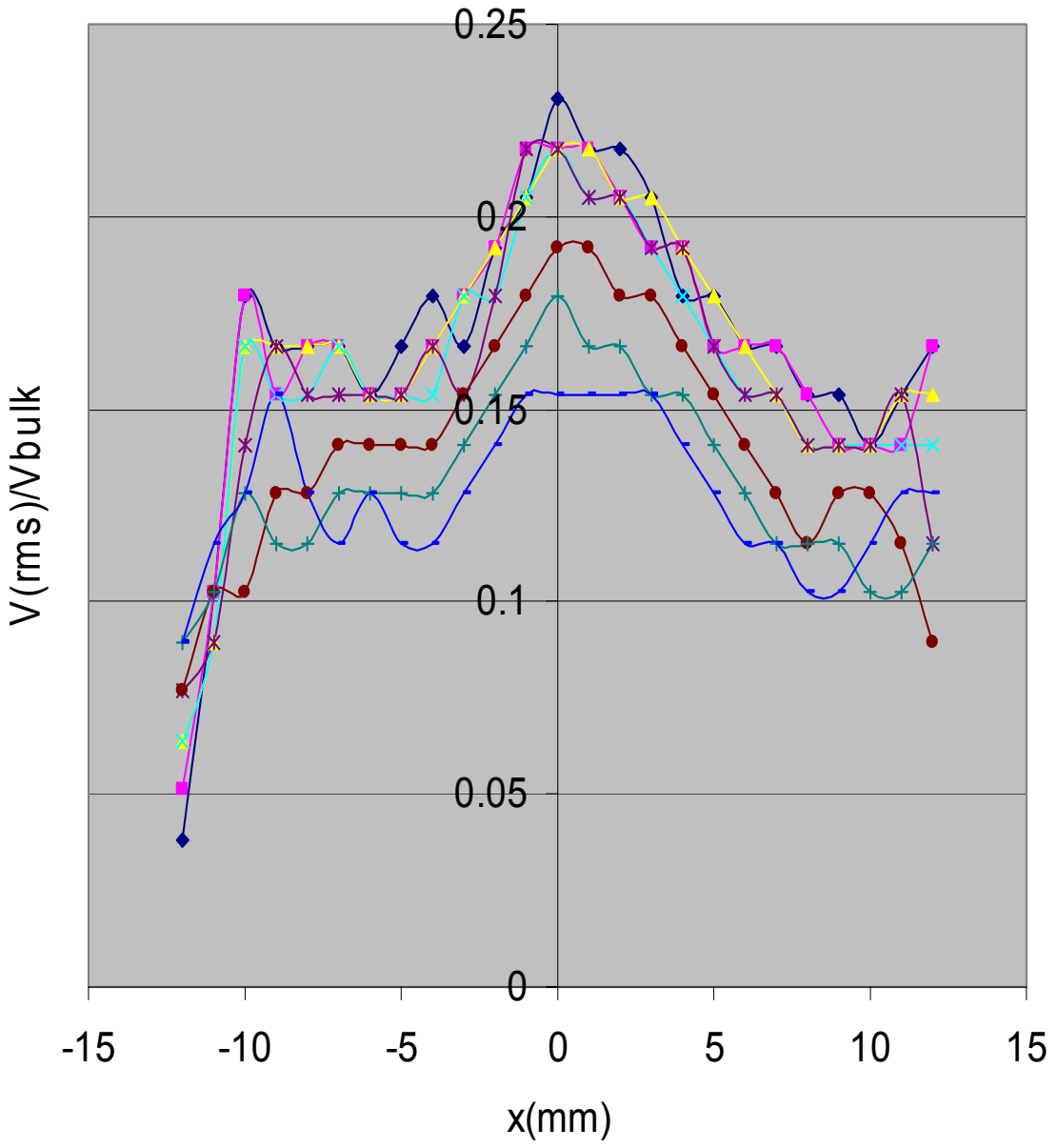
Graph 4: The v_{rms}/v_{bulk} relation with x and y coordinates for 3 mm disc.



Graph 5: The v/v_{bulk} relation with x and y coordinates for 4 mm disc.

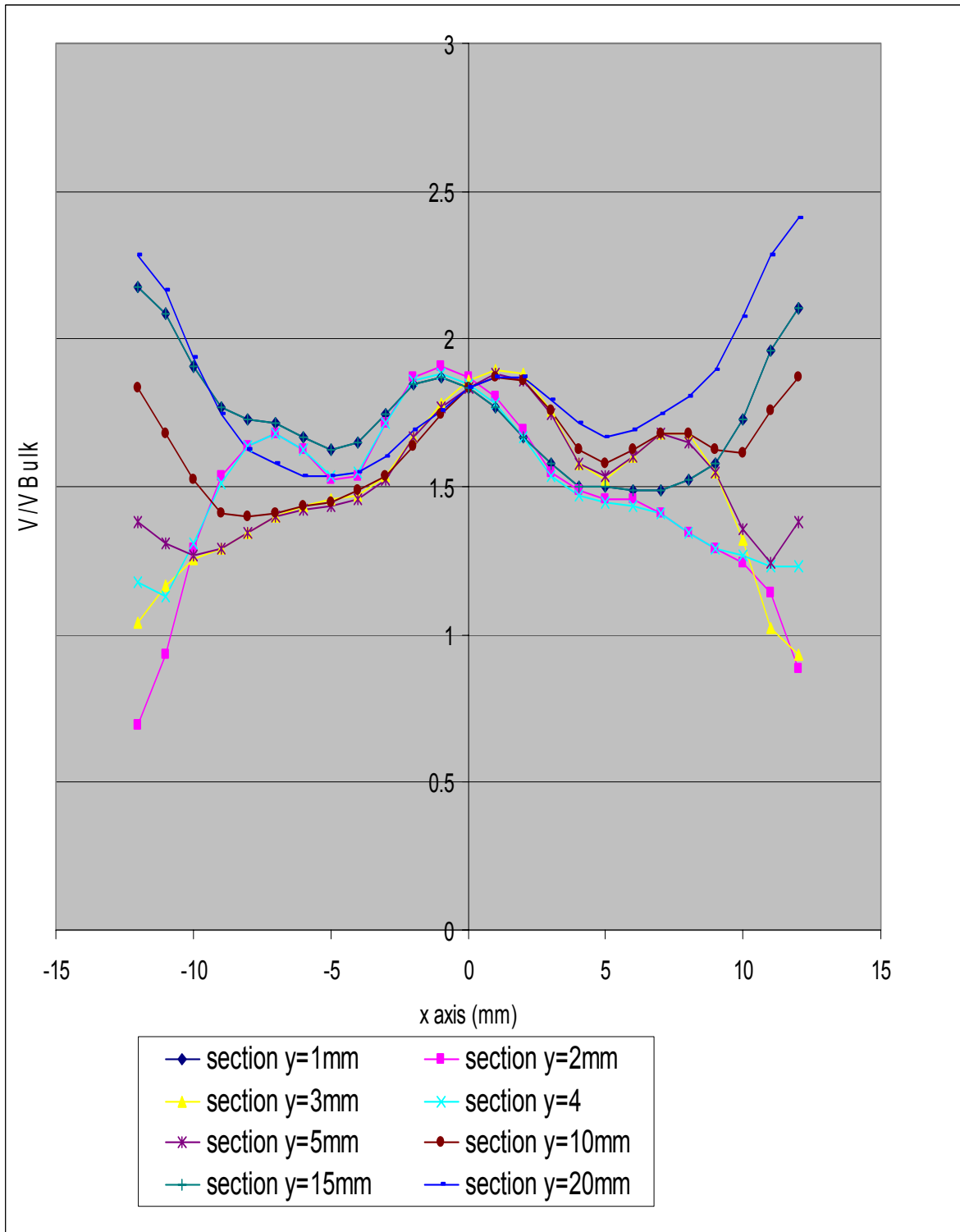


Graph 6: The v_{rms}/v_{bulk} relation with x and y coordinates for 4 mm disc.

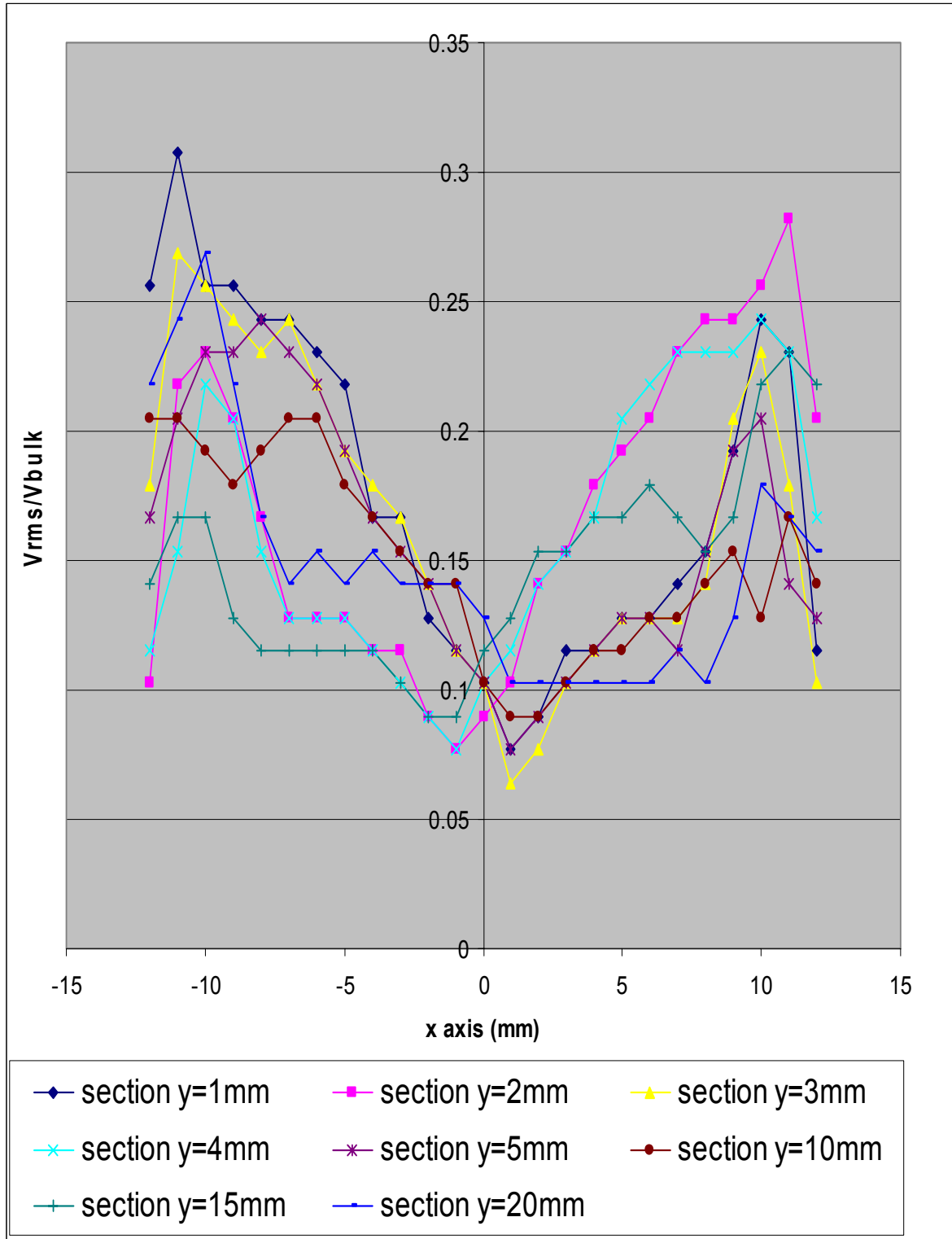


- ◆ section y=1mm
- ▲ section y=2mm
- ▲ section y=3mm
- ✖ section y=4mm
- ✱ section y=5mm
- section y=10mm
- + section y=15mm
- section y=20mm
- section y=2mm
- ✖ section y=4mm
- section y=10mm
- section y=20mm

Graph7: The v/v_{bulk} relation with x and y coordinates for a 25mm diameter tube.



Graph 8: The v_{rms}/v_{bulk} relation with x and y coordinates for a 25mm diameter tube.



5.1.5. The summary chart of the data (Makky chart):

This chart helps out the reader in pointing out directly which turbulence plate has a high or low v_{rms} / v_{bulk} value and the same can be conducted on the value v_{mean} / v_{bulk} . The four cases are represented in the graph. The chart is not that accurate because the method conducted in finding its parameters is averaging the v_{mean} / v_{bulk} for each y value and then taking the average for the averaged values the method is illustrated in the two equations:

$$(v_{mean} / v_{bulk})_{average} = \frac{(v_{mean} / v_{bulk})_{averaged}^{y=1} + (v_{mean} / v_{bulk})_{averaged}^{y=2} + \dots + (v_{mean} / v_{bulk})_{averaged}^{y=20}}{8} \dots (109)$$

$$(v_{rms} / v_{bulk})_{average} = \frac{(v_{rms} / v_{bulk})_{average}^{y=1} + (v_{rms} / v_{bulk})_{average}^{y=2} + \dots + (v_{rms} / v_{bulk})_{average}^{y=20}}{8} .. (110)$$

So to illustrate a 2mm turbulence plate we need two coordinates which are as follows

$$((v_{mean} / v_{bulk})_{average}^{2mm}, (v_{rms} / v_{bulk})_{average}^{2mm}).$$

Note: that the averaged quantities were divided over 8 because the data provided had been taken at the following cross sections y=1 ,y=2 ,y=3 ,y=4 ,y=5 ,y=10 ,y=15 ,y=20.

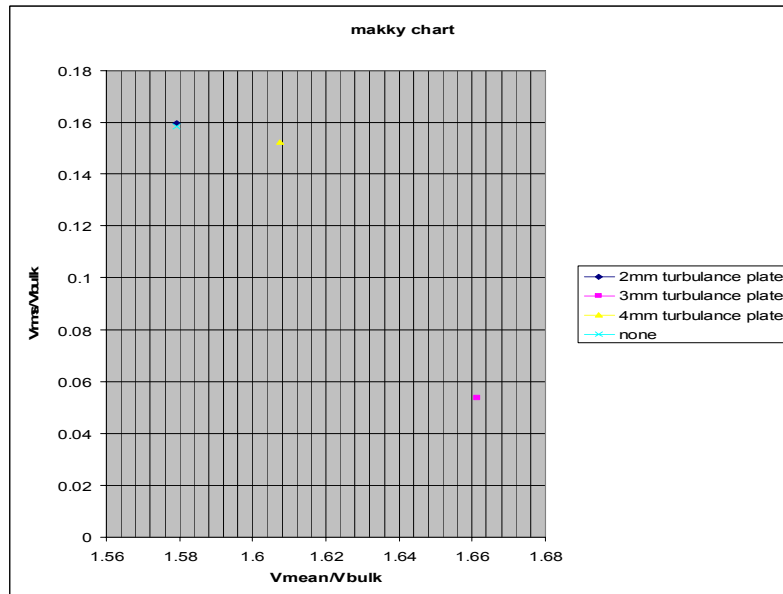


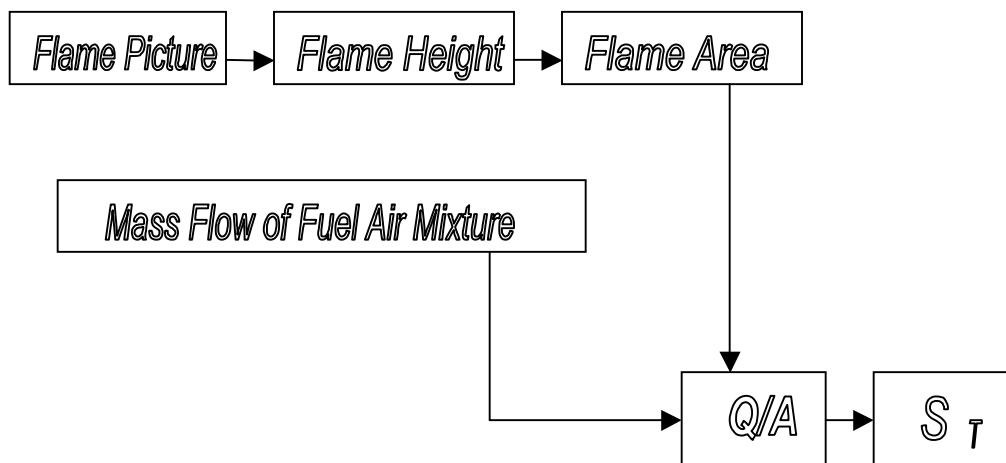
Figure 5-1: the make chart showing the relationship between v_{mean} / v_{bulk} and v_{rms} / v_{bulk} .

5.2. The burning velocity calculation:

5.2.1 Introduction:

More detailed and higher resolution pictures of the flames are illustrated which show clear marks of the scaling. Using Photoshop the change of the colouring of the original flame picture which was provided by a high frame rate camera and its colour had been changed into yellow to show exactly the amount of stretch the flame has because as we know that the flame height has an impact on the burning velocity calculation. With the use of Microsoft picture manger to magnify the picture and see its clear height to be as much accurate as possible in the conducted readings.

5.2.2. The Flow Chart of the calculation procedure for the calculation of the turbulent burning velocity:



This flow chart shows the input data which leads us to burning velocity output, from

Step one: by taking a picture of the flame and knowing the scaling we can measure the height of the flame and in conclusion we can evaluate the flame area.

Step two by just reading the flow meters for the fuel and air we can calculate the total volumetric flow rate.

5.2.3. The first method is using 3dmax software to calculate the flame area.

The description of the method:

The program 3dmax gives the user an option of tracing the flame profile as shown in the figure 1-18 on the right hand side illustration and then giving the lathe command to the profile, in conclusion the profile will be revolved around the mid axis which runs through the flame so the result is a 3d flame, 3dmax is provided with a command to calculate the area of the 3d model which in our case is the flame. At the end of the calculation and not forgetting to subtract the planner face (which has a circular shape) at the bottom of the 3d model so that it would be excluded from the area calculation.

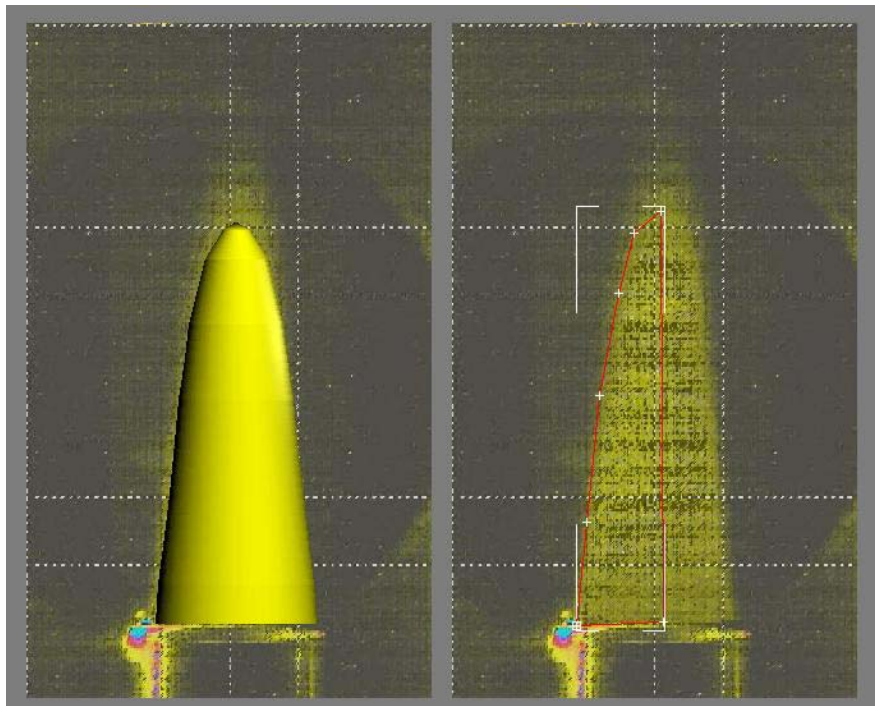


Figure 5-2: The flame is traced by taking points on the surface.

After conducting the previously discussed steps above for the turbulence plate that consists of 2mm holes the program output $267789 \text{ mm}^2 = 0.267789 \text{ m}^2$

5.2.4. The second method used to calculate the flame surface.

To check this calculation mathematically due to the similarity of the flame shape with half an ellipse we can use this equation [26]:

$$\frac{x^2}{a^2} + \frac{y^2}{b^2} + \frac{z^2}{c^2} = 1 \dots\dots\dots (111)$$

The flame has a cigar shape which is also called a Prolate $a = b < c$

$$(Area)_{Prolate} = 2\pi(a^2 + c^2 \frac{\alpha}{\tan \alpha}) \dots\dots\dots (112)$$

Where

$$\alpha = \arccos(\frac{a}{c}) \dots\dots\dots (113)$$

We know that $a=b=12,5\text{mm}$ and $c=65\text{mm}$

After substituting the constants in $\alpha = \arccos(\frac{a}{c})$ we find that $\alpha = 78.9^\circ$, for our case we

have to take half the area of the Porlate:

$$(Area)_{Prolate} = 2\pi(a^2 + c^2 \frac{\alpha}{\tan \alpha})$$

$$(Area)_{Prolate} = 205954.67\text{mm}^2 = 0.205954678\text{m}^2$$

Using the cone method [27] the flame area has the following answer:

$$2597.99\text{mm}^2 = 0.259799\text{m}^2$$

5.2.5. The third method assuming the flame area as a cone area.

The flow bulk velocity is calculated in the following way:

$$Q = AV_{Bulk} \Rightarrow V_{Bulk} = \frac{Q}{A} = \frac{0.000383}{3.14 \times (12.5 \times 0.001)^2} = 0.780694 \frac{\text{m}}{\text{sec}} = 78.0636 \frac{\text{cm}}{\text{sec}}$$

Finding the laminar burning velocity S_L :

We have the equivalence ratio which is $\phi = 1.43$ and we know that our gas is methane

$$CH_4 \text{ so from appendix D we can find the burning velocity } S_L = 31.2 \frac{\text{cm}}{\text{sec}} = 31.2 \times 10^{-2} \frac{\text{m}}{\text{sec}}$$

Finding the turbulent burning velocity S_T :

During the lab test readings were taken to know what the flow rate is Q , and it was as

$$\text{follows } Q = 23 \left(\frac{\text{liter}}{\text{min}} \right) = 3.83 \times 10^{-4} \left(\frac{\text{m}^3}{\text{sec}} \right) \text{ where H refers to the height of the cone and R}$$

the radius of the cone base.

$$A = \pi R \sqrt{(H^2 + R^2)} + \pi R^2 \dots\dots\dots (114)$$

But because we are only interested with the cone area and not the cone base area the second term is neglected in the equation so this leads us to following form:

$$A = \pi R \sqrt{(H^2 + R^2)} \dots\dots\dots (115)$$

Then just by the substitution of the parameters in the continuity equation this will lead us to the calculation of the turbulent burning velocity.

$$Q = AS_T \Rightarrow S_T = \frac{Q}{A} \dots\dots\dots (116)$$

The characteristic width flow in a jet flow L would be the local width of the jet at any axial location as can be seen on figure.

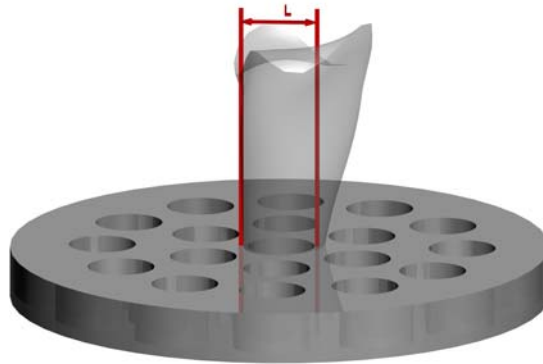


Figure 5-3: The turbulence plate and a flow existing one of the holes that has a diameter D which is equal to L.

$$\delta_l = \frac{D_m}{S_L} \dots\dots\dots (117)$$

The integral length scale of turbulence $L_T =$ The hole diameter

Laminar flame thickness = δ_l

$$\frac{L_T}{\delta_l} = \text{cons tan } t \dots\dots\dots (118)$$

Table 1: burning velocity calculation for a 2mm disc

Burning Velocity Calculation for 2mm Turbulance Plate :			
Height	0.065	m	
Cone diameter	0.01	m	
The Equivalence Ratio	1.43		
Area	0.002065013	m ²	
Flow Rate	0.000383	m ³ /sec	
Burning Velocity	0.185471024	m/sec	18.5471 cm/sec
$\frac{L_T}{\delta_l}$	29.71428571		
Integral Length Scale of Turbulence	2	mm	0.002 m
Laminar Burning Velocity	0.312	m/sec	31.2 cm/sec
Thermal Diffusivity	0.000021	m ² /sec	
Flame Thickness	6.73077E-05	(m)	0.067308 (mm)

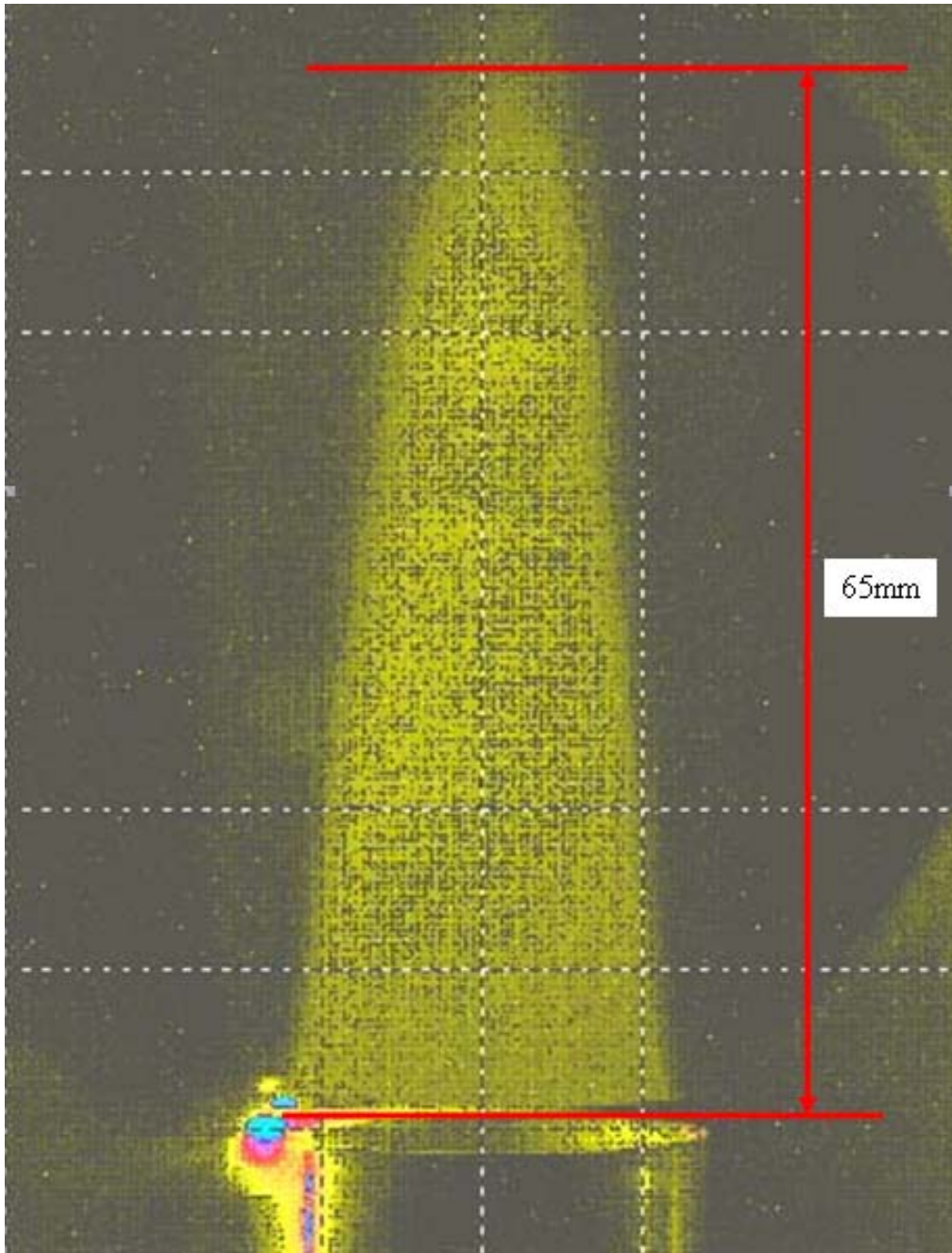


Figure5-4: shows the flame while a 2mm turbulence plate was tested and the scaling considered.

Table 2: burning velocity calculation for a 3mm disc

Burning Velocity Calculation for 3mm Turbulance Plate :			
Height	0.067	m	
Cone diameter	0.01	m	
The Equivalence Ratio	1.43		
Area	0.002127	m ²	
Flow Rate	0.000383	m ³ /sec	
Burning Velocity	0.180057	m/sec	18.0057 cm/sec
$\frac{L_T}{\delta_l}$	44.57143		
Integral Length Scale of Turbulence	3	mm	0.003 m
Laminar Burning Velocity	0.312	m/sec	31.2 cm/sec
Thermal Diffusivity	0.000021	m ² /sec	
Flame Thickness	6.73077E-05	(m)	0.067308 (mm)

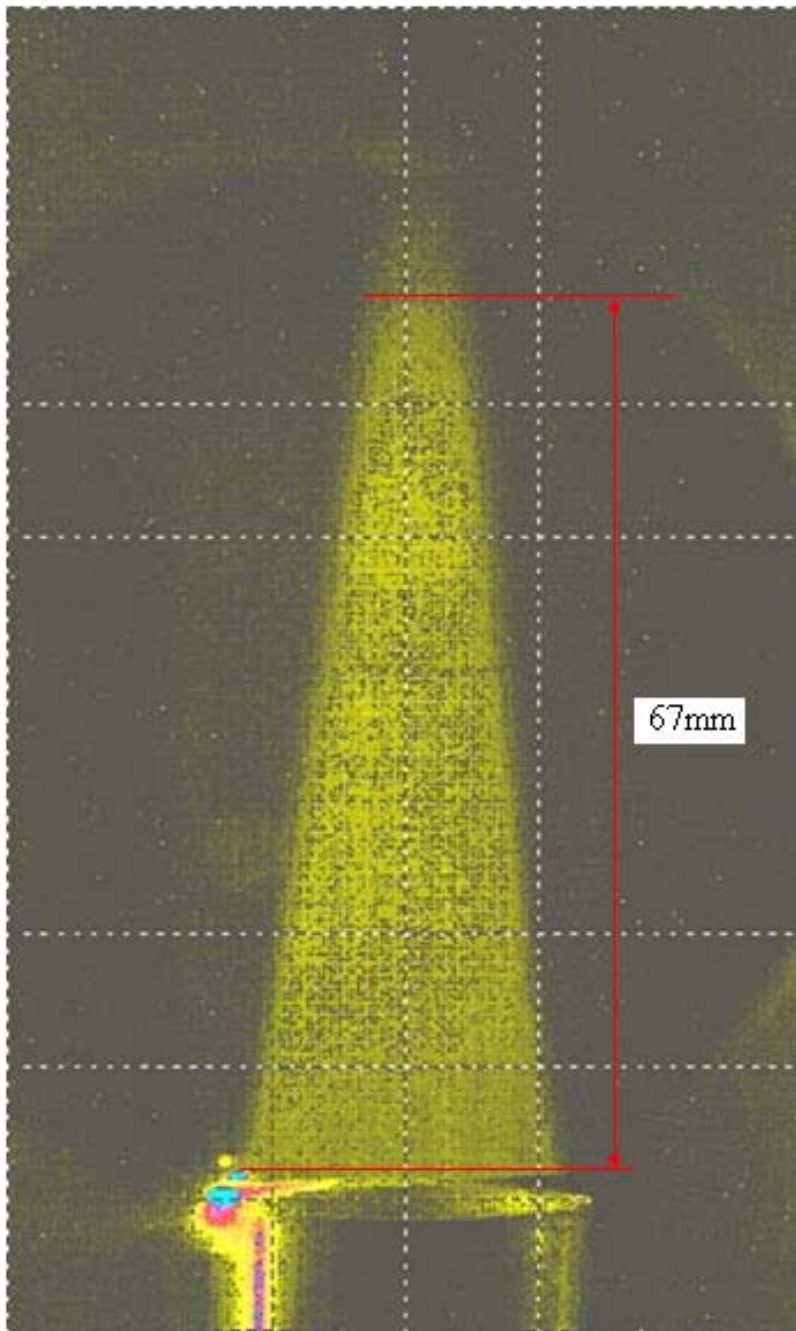


Figure5-5: shows the flame while a 3mm turbulence plate was tested and the scaling considered.

Table 3: burning velocity calculation for a 4mm disc

Burning Velocity Calculation for 4mm Turbulance Plate :			
Height	0.068	m	
Cone diameter	0.01	m	
The Equivalence Ratio	1.43		
Area	0.002158	m ²	
Flow Rate	0.000383	m ³ /sec	
Burning Velocity	0.177466	m/sec	17.74656 cm/sec
$\left[\frac{L_T}{\delta_l} \right]$	59.42857		
Integral Length Scale of Turbulence	4	mm	0.004 m
Laminar Burning Velocity	0.312	m/sec	31.2 cm/sec
Thermal Diffusivity	0.000021	m ² /sec	
Flame Thickness	6.73077E-05	(m)	0.067308 (mm)

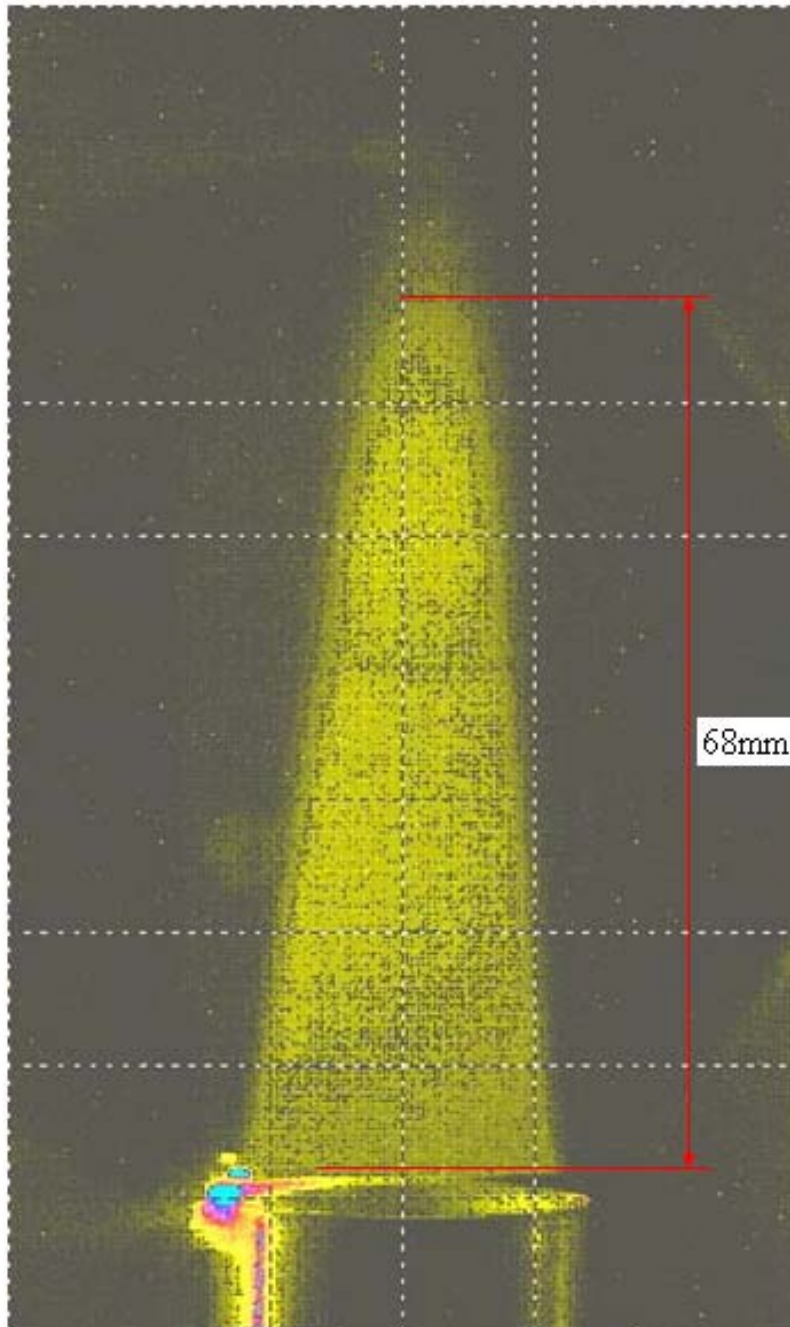


Figure5-6: shows the flame while a 4mm turbulence plate was tested and the scaling considered.

5.2.6. Flame thickness:

Flame thickness can be found by just having a picture of the flame and changing its colour status on Photoshop flame thickness can be visible where it is for the 2mm turbulence plate its about 1mm at the bottom of the flame and about 1.5mm at the top. This case for a turbulent flame in comparison with a laminar flame for an equivalence ratio of $\phi = 1.43$ the flame thickness is about 1.9mm [3].

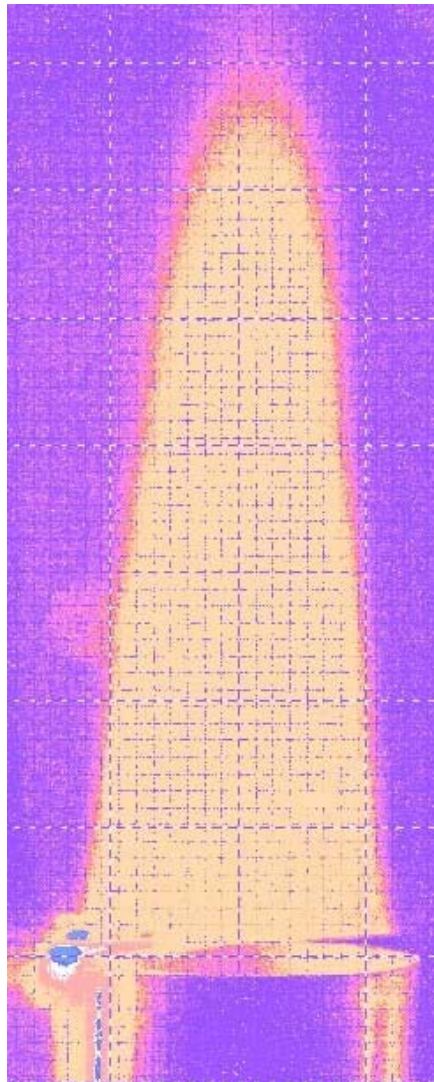


Figure5-7: flame thickness is visible with its several layers.

5.3. Turbulence plate parameters:

Table 4: 2mm Turbulence plate parameters

The 2mm Turbulence Plate Parameters:	
Number Of Holes	61
The Area of each Hole (mm)	3.14E-06
The Diameter of the Holes (mm)	2
The Diameter of the holes (m)	0.002
The Velocity Output (each hole)	1.999582
The total Flow Rate (m ³ /sec)	0.000383
The Mach Number Output	0.006402
The Flow Rate for each Hole (m ³ /sec)	6.28E-06
The Speed of sound for the Mixture (m/sec)	312.3485
The Temperature of the Mixture before the plate (K)	293
The Polytrophic Constant	1.03E+00
The Temperature of the Mixture(K)	313
The Ideal Gas Constant	321.7743
The Molar Mixture	25.83798
The Specific Heat Capacity at Constant Pressure of Air	1.004
The Specific Heat Capacity at Constant Pressure of Methane	36.20503004
The Percentage of the Air%	0.756767887
The Percentage of the Methane%	0.243232113
The Temperature of Air	20 C
The Temperature of Methane	20 C
	313 K
	313 K

Table 5: 2mm turbulence plate Reynolds number and pressure drop work sheet.

The 2mm Turbulence Plate Pressure Drop and Reynolds Number Work Sheet :			
The Mass Flow Rate(m ³ /sec)	6.27869E-06	Hole Diameter(m)	0.002
Air Kinematic Viscosity(m ² /s)	1.83E-06	Air Percentage%	0.756768
Fuel Kinematic Viscosity(m ² /s)	1.09E-04	Methane Percentage%	0.243232
Mixture Viscosity(m ² /s)	2.79E-05	Number of Holes	61
Pressure Drop for a Singe Hole(N/m ² /m)	-446.262		
Plate Thickness (mm)	3	Plate Thickness (m)	0.003
Single Pressure Drop(N/m ²)	-	Total Pressure Drop(N/m ²)	-81.6659
The Reynolds Number for a single hole	1.49E+02		
Air Density (m ³ /kg)	1.190475213		
Methane Density(m ³ /kg)	0.574712172		
Mixture Density(m ³ /kg)	1.040701867		
Velocity of Mixture(m/sec)	1.999582333		

Table 6: 3mm Turbulence plate parameters

The 3mm Turbulence Plate Parameters:	
Number Of Holes	37
The Area of each Hole (mm)	7.07E-06
The Diameter of the Holes (mm)	3
The Diameter of the holes (m)	0.003
The Velocity Output (each hole)	1.465159
The total Flow Rate (m ³ /sec)	0.000383
The Mach Number Output	0.004691
The Flow Rate for each Hole (m ³ /sec)	1.04E-05
The Speed of sound for the Mixture (m/sec)	312.3485
The Temperature of the Mixture before the plate (K)	293
The Polytrophic Constant	1.03E+00
The Temperature of the Mixture(K)	313
The Ideal Gas Constant	321.7743
The Molar Mixture	25.83798
The Specific Heat Capacity at Constant Pressure of Air	1.004
The Specific Heat Capacity at Constant Pressure of Methane	36.20503
The Percentage of the Air%	0.756768
The Percentage of the Methane%	0.243232
The Temperature of Air	20 C
The Temperature of Methane	313 K
	20 C
	313 K

Table 7: 3mm turbulence plate Reynolds number and pressure drop work sheet.

The 3mm Turbulence Plate Pressure Drop and Reynolds Number Work Sheet :	
The Mass Flow Rate(m ³ /sec)	1.04E-05
Air Kinematic Viscosity(m ² /s)	1.83E-06
Fuel Kinematic Viscosity(m ² /s)	0.000109
Mixture Viscosity(m ² /s)	2.79E-05
Pressure Drop for a Single Hole(N/m ² /m)	-145.329
Plate Thickness (mm)	3
Single Pressure Drop(N/m ²)	-0.43599
The Reynolds Number for a single hole	163.9729
Air Density (m ³ /kg)	1.190475
Methane Density(m ³ /kg)	0.574712
Mixture Density(m ³ /kg)	1.040702
Velocity of Mixture(m/sec)	1.465159
Hole Diameter(m)	0.003
Air Percentage%	0.756768
Methane Percentage%	0.243232
Number of Holes	37
Plate Thickness (m)	0.003
Total Pressure Drop(N/m ²)	-16.1315

Table 8: 4mm Turbulence plate parameters

The 4mm Turbulence Plate Parameters:	
Number Of Holes	19
The Area of each Hole (mm)	1.26E-05
The Diameter of the Holes (mm)	0.004
The Velocity Output (each hole)	0.000383
The Mach Number Output	2.02E-05
The Speed of sound for the Mixture (m/sec)	293
The Polytrophic Constant	313
The Ideal Gas Constant	25.83798
The Specific Heat Capacity at Constant Pressure of Air	1.004
The Specific Heat Capacity at Constant Pressure of Methane	36.20503
The Percentage of the Air%	0.756768
The Percentage of the Methane%	0.243232
The Temperature of Air	20 C
The Temperature of Methane	20 C
The Flow Rate for each Hole (m ³ /sec)	313 K
The Temperature of the Mixture(K) before the plate (K)	313 K
The Molar Mixture	25.83798

Table 9: 4mm turbulence plate Reynolds number and pressure drop work sheet.

The 4mm Turbulence Plate Pressure Drop and Reynolds Number Work Sheet :			
The Mass Flow Rate (m ³ /sec)	2.02E-05	Hole Diameter(m)	0.004
Air Kinematic Viscosity(m ² /s)	1.83E-06	Air Percentage%	0.756768
Fuel Kinematic Viscosity(m ² /s)	0.000109	Methane Percentage%	0.243232
Mixture Viscosity(m ² /s)	2.79E-05	Number of Holes	19
Pressure Drop for a Singe Hole(N/m ² /m)	-89.5459		
Plate Thickness (mm)	3	Plate Thickness (m)	0.003
Single Pressure Drop(N/m ²)	-0.26864	Total Pressure Drop(N/m ²)	-5.10412
The Reynolds Number for a single hole	239.4867		
Air Density (m ³ /kg)	1.190475		
Methane Density(m ³ /kg)	0.574712		
Mixture Density(m ³ /kg)	1.040702		
Velocity of Mixture(m/sec)	1.604928		

Table 10: General Data on all turbulence discs:

Discharge coefficient	0.55	0.57	0.63
Holes Diameter(mm)	2	3	4
Reynolds Number	149	164	239
L/D Ratio	1.5	1	0.75
Blockage Ratio%	61	47	51

5.4. The factors affecting the Turbulent Burning velocity:

1-The relation between the burning velocity and integral length scale over laminar flame thickness:

With the reliance on the data provided on (tables 4, 5, 6) the following graph can be plotted

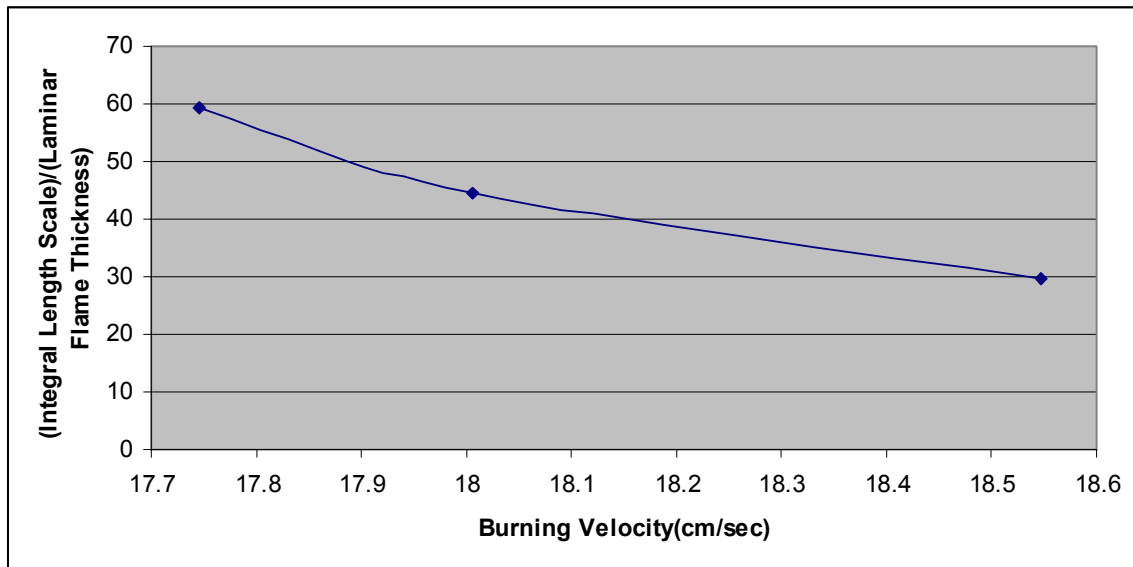


Figure5-8: The relation between the burning velocity and ratio L_T / δ_L .

What is clear is that with the increase in burning velocity there is a decrease in L_T / δ_L this also means for the case of a 2 mm turbulence disc there is bigger flame thickness than for the 4mm disc.

2-The relation between the burning velocity and the number of holes:

To plot this graph the data was gathered from tables (4, 5, and 6) for burning velocities and tables (7, 8, and 9) for the number of holes in each disc.

It is obvious that with the increase in burning velocity there is an increase in the number of holes on the turbulence disc.

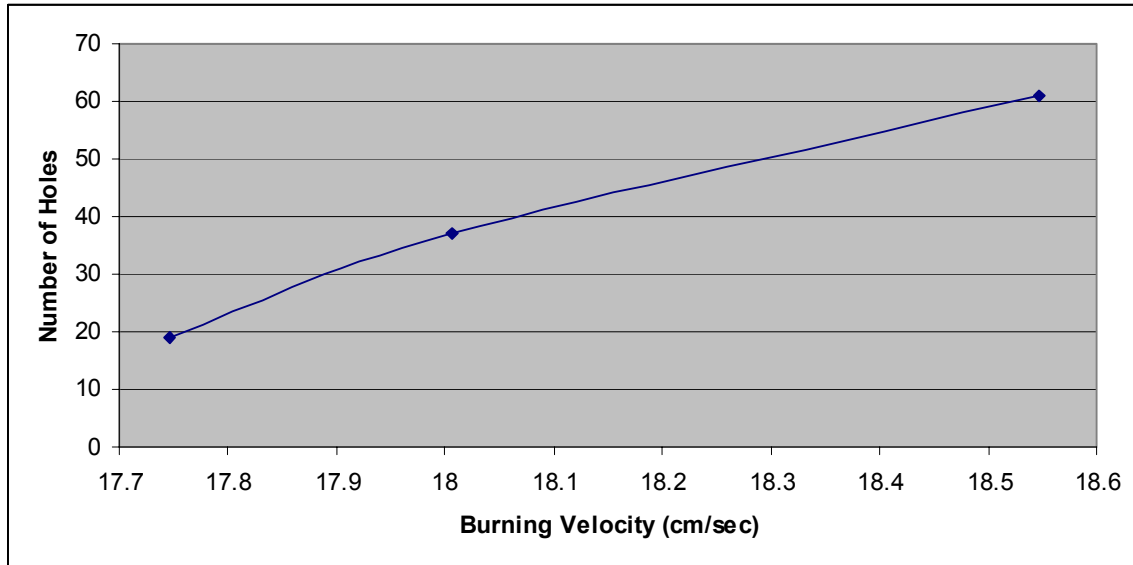


Figure 5-9: The relation between the burning velocity and the number of holes.

3-The relation between the burning velocity and the diameter of the holes:

The hole size in the turbulence disc has an effect on the burning velocity the smaller the hole size the better burning you have.

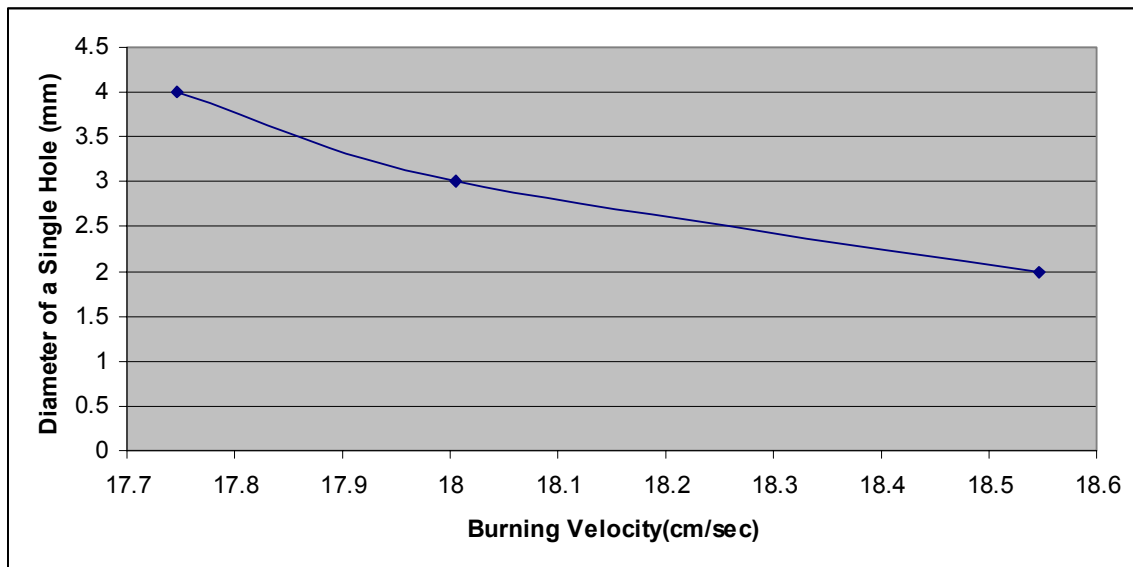


Figure 5-10: The relation between the burning velocity and the diameter of a single hole.

The data for this graph was taken from establishing a relation between the burning velocities in tables (4, 5, and 6) and hole diameters in tables (7, 8, and 9).

4-The relation between the burning velocity and the Reynolds Number:

The graph was plotted after establishing a relation between the burning velocity in tables (4, 5, and 6) and the Reynolds numbers in tables (7, 8, and 9).

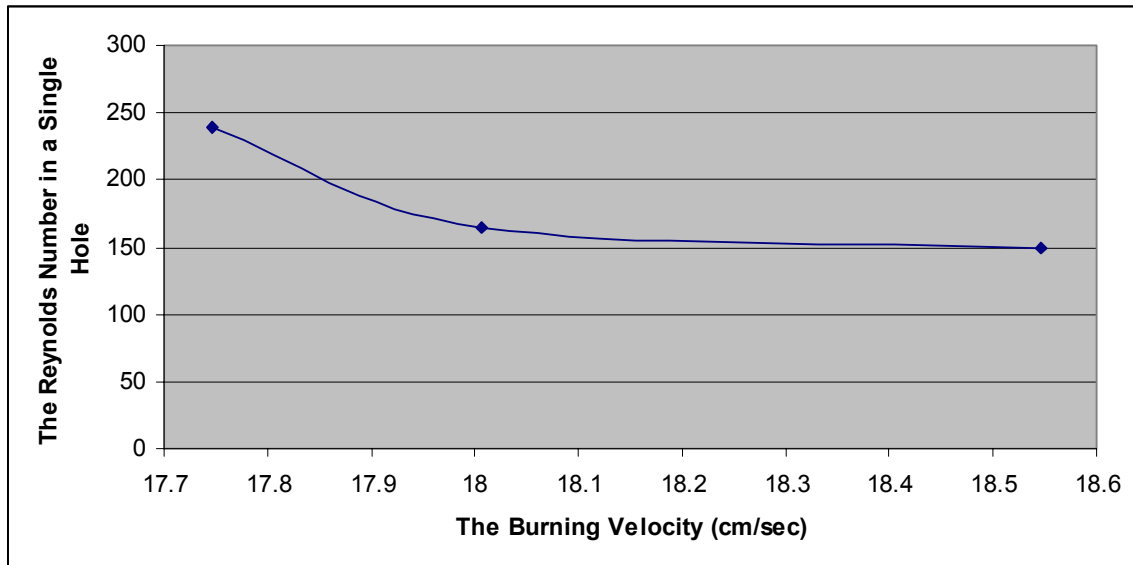


Figure 5-11: The relation between the burning velocity and the number of holes.

The smaller the Reynolds number the higher the burning velocity

5-The relation between the burning velocity and the discharge coefficient:

The graph was plotted after establishing a relation between the burning velocity in tables (4, 5, and 6) and data for discharge coefficients from reference [7]:

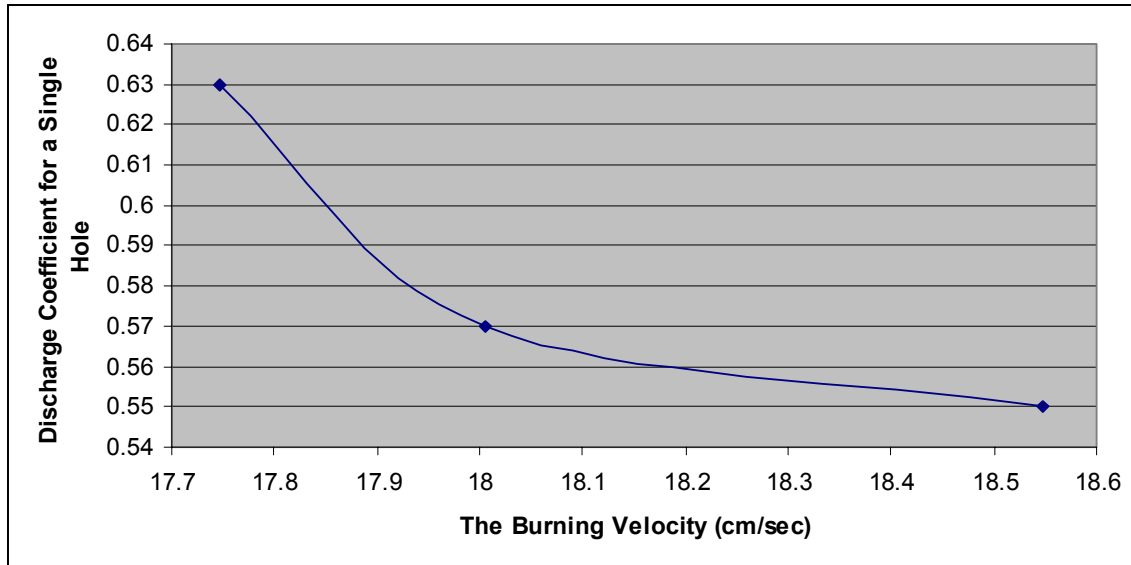


Figure 5-12: The relation between the burning velocity and the number of holes.

It's clear that having low discharge coefficient you means that there is a better burning velocity.

6-The relation between the burning velocity and the ratio l/D (plate thickness over hole diameter):

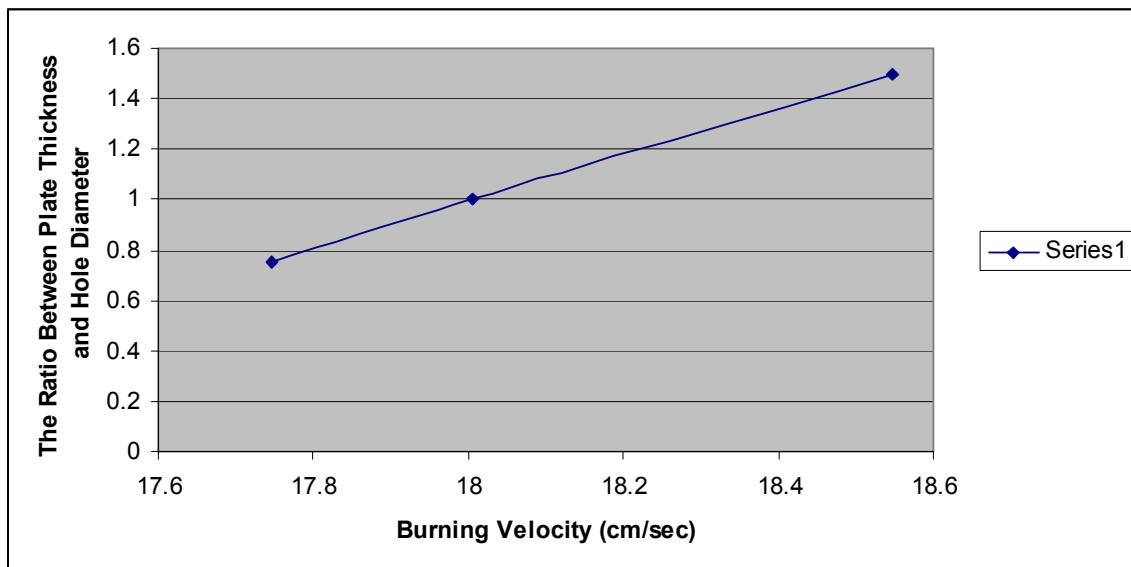


Figure 5-13: The relation between the burning velocity and the holes diameter.

Gathering and linking the info from tables (4, 5, 6) for the burning velocity with l/D in table 10 the figure is plotted.

7-The relation between the burning velocity and single hole pressure drop:

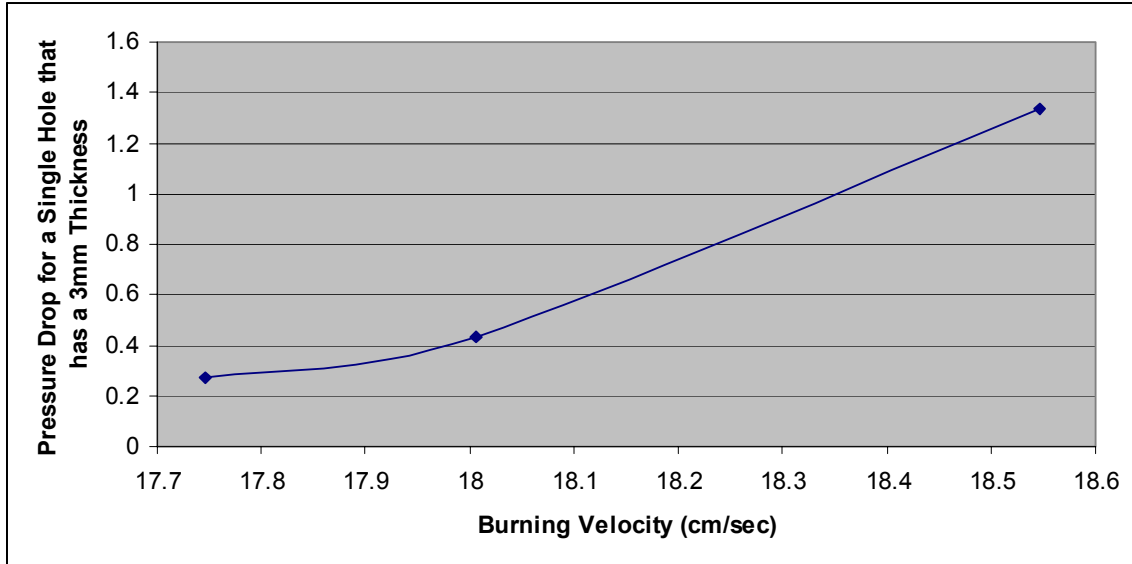


Figure 5-14: The relation between the burning velocity and the holes diameter.

By linking the info provided in table (4, 5, and 6) for burning velocities with the pressure drop for a single hole in tables (7, 8, and 9) the figure is plotted.

What is obvious the bigger the pressure drop the higher the burning velocity.

8-The relation between the burning velocity and Blockage Ratio%:

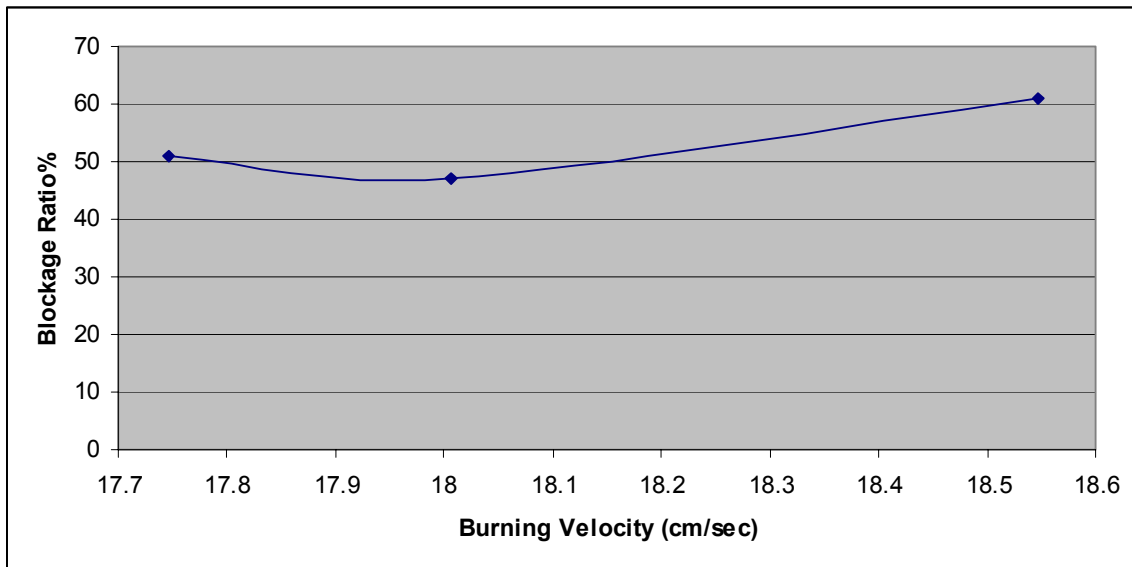


Figure 5-15: The relation between the burning velocity and blockage ratio.

Gathering and linking the info from tables (4, 5, and 6) for the burning velocity with the blockage ratio% in table 10 the figure is plotted.

The higher the blockage ratio the better results you get for burning velocities notice that for the mid point it's an inflection point.

5.5. The calculation of the Kolmogrov scales for the three turbulence discs:

A-2mm Turbulence disc:

$$l_0 = D_{2mm} / 10 = 0.2mm$$

$$Re_{2mm} = \frac{(v_{rms}^{y=1})_{average} D}{\nu} = \frac{0.138 \times 2 \times 0.001}{2.79 \times 10^{-5}} = 9.89$$

$$l_k^{2mm} = l_0 Re^{-3/4} = 0.035mm$$

B-3mm Turbulence disc:

$$l_0 = D_{3mm} / 10 = 0.3mm$$

$$Re_{3mm} = \frac{(v_{rms}^{y=1})_{average} D}{\nu} = \frac{0.034 \times 3 \times 0.001}{2.79 \times 10^{-5}} = 3.65$$

$$l_k^{3mm} = l_0 Re^{-3/4} = 0.113mm$$

C-4mm Turbulence disc:

$$l_0 = D_{4mm} / 10 = 0.4mm$$

$$Re_{4mm} = \frac{(v_{rms}^{y=1})_{average} D}{\nu} = \frac{0.1316 \times 4 \times 0.001}{2.79 \times 10^{-5}} = 18.86$$

$$l_k^{4mm} = l_0 Re^{-3/4} = 0.044mm$$

From this data what is visible that the Kolmogrov scales are smallest with the 3mm size of the holes.

5.6. The use of the Borghi to specify where the turbulence discs are situated:

A-For the flame using turbulence plate 2mm:

$$\frac{L_T}{\delta_L} = 30$$

$$\frac{u_{rms}}{S_L} = 0.442$$

B-For the flame using turbulence plate 3mm:

$$\frac{L_T}{\delta_L} = 44$$

$$\frac{u_{rms}}{S_L} = 0.108$$

C-For the flame using turbulence plate 4mm:

$$\frac{L_T}{\delta_L} = 59$$

$$\frac{u_{rms}}{S_L} = 0.42$$

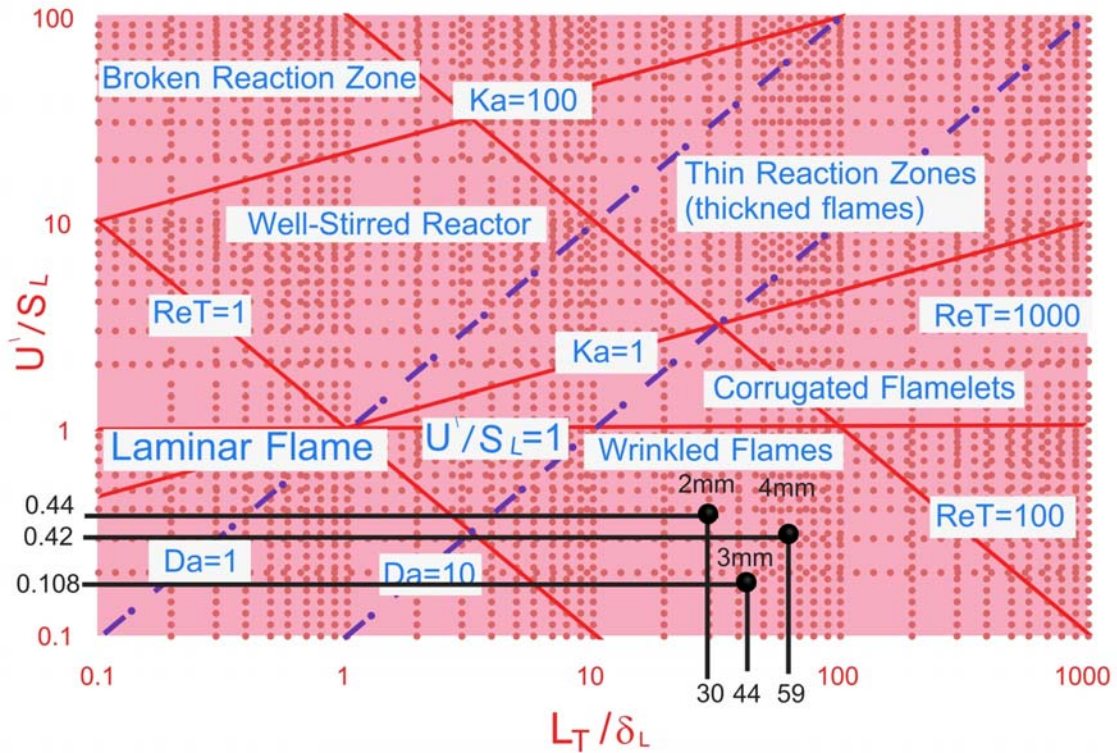


Figure 5-16: The turbulence discs are shown on the Borghi/Peters chart.

7. Conclusion:

1- The discharge coefficient of the turbulence plates has an effect on the burning velocity and that was noticed when low discharge coefficients were used higher burning velocities were achieved.

2- The number of holes and their size had an effect on the burning velocity the smaller the holes the better the burning whereas concerning the number of holes the larger the number of holes the better the burning was.

3- Pre-heat has also an effect on the size of the eddies on the turbulence plate which in turn should increase the v_{rms}/v_{bulk} .

4- The increase in loss of pressure has a noticeable effect on the burning velocity which mean that the fuel air mixture is given time to react in the and by looking at graph 2 what we can see is that due to the low velocity ratio in the core and the velocity ratio at the tips gives the fuel air mixture time and the proper place to burn.

5- The blockage ratio has an affect and that is in increasing the burning velocity, the loss in pressure and in increasing the Reynolds number.

6- My conclusion is that to consider that the flame has a cone shape and to be considered that it has that shape an external air flow must flow around the flame in a way the velocity vector should be perpendicular on the surface of tube outlet area.

7- More tests should be conducted to get more accurate results.

8- The pressure profile before the plate had a big impact on the profile of v_{rms}/v_{bulk} but the v_{mean}/v_{bulk} stayed the same having the same profile through out the four graphs the only difference was that the velocity ratios were better uniform with the use of turbulence plates than without.

This Equation is for Stoichiometric case and constant flow rates:

$$\frac{S_T}{S_T^i} = f\left(\frac{n_i}{n}, \frac{\zeta}{\zeta_i}, \frac{Re}{Re_i}, \frac{\phi_i}{\phi}, \frac{\alpha}{\alpha_i}, \frac{\beta_i}{\beta}, \frac{\sigma_i}{\sigma}\right)$$

$$\frac{S_T}{S_T^i} = \left(\frac{D_i}{D}\right)^2 \left(\frac{\mu}{\mu_i}\right) \left(\frac{Q_{real}}{Q_{real}^i}\right)^2 \left(\frac{\partial P_i}{\partial P}\right)^2 \left(\frac{n}{n_i}\right) \left(\frac{1 - \frac{n_i D_i}{D_{tube}}}{1 - \frac{n D}{D_{tube}}}\right) \left(\frac{v_i}{v}\right)$$

8. References

- [1]-Glassman, I., 1996, Combustion.3rd edition. Academic Press.
- [2]- E.L Houghton P.W.Carpenter., 2006,Aerodynamics for Engineering Students 5th edition .Butter worth-Heinemann ELSEVIER.
- [3]- Stephen, R.Turns., 2000,An Introduction to Combustion Concepts and Applications 2sec edition. McGraw-Hill Higher Education.
- [4]- Kanury, A.M., 1977, Introduction to combustion phenomena, 2nd edition, Gordon and Breach, Science Publishers.
- [5]- Griffiths, J.F and Barnard, J.A., 1995, FLAME AND COMBUSTION.3rd edition. BLAKIE ACADAMIC AND PROFESSIONAL.
- [6]- BENNETT,C.O AND MYERS,J.E.,1962,MOMENTUM,HEAT,AND MASS TRANSFER. McGraw-Hill Book Company Inc.
- [7]-Lefebvre, Arthur. H., 1989, Atomization and Sprays, Taylor and Francis.
- [8]- LEWIS, BERNARD. VON ELBE ,GUENTHER .,1987, COMBUSTION, FLAMES and EXPLOSIONS of GASES, Third edition. Academic Press.
- [9]- Hill, Philip. , Peterson, Carl., 1992, Mechanics and Thermodynamics of propulsion 2 edition, ADDISON-WESLEY PUBLISHING COMPANY .
- [10]- SCHLIGHTING, HERMANN., 1979, BOUNDARY-LAYER THEORY, Seventh edition ,McGraw-Hill BOOK COMPANY .
- [11]-Meherwan ,P.Boyce.,2002,Gas Turbine Engineering Handbook, second edition, Gulf Professional Publishing .
- [12]-“Methane”
<http://en.wikipedia.org/wiki/Methane> {last Accessed on 1 September 2007}.
- [13]-“Adiabatic Flame Temperature”
http://en.wikipedia.org/wiki/Adiabatic_flame_temperature{last Accessed on 1 September 2007}.
- [14]- “Photron Ultima Camera Manual”
http://www.itronx.com/pdf/Photron_Ultima_APX-RS.pdf
(Last Accessed on 6 September 2007).
- [15]- PSA FLOW MANUUAL Version 3

[16]- (PIV Theory)

www.ce.utexas.edu/prof/kinnas/319LAB/PIVa.doc

(Accessed on 6 September 2007)

[17]- (The turbulent burning flame picture)

http://utias.utoronto.ca/~groth/research_combustion.html

(Last Accessed on 6 September 2007).

[18]- “SCIENCE AT NASA “

http://science.nasa.gov/headlines/y2000/ast12may_1.htm

(Last Accessed on 6 September 2007).

[19]-“General Flame Picture”

<http://www.flickr.com/photos/shigeru/122353430> {last Accessed on 6 September 2007}.

[20]-”Heat of combustion for methane “

<http://www.chm.davidson.edu/ChemistryApplets/calorimetry/HeatOFCombustionOfMethane.html>

{Last Accessed on 6 September 2007}.

[21]- Siewert , Piotr .,2002,Flame front characteristics of turbulent lean premixed methane / air flames at high-pressure ,degree of Doctor of Science ,SWISS FEDERAL INSTITUTE OF TECHNOLOGY ZURICH.

[22]-“ Methane“

<http://scifun.chem.wisc.edu/chemweek/methane/methane.html>

(Last Accessed on 7 September 2007).

[23]-“Methane”

<http://www.historyoftheuniverse.com/methane.html>

(Last Accessed on 7 September 2007).

[24]-Huenecke, Klaus.,1997,Jet Engines Fundamentals theory and design ,Airlife Publishing Ltd.

[25]-Duncan,W.J. ,Thom,A.S. ,Young,A.D., MECHANICS OF FLUIDS,1985 ,second edition, Edward Arnold.

[26]-“ Ellipse Area”

<http://en.wikipedia.org/wiki/Ellipsoid>

(Last Accessed on 8 September 2007).

[27]-“Cone Area”

<http://www.uwm.edu/~ericskey/TANOTES/Geometry/node15.html>

(Last Accessed on 8 September 2007).

Appendix A: List of figures

Figure 1-1: Range of bumable fuel-air ratios versus combustor gas velocity.....	-2-
Figure 1-2: a gas turbine used to generate electricity with all its components excluding the Alternator shows how difficult it is for a designer to get all the components to work at its best [11].....	-3-
Figure1-3: A cross section in a combustor of an early model jet engine and how complicated it is for the designer to get every component running at its best [24].....	-4-
Figure 2-1: Methane 3d balls.....	-6-
Figure 2-2: This shows the chemical structure of Methane.....	-6-
Figure 2-3: variation of flame temperature with the increase of equivalence ratio.	-8-
Figure 2-4: This shows the exact volume of oxidizer equals the exact volume of fuel which refers to the Stochiometric ,but due to difference in density they don't have the same volume	-11-
Figure 2-5: This shows the exact amount of fuel equals the excess amount of oxidizer which refers to the fuel lean case.....	-13-
Figure 2-6: This shows the exact amount of oxidizer equals the exact amount of fuel in addition to it excess fuel this refers to the fuel rich case.....	-13-
Figure 2-7: Tracer transport in laminar flow.....	-19-
Figure 2-8: Tracer transport in turbulent flow.....	-20-
Figure 2-9: Velocity recorded at random point in figure 2-8.....	-21-
Figure 2-10: Velocity recorded at random point which has turbulence effects on both the x and y axis.....	-22-
Figure 2-11: The transfer of data from a none uniform structure(graph shown on the left) to a uniform structure(graph on the left).....	-23-
Figure 2-12: The effects of turbulence intensity and how it is shown graphically.....	-25-
Figure 2-13: The turbulence fluctuating plays a vital role in the Borghi /Peters chart...-	-25-
Figure 2-14: The image of a number of flames which illustrate the similarity of flames in the way they burn and there flame structure similarity [19].....	-26-
Figure 2-15: the description of a stationary shock wave, subscripts 1 and 2 refer to the pre-and post-shock gases respectively.....	-27-

Figure 2-16: concentration and temperature profiles associated with a one dimensional, premixed, adiabatic flame.....	-30-
Figure 2-17: shows the burning velocity vector which is normal to the wave surface...	-31-
Figure 2-18: velocity vectors in a Bunsen core flame.....	-32-
Figure 2-19: General description of laminar Bunsen burner flame.....	-33-
Figure 2-20: A small slice is taken from the flame to be studied.....	-34-
Figure 2-21: The balance between zone I and zone II.	-35-
Figure 2-22: The balance across a methane flame differential element.....	-38-
Figure 2-23: The temperature at different time intervals.....	-41-
Figure 2-24: a comparison between a sinusoidal combustion wave at the top and a real combustion wave at the bottom [17].....	-43-
Figure 2-25: The approximation of the turbulent flame to a cone shape.....	-44-
Figure 2-26: Model of combustion wave in a turbulent flow.....	-45-
Figure 2-27: The difference with height at time intervals gives us the turbulence fluctuation.....	-46-
Figure 2-28: shows the laminar burning velocity at one of the cross sections of the flame.....	-46-
Figure 2-29: A 3D look on a combustion wave in a turbulent flow with a slice of a flame profile taken from a larger flame.....	-48-
Figure 2-30 : LES predictions of a free-propagating turbulent premixed methane-air flame using thickened flame with power-law flame wrinkling subfilter scale models[17].....	-49-
Figure 2-31: shows due in a flow which illustrates large eddies with low frequency and large wave length.....	-50-
Figure 2-32: Borghi /Peters chart illustrating different types of burning regimes.....	-53-
Figure 2-33: the classification of flame regimes based on three characteristic numbers [21].....	-55-
Figure 3-1: Shows the cylindrical atmospheric test facility.....	-57-
Figure 3-2: shows different types of blockage plates.....	-58-
Figure 3-3: a cross section through the cylindrical atmospheric test bench.....	-59-

Figure 3-4: is a clear diagram of the Dantec module showing the x, y and z axis of movement.....	-60-
Figure 3-5: The whole test apparatus with all of it secondary circuits.....	-61-
Figure 4-1: Particle Image Velocimetry [16].....	-62-
Figure 4-2: Interrogation areas the seeding particles where the grey particles where taken at time t1 and the red particles taken at t2.....	-63-
Figure 4-3: showing the camera and the particles and the interrogation areas.....	-64-
Figure 4-4: shows the vectors plotted by the soft wear after the collection of data and its analysis been conducted.....	-65-
Figure 4-5: Principles of backscatter LDA.....	-66-
Figure 4-6: laser beam with Gaussian intensity distribution.....	-66-
Figure 4-7: Light scattering from a moving seeding particle.....	-67-
Figure 4-8: Light scattering from a moving seeding particle.....	-69-
Figure 4-9 :Fringes from where two coherent laser beams cross.....	-70-
Figure 4-10: shows the high imagery used in the experiments [14].....	-73-
Figure 5-1: the make chart showing the relationship between v_{mean} / v_{bulk} and v_{rms} / v_{bulk}	-84-
Figure 5-2: The flame is traced by taking points on the surface and then revolving the profile around the tube axis.....	-86-
Figure5-3: The turbulence plate and a flow existing one of the holes that has a diameter D which is equal to L.	
Figure5-4: shows the flame while a 2mm turbulence plate was tested and the scaling considered.....	-90-
Figure5-5: shows the flame while a 3mm turbulence plate was tested and the scaling considered.....	-92-
Figure5-6: shows the flame while a 4mm turbulence plate was tested and the scaling considered.....	-94-
Figure5-7: flame thickness is visible with its several layers.....	-95-
Figure5-8: The relation between the burning velocity and ratio L_T / δ_L	-102-
Figure 5-9: The relation between the burning velocity and the number of holes.....	-103-

Figure 5-10: The relation between the burning velocity and the diameter of a single hole.....	-103-
Figure 5-11: The relation between the burning velocity and the number of holes.....	-104-
Figure 5-12: The relation between the burning velocity and the number of holes.....	-105-
Figure 5-13: The relation between the burning velocity and the holes diameter.....	-105-
Figure 5-14: The relation between the burning velocity and the holes diameter.....	-106-
Figure 5-15: The relation between the burning velocity and blockage ratio.....	-106-
Figure 5-16: The turbulence discs are shown on the Borghi/Peters chart.....	-108-

Appendix B: List of Tables

Table 2-1: A summary of hydro-carbons.....	-5-
Table 2-2: Approximate flame temperatures of various Stoichiometric mixtures critical temperature 298(K).....	-8-
Table 3-1: The Turbulence Plates characteristics.....	-58-
Table 1: burning velocity calculation for a 2mm disc.....	-89-
Table 2: burning velocity calculation for a 3mm disc.....	-91-
Table 3: burning velocity calculation for a 4mm disc.....	-93-
Table 4: 2mm Turbulence plate parameters.....	-96-
Table 5: 2mm turbulence plate Reynolds number and pressure drop work sheet.....	-97-
Table 6: 3mm Turbulence plate parameters.....	-98-
Table 7: 3mm turbulence plate Reynolds number and pressure drop work sheet.....	-99-
Table 8: 4mm Turbulence plate parameters.....	-100-
Table 9: 4mm turbulence plate Reynolds number and pressure drop work sheet.....	-101-
Table 10: General Data on all turbulence discs.....	-102-

Appendix c: List of Graphs

Graph 1: The v/v_{bulk} relation with x and y coordinates for 2 mm disc.....	-76-
Graph 2: The v_{rms}/v_{bulk} relation with x and y coordinates for 2 mm disc.....	-77-
Graph 3: The v/v_{bulk} relation with x and y coordinates for 3 mm disc.....	-78-
Graph 4: The v_{rms}/v_{bulk} relation with x and y coordinates for 3 mm disc.....	-79-
Graph 5: The v/v_{bulk} relation with x and y coordinates for 4 mm disc.....	-80-
Graph 6: The v_{rms}/v_{bulk} relation with x and y coordinates for 4 mm disc.....	-81-
Graph7: The v/v_{bulk} relation with x and y coordinates for a 25mm diameter tube.....	-82-
Graph 8: The v_{rms}/v_{bulk} relation with x and y coordinates for a 25mm diameter tube.....	-83-

Appendix D:

TABLE 1 Burning Velocities of Various Fuels at 25°C Air-Fuel Temperature (0.31 mol% H₂O in Air). Burning Velocity *S* as a Function of Equivalence Ratio ϕ in cm s⁻¹

<i>F_{fuel}</i>	$\phi = 0.7$	0.8	0.9	1.0	1.1	1.2	1.3	1.4	<i>S_{max}</i>	ϕ at <i>S_{max}</i>
Saturated hydrocarbons										
Ethane	30.6, 22.0L	36.0, 29.0L	40.6, 36.5L	44.5, 42.5L	47.3, 43.0L	47.3, 42.5L	44.4, 40.0L	37.4, 27.5L	47.6	1.14
Propane	—	—	42.3, 39.5L	45.6, 44.0L	46.2, 45.0L	42.4, 43.5L	34.3, 37.0L	—	46.4	1.06
<i>n</i> -Butane	24.0L, 23.0L2	32.0L, 30.0L2	37.0L2	39.0L2	41.0L2	40.5L2	33.5L2	28.0L, 25.0L2	44.9	1.03
Methane	—	38.0	42.6	44.8	44.2	41.2	34.4	25.0	44.8	1.08
	20.5L, 17L2	30.0, 28.0L	38.3, 36.0L	43.4, 40.5L	44.7, 42.0L	39.8, 37.0L	31.2, 27.0L	—	44.8	1.08
		25.0L2	33.0L2	38L2	38.5L2	34.0L2	24.0L2	13.5L2		

The source of this table is [1].